UNIVERSITÀ DEGLI STUDI DI PADOVA

DIPARTIMENTO DI INGENGERIA INDUSTRIALE

CORSO DI LAUREA MAGISTRALE IN CHEMICAL AND PROCESS ENGINEERING

Tesi di Laurea Magistrale in
Chemical and Process Engineering

Nitrogen fixing cyanobacteria for protein production: experimental and computational approach

Relatore: Prof.ssa Eleonora Sforza

Laureando: LEONARDO PATTARO

ANNO ACCADEMICO 2022 – 2023

Riassunto

Al fine di indirizzare l'industria alimentare verso un approccio più sostenibile, la produzione di composti da fonti vegetali, come le proteine o i pigmenti, rappresenta un importante ambito di ricerca. A tal riguardo, l'interesse è incentrato verso i cianobatteri azoto-fissatori, capaci di fissare l'azoto atmosferico e immagazzinarlo in forma di molecole a base di azoto.

Rispetto ad una loro potenziale applicazione in ambito industriale, le caratteristiche di crescita di *Nostoc* PCC 7120 sono state investigate mediante colture in scala di laboratorio, sia in discontinuo che in continuo. Per la prima categoria, è stato impiegato un bioreattore pilota da 275 L, al fine di verificare le capacità di adattamento ad una più grande scala operativa, mentre per la seconda fotobioreattori da 200 mL per determinare l'effetto di alcune variabili di processo. Rispetto all'intensità di luce, la condizione ottimale è stata individuata a 550 μmol m^{-2} s^{-1}, come miglior compromesso tra produttività di biomassa e contenuto di composti dall'elevato valore aggiunto. In secondo luogo, è stato condotto uno studio dettagliato sulle prestazioni di crescita della specie in condizioni di azoto-fissazione, modulando la quantità e l'origine dell'azoto all'interno dell'ambiente di coltura; lo sfruttamento di tale processo metabolico è risultato essere determinante per ridurre i costi capitali relativi all'approvvigionamento di nutrienti e migliorare le prestazioni della coltivazione.

Inoltre, l'esito favorevole di tale processo a livello industriale dipende anche dalla possibilità di prevedere il comportamento della specie. Pertanto, è stato sviluppato un modello matematico per simulare la crescita dei cianobatteri azoto-fissatori *Anabaena* PCC 7122 e *Nostoc* PCC 7120. Nel dettaglio, il modello si basa sulla teoria della quota interna di nutrienti di Droop, nella quale la variazione del tasso di crescita della biomassa dipende dalla quantità interna di nutrienti immagazzinata nella stessa. Rispetto ai vari modelli predittivi già presenti in letteratura, focalizzati sulla biomassa totale, l'introduzione di tale cinetica permette di tenere in considerazione simultaneamente entrambe le tipologie di cellule caratterizzanti le specie in questione, ossia cellule vegetative ed eterocisti. In accordo con il contesto sperimentale di questo lavoro, il modello è stato sviluppato per coltivazioni in continuo, prevedendo il comportamento della coltura rispetto al tempo di residenza. I risultati derivanti risultano in linea con dati raccolti durante precedenti campagne sperimentali, utilizzati per il fitting di alcuni parametri incogniti presenti nel modello.

Abstract

To convey the food and feed industry towards a more sustainable approach, the production of vegetal-derived compounds, as proteins or pigments, represents a relevant topic of research. In that regard, nitrogen-fixing cyanobacteria are of interest thanks to their capability to fix atmospheric nitrogen into valuable N-based macromolecules.

Looking for a potential industrial exploitation, laboratory experiments were conducted to assess *Nostoc* PCC 7120 cultivation features, both in batch and continuous configurations. Discontinuous cultivation was conducted in a 275-L pilot scale bioreactor in order to assess species performances in a larger operational scale, while 200-mL continuous photobioreactors were used to evaluate the effects of operating variables on harvested biomass and production of valuable compounds. With respect to enlightenment conditions, an optimal light intensity of 550 μmol m^{-2} s^{-1} was found, as the best compromise between biomass productivity and embedded valuable compounds. Secondly, a detailed study on diazotrophic growth performances was conducted, by varying the amount and source of nitrogen within the culture environment. The exploitation of such peculiar metabolic path seems to be a promising choice, since it contributes to lower nutrients-related capital costs as well as improve cultivation outcomes.

Moreover, successful industrial exploitation relies also on the possibility of predicting such outcomes. Therefore, the development of a simulation model for two cyanobacterial species, namely *Anabaena* PCC 7122 and *Nostoc* PCC 7120, was considered. In detail, the model embeds the Droop theory based on the nutrient quota, accounting for the variation of biomass growth rate based on the amount of nutrients within the biomass itself. Compared to the various predictive models already available in literature, focusing only on overall biomass, the introduction of such peculiar kinetics allows then to simultaneously account for both the two typologies of cells characterizing the species in question, namely vegetative cells and heterocysts. According to the experimental background of this work, the model was developed for continuous operations, predicting cultivation outcomes with respect to the operating residence time. The derived computational outcomes seem in line with data collected in previous experimental campaigns, which were also used for the fitting of additional unknown model parameters.

Table of contents

Introduction

The most crucial challenge that nowadays society has to face regards climate change, with a relevant negative contribution offered by the food and feed industry. Indeed, also due to the constant growth of worldwide population, projected to reach the threshold of 10 billion inhabitants by the year 2059, the request for food is constantly arising; as a matter of example, the request for proteins is expected to be 14% higher by 2030. This aspect puts a lot of pressure on the meat production chain, with the need for process intensification in order to sustain the increasing demand. Since this is of particular concern in terms of sustainability, it is necessary to find alternative solutions. About that, microalgae represent a potential feedstock as they are characterized by a protein content up to 70%. In addition to that, they are rich in other valuable compounds, such as essential ammino-acids and antioxidants, showing interesting applications also besides the food and feed sector. As generally photoautotrophs, their main metabolic path is photosynthesis. However, a smaller group composed by cyanobacteria is characterized by an additional metabolic process, through which is possible to fix atmospheric dinitrogen from the outer environment and directly convert it into nitrogen-based compounds embedded in biomass. These nitrogen-fixing cyanobacteria, first implemented in biofertilizers production, are now under investigation due to their peculiar nutritional profile.

Obviously, such microorganisms versatility has progressively gained more interest also from an economical perspective, to such an extent as to carve out a significant slice of the market: projections forecast that microalgae-based products will reach $ 3.08 billion by 2030, corresponding to 100,788 tons in volumetric terms.

From an operational perspective, microalgal biomass is still mainly produced according to batch rationales, as the know-how is quite spread and reliable. However, this approach is characterized by a time-dependent productivity, which does not allow to exploit at their most potential the adopted cultivation apparatuses. In order to overcome this aspect, researchers focus their attention on continuous systems, which can ensure steadiness to cultivation productivity and quality, as well as a more responsive system with respect to operating variables variations.

According to what has been stated so far, the cultivation of nitrogen-fixing cyanobacterium *Nostoc* PCC 7120 for further application in the food and feed industry represents the cornerstone of this work. For this purpose, an experimental assessment on growth performances is drawn, by exploiting both batch and continuous cultivation systems. Regarding the latter configuration, the effects of light intensity and nitrogen source and availability are investigated, in order to find the optimum conditions for ensuring satisfying biomass quality and quantity. Furthermore, a mathematical model was developed in order to predict cultivation outcomes for such species, exploiting experimental data collected for two similar species, namely *Anabaena* PCC 7122 and *Nostoc* PCC 7120.

This thesis is articulated in five chapters.

Chapter 1 provides a general overview concerning microalgae and cyanobacteria. Indeed, the biological description of the latter metabolic processes is then functional for the general presentation of the various fields of application, with a deeper focus on the food sector; in order to contextualize from an economic perspective this new rising market. Then, the different cultivation systems are presented, both from a structural perspective, namely as open or closed configurations, and from an operational perspective, considering batch and continuous configurations.

Chapter 2 lists all the materials and methodologies implemented along the experimental campaign, along with a brief explanation of the statistical approach used in view of the final elaboration for the collected results.

Chapter 3 focuses on the mathematical model. The first part focuses on the Droop kinetics, that has to be considered as the main novelty of such a model. Indeed, after its historical derivation, a comparison with respect to Monod kinetics is drawn, namely the other widespread biomass kinetic law. Secondly, the various model equations are presented, based on the several phenomena aimed to model.

In the last two chapters the results are then discussed. Starting from chapter 4, the focus is on *Anabaena* PCC 7122 in which the computational model results are presented. Chapter 5 instead deals with *Nostoc* PCC 7120, both from an experimental and computational perspective.

Chapter 1

State of the art

In the following chapter, a broad overview of the context is proposed. First of all, an in-depth analysis on potential applications of microalgae, and more specifically of cyanobacteria, is developed, along with the description of cyanobacterial metabolic key aspects. Following, an actual contextualization concerning the markets previsions and demands of such bio-based products is drawn, as a reflection of their potential applications. In the end, the focus moves towards the different cultivation processes that are used nowadays for microalgae production, both at industrial scale and at laboratory scale.

1.1 Prospects and challenges in today food industry

Due to the climate change scenario, the need of improving the variety of food and feed production sources becomes increasingly urgent, and nowadays it has developed in a serious issue that has to be addressed within the short-term period. In addition to that, the problem is also even more relevant if a constantly increasing world population is taken into account. In fact, starting from 1960, it has increased by 167%, with the mathematical projections forecasting the achievement of 10 million inhabitants by approximately the year 2059 (*World Population Prospects - Population Division - United Nations*, 2022) . Along with such a rapid increase, also an augmented demand for food consumption is expected, and the Food and Agriculture Organization (FAO) projects a global consumption of meat-based proteins increment by 14% by 2030 compared to the average of 2018-2020 (*OECD-FAO Agricultural Outlook 2021-2030*, 2021). Another crucial point related to the meat production sector is the environmental footprint that all the involved processes are characterized by. Considering its carbon footprint, and more specifically the sector impact on Green House Gases (GHG) emissions, the previously quoted study highlights that GHG emissions from meat production comprised about 54% of total emissions from agriculture during the 2018-2020 period, and an

increase of 5% by 2030 is expected. Fortunately, such increase is shown to be considerably less compared to the one in meat production, due to improvements in the sector, aimed at optimizing the meat output from a given stock of animals, but also to the new technologies available for reducing methane emissions (*OECD-FAO Agricultural Outlook 2021-2030*, 2021). As for the carbon footprint, also the water footprint can be presented as a key indicator for the non-sustainability of such a sector. Even though some differences can be highlighted for the different types of animal products, as well as production methods and geographical areas, as a matter of reference the average worldly water footprint value for beef products is 15400 L kg^{-1} (Mekonnen & Hoekstra, 2010), and obviously this value is expected to increase. The abovementioned issues related to such food sectors open the path to new strategies in order to slow down the possible adverse effects related to intense meat consumption and production. As a matter of example, in high income countries, new dietary preferences were developed, such as vegetarian and vegan diets. The common rationale of these alimentary regimes is based on the reduction of animal-based proteins consumption, while showing a greater interest in other protein sources. Due to this factor, together with the need of finding more sustainable solutions for food increased demands and a more environmentally focused way of thinking, interest in alternative protein sources has been developed along the years. With respect to this, a potential idea is to boost agricultural production, known to provide alternative foods with respect to animal ones. However, satisfying the population needs by relying only on agriculture is still crucial, as this regime would imply massive deforestations and intense use of fertilizers and pesticides, compromising the overall sustainability of the approach.

These considerations lead to the determining role of alternative feed sources, that are capable of providing a lower intensification of livestock and crop productions, while enlarging the variety of sources available for customers. The development of foods with an increased nutritional content is another key objective that companies are pursuing. In fact, adding functional foods in the everyday diet, would help preserving and boosting human health, with a particular reference to elderly, for which the protein deficiency is one of the most relevant concerns (Villaró et al., 2021).

According to a more sustainable protein production, the FAO recently reported that plant-based proteins are 38-91% less land intensive, 53-95% less water intensive, and 69-92% less carbon intensive than meat-based ones, thus reducing, at European level, global warming potential,

water use and land use by over 80% (*Alternative Proteins Top the Bill for the Latest FAO–International Sustainable Bioeconomy Working Group Webinar | Sustainable and Circular Bioeconomy for Food Systems Transformation | Food and Agriculture Organization of the United Nations*, *2022*).

Within all the alternative protein sources, microalgae represent a potential feedstock since, from a nutritional point of view, are characterized by a protein content up to 70%. In addition to that, other studies proved that they are rich in essential ammino-acids and antioxidants, and they contain phycobiliproteins, a particular kind of pigment which showed anti-inflammatory properties (Batista et al., 2013) (Barkia et al., 2019).

1.1.1 Microalgae and cyanobacteria potentialities

With the general term microalgae, reference is made to all photosynthetic unicellular microorganisms capable of living either in saline or freshwater environment, converting sunlight, nutrients, and carbon dioxide into algal biomass (Tan et al., 2011). Clearly, this hints at the possibility of including a wide variety of different organism under this name; indeed, within the abovementioned category, it is possible to comprehend two subgroups, based on their inner structure and behavior (Shaikh et al., 2022). The first one is composed by more complex entities, belonging to the Eukaryotic domain, while the second subgroup is composed by microorganisms comprised within the Prokaryotic domain as cyanobacteria (Shaikh et al., 2022). Over the years, these microorganisms have achieved considerable success in many application sectors, due to the intrinsic environmental advantages related to bio-based processes with respect to conventional ones (Khan et al., 2018).

In detail, the application of microalgae in the food sector dates back to several centuries ago. Indeed, there are numerous records of historical usage of microalgae, and primarly cyanobacteria, in human diet (Gantar & Svirčev, 2008). As a matter of example, *Nostoc commune*, a filamentous cyanobacterium growing in the form of large gelatinous sheets, was implemented in everyday Asian diet. Evidence reports its raw consumption, as well as dried, stir-fried, in soups and as thickener for other foods (Facciola, 1990). Moreover, another strain of the genus *Nostoc, Nostoc punctiforme*, is historically part of the traditional dietary regime in China, Mongolia and South America. In the latter geographical region, it is still commercialized with the common name of “Lakeplum” (Trainor, 1978).

After that, the first systematic studies concerning the application of these microorganisms into the food chain are related to the production of bio-based fertilizers. As explained in previous section *§1.1*, one possibility to tackle the constant increasing demand for food is to boost agricultural production. In turn, in order to accomplish such objective, it is fundamental to replenish soils with all the nutrients needed to maintain their optimal fertility. Regarding nitrogen-based fertilizers, the most widespread typology, the Haber-Bosch process was depicted as the primary solution for a concrete production boost (Liu, 2014). In numbers, about 80% of the ammonia produced globally is used for nitrogen-based fertilizers, mainly produced nowadays with such industrial setup. Such technique, from a practical perspective, involves the fixation of atmospheric dinitrogen N_2, so its conversion into ammonia through a high-pressure reaction. By circulating nitrogen and hydrogen over a proper catalyst at 150-200 atm and at a temperature of about 500°C, an industrially relevant production of ammonia can be achieved (Chen et al., 2019). Apart from the great product volumes obtained, potential drawbacks can be however pointed out: the massive need of hydrogen as input for the process (Rafiqul et al., 2005), as well as the high operative temperature and pressure involved. Under this optic, finding an alternative path for ammonia production becomes of primary importance, and some cyanobacteria fit such role perfectly. More specifically, the biological fixation performed by nitrogen-fixing cyanobacterial species represent the basis for a sustainable agricultural system, with a reduced impact on the surrounding environment.

The culmination of microalgae involvement for alimentary purposes occurs with numerous attempts to produce biomass and commercialize it in various forms (Trainor, 1978). Indeed, works on controlled cultivation of *Chlorella vulgaris* suggest that the high nutritional content of such microorganism can make it a suitable food source. In general, it must be reported that each singular species is characterized by a specific nutritional value and digestibility, but, along with that, also the technological process applied for biomass production can have a significant impact on such aspects (Soeder, 1980). The species nutritional profile has to be defined by looking at several compounds simultaneously, in order to assess the optimal ones for food and feed purposes. Starting from protein content, this is considered as the most important component of algal biomass (Trainor, 1978): its content can be manipulated by acting on the cultivation conditions, like availability of nutrients such as potassium, sodium, and nitrogen (Mostert & Grobbelaar, 1987), culture growth phase and light availability (Fontes et al., 1987).

The lipid content, is variable among the different species, reaching up to 53% of the algal dry weight, and it can be varied thanks to ecological factors applied during growth (Trainor, 1978). Another interesting feature is the production and accumulation of polyunsaturated fatty acids, as docosahexaenoic acid (DHA), recognized for its benefits on cardiovascular health and neural development (Jiang et al., 2004). In addition, specifically for eukaryotic algae, the presence of approximately 10% carbohydrates, such as cellulose, mannose and xylose, is remarkable, making their biomass more easily digestible and thus suitable for human consumption (Richmond & Preiss, 1980). Carbohydrates are usually accumulated and account up to 50% of the whole biomass (Aaronson & Dubinsky, 1982). In addition, microalgae and cyanobacteria vitamin profile cannot be overlooked, as they are a rich source. For example, the cyanobacterium *Arthrospira platensis* (commercially known as *Spirulina*) has the highest content of vitamin B_{12} with respect to any fresh plant or animal derived food, and the same can be said for provitamin A, vitamin E, thiamine, cobalamin, biotin, and inositol (Trainor, 1978). However, the applicability of algae and cyanobacteria for human consumption has also some limitations that must be considered, primarily the high nucleic acids content. The major concern is related to their metabolization to uric acid, which results in adverse health effects such as gout and kidney stones (Soeder, 1980). With respect to that, cyanobacteria are considered safer than other eukaryotic microalgae. In fact, *Spirulina* has 4.2-6% nucleic acids content, not inducing any particular concern with respect to the derived uric acid levels (Trainor, 1978).

Among the different groups of cyanobacteria, nitrogen fixing species are attractive for the production of biomass and chemicals. For example, a study conducted on several strains of filamentous heterocystous nitrogen-fixing species, such as *Anabaena* sp. and *Nostoc* sp., reported a biochemical profile similar to the one characterizing *Spirulina*, which is considered to have high nutritional value (Vargas et al., 1998; Henrikson et al., 1989). In addition to that, their peculiar metabolism is also a relevant aspect to be considered, since they are capable of fixing atmospheric dinitrogen N_2 under aerobic conditions. This opens to positive economic implications, since nitrogen-based compounds are not required in medium, as well as reduction of culture contamination by other microorganisms (Vargas et al., 1998).

1.2 Nitrogen-fixing cyanobacteria

The cyanobacteria phylum contains over 2000 species, arranged in 150 different genera. Commonly speaking, it is also denoted as "blue-green algae" phylum, due to the photosynthetic pigments which are preferably developed by such microorganisms. Historically, they represent the precursor of eukaryotic chloroplast (Lane, 2017). Another relevant peculiarity which makes them distinguishable from the other prokaryotes regards the presence of the characteristic gram-negative cell wall.

Metabolically, cyanobacteria are photoautotrophic microorganisms, meaning that photosynthesis is the dominant mechanism through which they produce all the organic materials fundamental to the species development and maintenance.

During photosynthesis, light is absorbed and then converted into chemical energy. More specifically, the absorbed photons induce the production of energized electrons, that are then moved to the cell reaction center for the conversion to chemical energy. The latter, in the form of adenosine triphosphate molecules (ATP), is chemically synthetized as a result of such electrons movement, which generate a proton gradient between inner and outer cell environment allowing the functioning of ATP synthase (Assunção et al., 2022).

Along this way, carbon dioxide can be fixed through the Calvin cycle and later converted into molecules that can be exploited by the cells as building blocks. The key elements involved in the entire process are the thylakoid membranes, where the photosynthetic reactions occur (Assunção et al., 2022). All the systems involved in such a process are present above their surfaces. The primary pigments involved in light absorption are chlorophyll a, specifically used in oxygenic photosynthesis, and carotenoids; these allow the system to harvest light at different wavelengths. In addition, cyanobacteria are also equipped with phycobilisomes, namely the cyanobacterial light-harvesting system (LHS). From a functional point of view, LHS acts as an antenna placed on the surface of thylakoid membranes, needed to help absorbing incident light, due also to their inner mobility along the photosynthetic chain (Saini et al., 2018). The building blocks of such antenna are phycobiliproteins, secondary pigments which can be differentiated into four different groups, based on the specific range of absorbed wavelengths and the species: phycocyanin, allophycocyanin, phycoerythrin, and phycoerythrocyanin.

Table 1.2. *Cyanobacterial pigments absorption spectra* (Saini et al., 2018).

Pigment	Absorption spectrum [nm]	Reference
Phycocyanin	610-625	(Tavanandi et al., 2018)
Allophycocyanin	650-660	(Rastogi et al., 2016)
Phycoerythrin	490-570	(Sonani et al., 2018)
Phycoerythrocyanin	560-600	(Chandra et al., 2016)

Cyanobacterial cells are usually mostly prone to produce the first two types. In fact, the reason behind the historical name of cyanobacteria can be attributed exactly to the presence of phycocyanin, as it is a blue-emitting pigment (Assunção et al., 2022).

The architecture of a phycobilisome comprises a central core and several perimetral elongations, providing the whole element a fan-like appearance (Lundell et al., 1981). The core is mainly made of allophycocyanin, while the elongations are a mixture of phycocyanin for their basis, and phycoerythrin for the outermost sections, as illustrated in figure1.1.

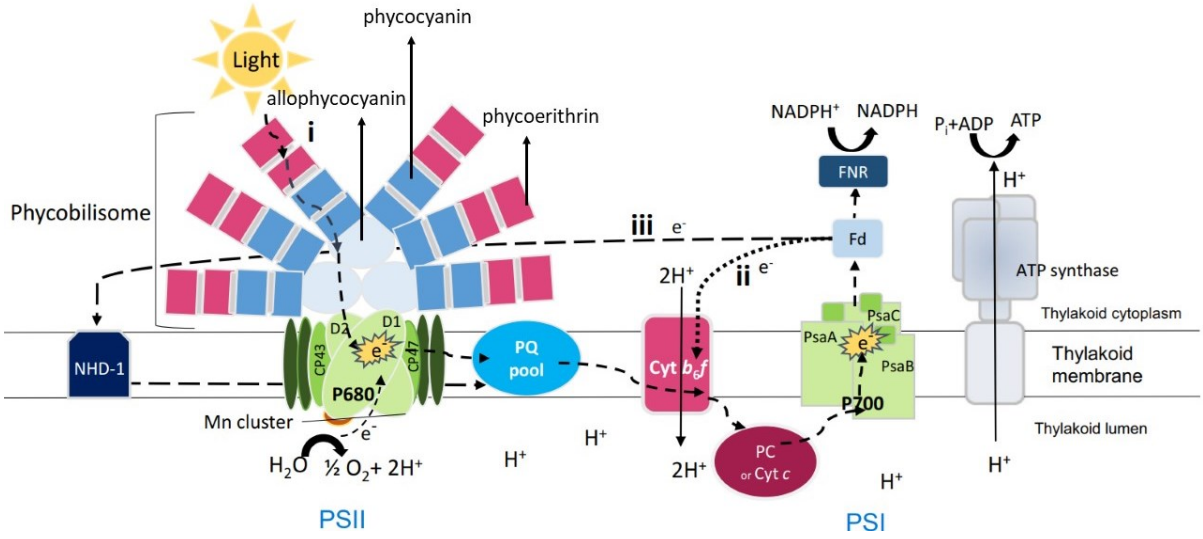

Figure 1.1. *Electron transport routes during photosynthesis* (Assunção et al., 2022).

Moving to the details concerning the electron transport process, the starting point is represented by photons collection through two pigment-protein complexes within the thylakoid membrane, namely photosystem I (PSI) and photosystem II (PSII) (Masojídek et al., 2013). Specifically for the latter, the harvesting of light is helped by the presence of the antenna system, which is then transferred to PSII according to a decreasing energy gradient (Masojídek et al., 2013). Such reaction center is used to catalyze water photolysis reaction, through which two electrons

are extracted from water, and transferred through a chain of electron carriers (Masojídek et al., 2013). The electron transport between these two complexes is linked via cytochrome b_6f and performed by two kinds of mobile carriers: plastoquinones and plastocyanin. Within PSI a photochemical reaction takes place, aimed at generating the low redox potential necessary for reducing ferredoxin and lately producing NADPH. In parallel, protons are transported from an external space (stroma) into the intra-thylakoid space (lumen) inducing a pH gradient, which is essential for ATP synthesis from ADP in ATP synthase, source of chemical energy for cyanobacteria (Masojídek et al., 2013).

Moreover, by considering a smaller group of cyanobacteria, known as nitrogen-fixing (or diazotrophic) cyanobacteria, nitrogen fixation represents a peculiar metabolic pathway, allowing fixation of inorganic dinitrogen directly from the outer environment.

The possibility of acquiring such macronutrient directly from an inorganic source as air, is explained in the following reaction (Bothe et al., 2010):

$$N_2 + 16ATP + 8H^+ + 8e^- \rightarrow 2NH_3 + H_2 + 16ADP + 16P \quad (1.1)$$

Such dinitrogen reduction is energy-consuming, as it involves 16 ATP molecules per reduced N_2 molecule. Due to the high energy demand, the process is unfavorable, and indeed other ways in order to acquire nitrogen are preferable, when available. The key enzyme for reaction catalysis is nitrogenase (K. Kumar et al., 2010). It is composed by two metalloproteins, namely the iron (Fe) protein, also denoted as dinitrogenase reductase, and the molybdenum-iron (MoFe) protein, also called dinitrogenase. In some cyanobacteria species, the latter one can be also substituted by the homologous alternative vanadium (VFe) or iron only (FeFe) proteins (Pratte et al., 2006). Dinitrogenase reductase serves to transfer electrons from electron donors to dinitrogenase (K. Kumar et al., 2010).The most relevant peculiarity related to such enzyme is the sensitivity with respect to oxygen, which irreversibly inactivates it. Therefore, a prerequisite for N_2 fixation has to be find in developing an anoxic environment, to ensure the right activity of such enzyme (Gallon, 1992). In order to prevent this phenomenon, different strategies were adopted, depending on the nature of the species considered.

Many cyanobacteria can apply the so-called temporal differentiation depending on the light-dark condition, they are capable of selectively performing photosynthesis or nitrogen fixation (K. Kumar et al., 2010). More precisely, under light regime they perform photosynthesis, by

absorbing light to fix inorganic carbon and produce oxygen, while under dark regime they fix inorganic nitrogen, due to the lack of photosynthesis combined with an increased respiration rate, enabling a significant reduction in oxygen concentration within the cell. In the latter condition, energy can be only derived by fermentation of previously stored carbohydrates.

On the other hand, some cyanobacteria have developed a different strategy to overcome the abovementioned issue, namely, to spatially differentiate the two metabolic processes by differentiating specialized cells for the different cycles (K. Kumar et al., 2010). In this case, heterocystous cyanobacteria are considered an exceptional category, because this feature is unusual among bacteria (Muro-Pastor & Hess, 2012). The differentiation process involves the possibility of having simultaneously two different types of cells: vegetative and heterocystous cells, responsible for carbon and nitrogen fixation, respectively. The development of the latter from a vegetative cell occurs under nitrogen depletion, which induces a series of modifications, both at a metabolic and morphological level, up to the formation of the final specialized cell (K. Kumar et al., 2010). Among the different changes, some are of crucial importance to sustain the new metabolic cycle that has to be carried out. From a structural point of view, they appear larger and rounder with respect to vegetative cells. While metabolically, the first change regards photosystems I and II, with the presence of the first and the absence of the second (Wolk et al., 1994): in this way light can be still harvested by the heterocyst and used for ATP production, but oxygen production can be inhibited, producing the desired anoxic condition, along with an increased respiration rate, another heterocysts peculiarity (Wolk et al., 1994). Moreover, the heterocystous cell is usually characterized by a decreased concentration of phycobiliproteins, making it lighter in coloration and with poorer autofluorescence with respect to a vegetative cell. In the end, heterocysts have a thicker cell wall, due to the presence of an additional extracellular envelope, made by glycolipids, to act as a further barrier for oxygen diffusion (Walsby, 1985).

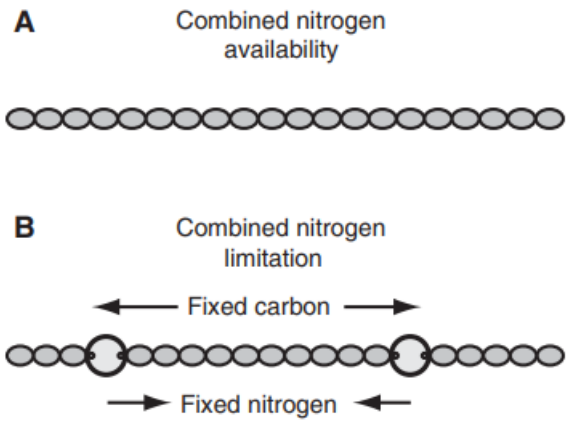

Figure 1.2. *Heterocyst development in Anabaena PCC 7120 grown in medium with a nitrogen source (A) or without nitrogen available in culture medium (B)* (K. Kumar et al., 2010).

As schematized in figure 1.2, the differentiation process brings a condition of dependency between the different typologies of cells within the same environment. Indeed, vegetative cells provide carbon, in the form of glutamate, to heterocysts, and at the same time they receive part of fixed nitrogen, in the form of amminoacids, from heterocysts themselves (Martín-Figueroa et al., 2000; Meeks et al., 2002). The exchange of metabolites is accommodated by the filamentous structure, presenting vegetative cells and heterocysts alternated along the chain, with a semiregular interval. The presence of heterocysts along the filaments is regulated by a pattern, comprising one every 10-20 vegetative cells (K. Kumar et al., 2010). The appearance frequency is related to nitrogen availability, considering that it depends also on the source of nitrogen that is provided to the culture. Apart from cells arrangement, the movements of molecules along filaments is physically achieved by means of the presence of channel proteins named microplasmodesmata, acting as natural connections between adjacent cells (Giddings & Staehelin, 1981), highlighted in figure 1.3 below.

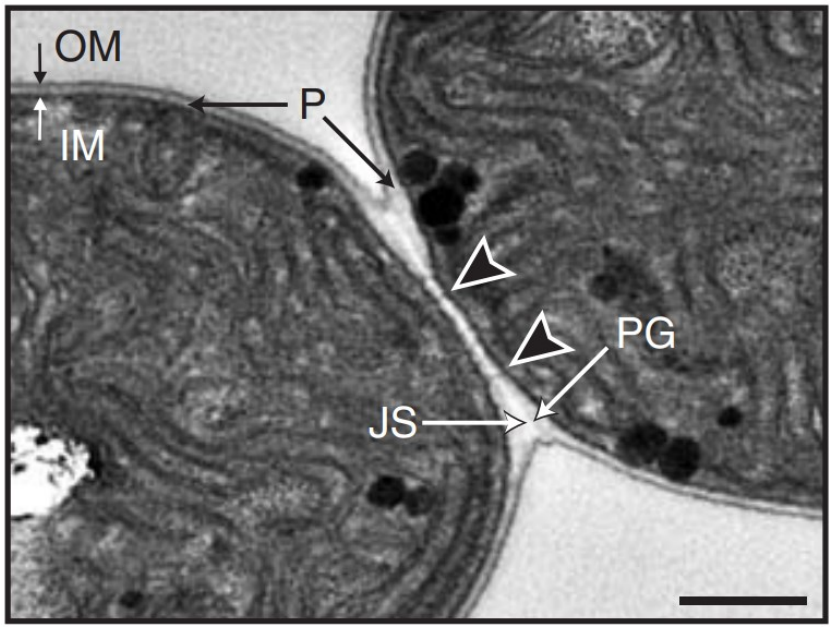

Figure 1.3. *Transmission electron micrograph of the junction between two vegetative cells. In detail, arrows indicate microplasmodesmata within the periplasm (P)* (K. Kumar et al., 2010).

1.3 Other applications

Due to the wide variety of compounds that can be produced and extracted from microalgae and cyanobacteria, the market demand is not only focused on biomass exploitation for feedstock purposes, but also on other valuable sectors.

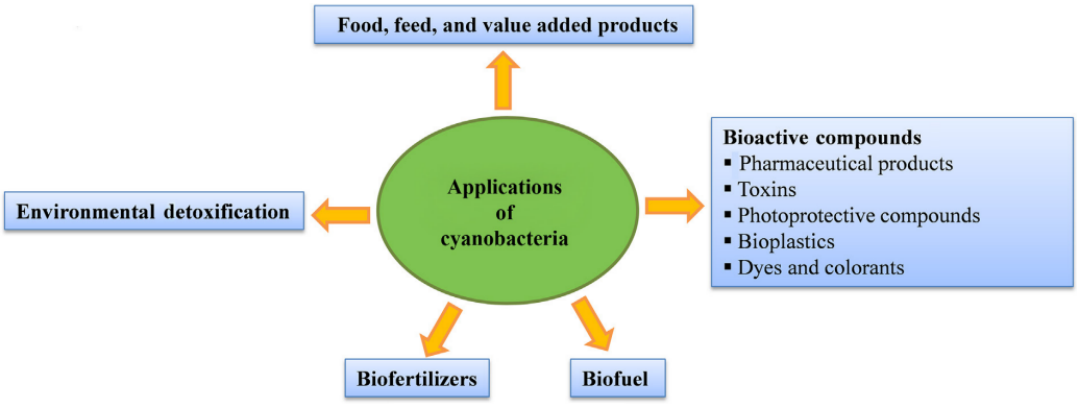

Figure 1.4. *Potential fields of application for cyanobacterial production* (J. Kumar et al., 2018).

With respect to bioremediation processes cyanobacteria represent a possible solution, since they are characterized by a trophic independence for nitrogen and carbon (Touliabah et al., 2022). The reference biological process is called "phycoremediation", in which biomass is capable of accumulating organic and inorganic toxic substances in their cells and subsequently degrade them through excretion of specific enzymes, converting them into nontoxic compounds (Opeolu et al., 2010). As a matter of example, cyanobacterial species as *Anabaena sp.*, *Aphanothece conferta*, *Phormidium sp.*, *Nostoc sp.*, and *Synechocystis aquatilis* can degrade a wide variety of petroleum hydrocarbons (Abed, 2009), (Ibraheem, 2010).

Such operation rationale does not only avoid sludge production characterizing conventional remediation processes (Crini & Lichtfouse, 2019) , but it is also considered as a cost-effective solution. Indeed, the starting investment for setting up the biological process is 5-20 times less than the conventional chemical treatment, and running costs are 3-10 times lower (Karthik et al., 2015)

Besides that, cyanobacteria are also known for producing a wide variety of products out of their metabolic processes, the so-called metabolites, that can be implemented in several areas of interest. Depending on the metabolic path dealing with their synthesis, it is possible to distinguish between primary and secondary metabolites. Primary metabolites, as proteins, carbohydrates, lipids presented in *section §1.1.1* are the ones strictly involved in primary biomass processes, such as reproduction, growth, and cell division (Mazard et al., 2016). On the contrary, secondary metabolites are developed during side metabolic paths, or produced for defensive purposes as a response to environmental stresses (Chomel et al., 2016). Within the latter category, the most commonly produced include pigments, toxins, phenolic compounds, essential oils, alkaloids, steroids, and antibiotics (Baselga-Cervera et al., 2014), (D. P. Singh et al., 2017), (Khalifa et al., 2021). Among all the application sectors, relevant is the nutraceutical one, aimed at enhancing food nutritional properties by exploiting cyanobacterial secondary metabolites. As a matter of example, cyanobacterial phycocyanin and carotenoids can be exploited as antioxidant compounds, capable to prevent reactive oxygen species (ROS) and scavenge them (Halliwell, 2003). Additionally, these compounds are used nowadays in food supplements, sold in form of tablets, granules and capsules, or food additives (Żymańczyk-Duda et al., 2022).

1.4 Market demand and forecasts

Economic data concerning cyanobacterial species usually focus on *Spirulina* sp., as it is the most important microorganism exploited at industrial level so far. However, more often, a global analysis for market demands and possible forecasts for the following years are provided for the general category of microalgae. Even if it includes other species apart from cyanobacteria, the analysis can still be useful for depicting a general frame of contemporaneous industrial society, aimed at pursuing a new bio-based approach for modelling the newborn industrial production processes, as a response to the major crucial issues that has to be faced nowadays.

The global market for microalgae-based products is expected to reach $ 3.08 billion by 2030, at a Compounded Average Growth Rate (CAGR) of 9.4% within the 2023-2030 range. In a volumetric perspective, it is expected to reach 100,788 tons by 2030 at a CAGR of 12.8% during the same year span (*Microalgae Market to Reach $3.08 Billion by 2030 - Market Size, Share, Forecasts, & Trends Analysis Report with COVID-19 Impact - Bloomberg, 2023)*.This rapid growth is supported by several reasons, but the most relevant contribution is provided by food and related industry, being the largest share of the market.

Due to the consumers growing interest in alternative, natural and healthy products, along with an increased awareness regarding the link between nutrition and health, researchers and industries were encouraged to develop novel products with functional ingredients. For the purpose, microalgae cover an active role, due to the excellent nutritional profile, with the subsequent products being consumed as supplements to enhance immunity. Also, the booming nutraceutical sector provides a relevant contribution in such market boost, being the propeller of these new trends focused on alternative dietary regimes.

Considering species-based market sharing, in 2023 *Spirulina* is expected to account for the largest segment of the global microalgae market, but on the other side it has to be underlined that the *Heamatococcus pluvialis* segment is projected to register the highest CAGR within the 2023-2030 forecast span. Such growth is due to the increasing demand for natural astaxanthin, a molecule with powerful antioxidant properties, as well as for natural food colorants.

From a geographical perspective, the microalgae market is fragmented mainly in five regions, namely North America, Europe, Asia-Pacific, Latin America, and Middle East & Africa. During 2023, the North America segment is expected to be the dominant one, followed by

Asia-Pacific and Europe. This has to be related to the huge consumption of health supplements, strict regulations concerning synthetic colors use, and growth of subsidiary industries like cosmetics and biofertilizers. On the contrary, the European sector is expected to lead the following years in growth, as a result of an increased adoption of microalgae for therapeutical and nutritional purposes, and significant investments from leading color stakeholders in the phycocyanin area of interest (*Microalgae Market by Size, Share, Forecasts, & Trends Analysis*, *2023*).

Despite the previously mentioned marker forecasts, it has to be acknowledged that, compared with other conventional markets, it is still a niche market. This is due to the fact that microalgal biomass potentialities are not exploited at their full regime nowadays, being most of them still at research level due to the presence of several challenges, from the social acceptance perspective to the engineering ones, that combined together slow down the actual industrial and economic feasibility. With respect to the latter aspect, more in-depth analyses are required, in order to find the right compromise between optimal biomass production volumes and quality, and the reduction of the capital and operative expenses. More in detail this analysis involves the assessment of optimal growth conditions, proper cultivation system, as well as all the auxiliary facilities usually involved in an industrial plant.

1.5 Microalgae and Cyanobacteria cultivation systems

Maximizing biomass production and productivity represents the major challenge that industries have to pursue. Moreover, to be competitive in such a fast-growing market, capital and operation costs must be kept at minimum. In order to find the right compromise between these two aspects, the innovation process covers a leading role in the subject, by assessing how operation factors can affect microbial growth efficiency, and by improving cultivation equipment.

1.5.1 Growth factors affecting microalgal cultures

Several operation factors contribute to modify the way under which microalgae can grow. Among them, the most relevant ones are temperature, light intensity, pH conditions, and the

availability of nutrients. In the following sections, a brief description of their effects is proposed.

1.5.1.1 Temperature

Operating temperature covers a central role in the control of microorganism growth, and more specifically in the kinetics of the metabolic processes. In fact, photosynthesis and related carbon fixation is strictly linked to this factor (Venkata Mohan et al., 2015). The effect of temperature on metabolism obviously differs with respect to the species. Based on the temperature range allowing for the optimum species growth, microalgae can be classified into psychrophiles, mesophiles and thermophiles.

Table 1.2. *Classification based on optimum growth temperature for some cyanobacterial species.*

Strain	Classification	Reference
Nostoc commune	Psychrophile	(Vincent & Quesada, 2011)
Synechocystis sp.	Mesophile	(Yu et al., 2013)
Arthrospira platensis	Mesophile	(Delrue et al., 2017)
Synecochoccus sp.	Thermophile	(Pedersen & Miller, 2017)

The optimal temperature interval is mainly related to the carbon fixation process, since it can enhance CO_2 absorption, but it has to be acknowledged that higher temperatures contribute also to a sharp reduction in the respiration process (Zuccaro et al., 2020).

The possibility of having certain optimum conditions implies, on the contrary, the presence of boundaries for this parameter, as no photosynthetic organisms are capable to grow beyond 75°C, due to chlorophyll instability. Furthermore, outside the optimum condition, temperature can be exploited as a stress factor, to induce the production of certain valuable metabolites (Zuccaro et al., 2020). Despite that, the majority of species nowadays exploited are within the mesophilic group; this implies that optimum growth conditions range from 24 to 35 °C. From an industrial perspective, these operative conditions do not represent a limiting factor, but rather an advantage, considering the possibility of reducing energy expenditure.

1.5.1.2 Light

As photosynthetic microorganisms, light is a key factor affecting growth and thus the cultivation process. Light can be naturally or artificially supplied. Thanks to the technological development of more efficient light sources, such as LED, it is now possible to modulate light

more accurately according to photosynthetic needs, ensuring modifications in productivity of microalgal biomass, and different accumulation of valuable compounds in it. The main parameters involved in this process are light intensity, duration of lighting and the use of rays of different spectral composition. These aspects can be changed either individually or combined together to reach the desired cultivation outcomes (Maltsev et al., 2021). As explained in section *§1.2*, the simultaneous presence of different pigments working at different spectral interval suggest the possibility of implementing, when cultivating microalgae, light with different spectral composition (Teo et al., 2014). Indeed, as the red part of the spectrum contains an insignificant part of light energy, implementation of LED lamps allows to create monochromatic light or light fluxes with a selected spectral composition (Schulze et al., 2014). So, it is possible to change metabolic processes in microalgae cells, shifting them towards the predominant accumulation of proteins, carbohydrates, or lipids (Raqiba H & Sibi G, 2019). As a matter of example, blue light increases carbohydrate content, while green light can increase protein content in *Arthrospira platensis* (Mao & Guo, 2018). Moving to the light duration parameter, the use of lightning systems with dark cycles can increase the productivity of microalgae by increasing the efficiency of light absorption while reducing energy consumption, relevant aspect to seek in optic of process profitability (Maltsev et al., 2021). In addition to that, continuous light can initiate photoinhibition processes; on the other hand, introducing dark periods can help restoring damages to photosystems (Yustinadiar et al., 2020). Along with productivity, such parameter can modulate species biochemical composition; for example, *Nostoc calcicola* at a light intensity of 21 μmol m^{-2} s^{-1} with a photoperiod of 8/16 h light/dark tend to accumulate proteins and phycobiliproteins, while at 63 μmol m^{-2} s^{-1} and longer illumination (16/8 h) carbohydrates and carotenoids preferably (Khajepour et al., 2015). Along with the previous two, the intensity of the light source represents a significant aspect affecting microalgae growth. A key relationship between this parameter and the rate at which photosynthesis is carried out has been highlighted (Zuccaro et al., 2020). To better explain this concept, it is possible to observe different outcomes depending on three different light regimes, as in figure 1.5. First of all, at low light intensities the relationship is linear, and so the photosynthetic rate tends to grow linearly with the operating parameter of interest. Then, beyond a specific threshold value, a light saturation condition occurs, as a further increase in light intensity is not capable of stimulating an increase in microbial growth anymore.

Obviously, saturation condition can degenerate into an inhibition phase, under which very high levels of light induce a state of stress capable of inhibiting microbial growth, due to damages in photosynthetic systems (Razzak et al., 2013). In response to this phenomenon that can compromise biomass growth, microalgae have developed some strategies to partly counteract the excess of light radiations, namely by producing antioxidants such as β-carotene and astaxanthin (Raven & Ralph, 2015). Photoinhibition is also associated with self or mutual shading effects inside the photobioreactors, namely states under which cells are shaded by the others much closer to the surface. To limit this phenomenon by ensuring proper mixing and a proper light distribution to the whole culture, a proper design of the cultivation apparatus is required.

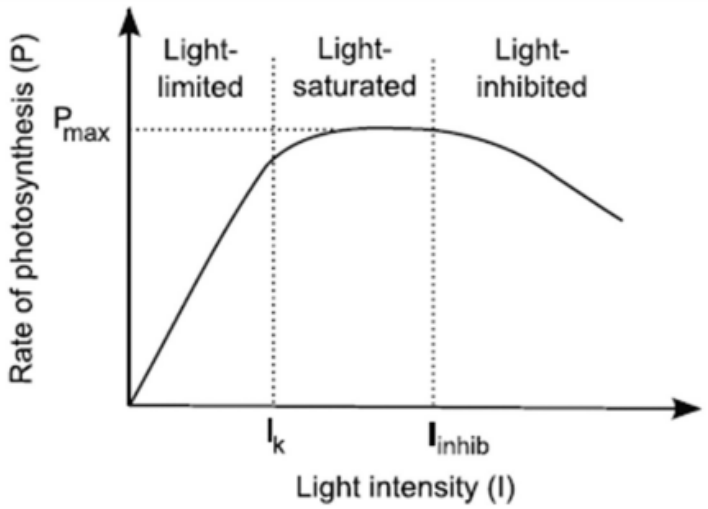

Figure 1.5. *Relationship between light intensity and photosynthetic rate* (Béchet et al., 2013).

In the end, the highlighted trend opens the door also to the concept of optimum light intensity conditions, capable of allowing the biomass grow at the highest possible rates, while optimizing electricity costs, due to the reduction of photoinhibition and photosaturation phenomena (Zuccaro et al., 2020). Such values, dependent on the species of interest, can range between 200 and 400 μmol m^{-2} s^{-1}.

1.5.1.3 pH

Microalgal metabolism is also strictly related to pH since it contributes to regulate the uptake of ions, enzymatic activity, phosphorus, and inorganic carbon availability (Havlik et al., 2016). Most microalgal species are quite sensitive to changes in pH conditions, and the optimum range

of values is 6.0-8.0 in freshwater cultivations, with some exceptions concerning extremophile species (Zuccaro et al., 2020). In order to maintain the desired pH value within the system, the control of such process variable is usually achieved by insufflating CO_2 or by using inorganic or organic acids, that can counteract potential pH changes due to degradation and/or release of metabolites within the environment ("Handbook of Microalgal Culture," 2003).

1.5.1.4 Nutrients availability

In order to perform all the metabolic cycles that allow the survival of the species, microalgal cultures require several nutrients. Depending on the amounts needed, they can be divided in macronutrients and micronutrients. Within the first category essential elements as C, N, and P are required in large amounts, while the second one comprises elements such as Fe, Mo, Co, Mg etc. that are usually in traces since they are only necessary as cofactors for enzymes activity. Cultivation media are characterized by nutrient concentration adapted and adjusted with respect to the metabolic needs of the microbial species of interest, and to the environmental conditions suitable for the cultivation purpose (Arrigo, 2005).

Carbon represents the main element of microalgal biomass, equal to 50%-65% of the dry weight (Zuccaro et al., 2020). It is mainly taken up in its organic form through photosynthesis, but it is also possible to provide it as organic carbon substrate, depending on the selected production system. Indeed, the first route, which exploits light availability to fix C from the external environment is called autotrophic production, while second one is the heterotrophic cultivation, allowing, under dark regimes, to rise biomass by providing organic C sources. A third option is also available, namely mixotrophic cultivation, combining both autotrophy and heterotrophy: light and inorganic carbon are used for photosynthesis, while organic carbon for respiration (Peter et al., 2022).

Nitrogen is the second most abundant element within microalgal biomass, with a concentration equal to 1%-14% of total dry weight ("Handbook of Microalgal Culture," 2003). It is a fundamental constituent of DNA, RNA, proteins, and pigments, such as chlorophyll and phycocyanin. From an operative perspective, nitrogen is usually supplied in inorganic form, by adding nitrates, nitrites, or ammonium compounds in the medium, and sodium nitrate ($NaNO_3$) is the most frequently used supplier, but sometimes also in organic form, as urea or ammino acids. In addition to that, according to section *§1.2* diazotrophic cyanobacterial species are also capable of assimilating dinitrogen (N_2) coming from the outer environment as nitrogen

source, in a particular metabolic cycle called nitrogen fixation; this allows also to conceive culture mediums with no external nitrogen source.

The third important macronutrient in the list is phosphorus, with a concentration in biomass ranging between 0.05% to 3.3% ("Handbook of Microalgal Culture," 2003), and it is a limiting nutrient for microalgae. Several organic molecules, such as RNA, DNA, and ATP contain phosphorus, and it is usually supplied within the medium in form of ortophosphates.

1.5.2 Batch cultivation systems

Batch cultivation mode of microalgae and cyanobacteria represents the first strategy developed, as well as the most used technique implemented nowadays at industrial level. Under batch regime, biomass is allowed to grow in a close environment, relying on the applied growth factors, such as medium composition, light availability, and temperature. Along time, it is possible to denote the specific trend in figure 1.6 for a batch cultivation system, involving several peculiar phases (Wanner & Egli, 1990).

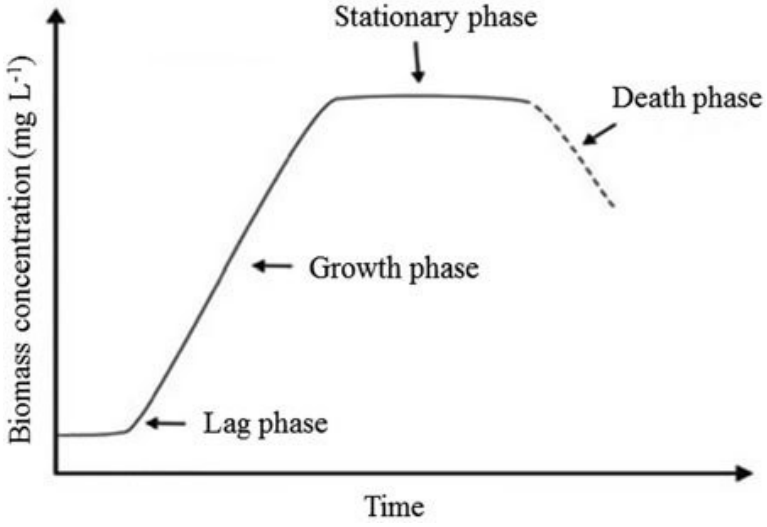

Figure 1.6. *Typical growth curve for a batch system* (Nasr, 2018).

In the lag phase, possibly occurring after inoculation, biomass is adapting to the new environmental conditions, thus no relevant increase in population number is expected. After that, biomass grows exponentially, at specific growth rate that is the maximum one μ_{max}, till reaching a stationary phase characterized by a constant concentration; usually this condition is derived by the accumulation of a side product acting as a growth inhibitor, or by limitations

derived by the consumption of a limiting nutrient. In the end, microbial cells start to die, inducing a progressive reduction in concentration (Wanner & Egli, 1990).

At an operation level, it is possible to highlight different culture systems, depending on the design features characterizing the cultivation facilities. The most important classification is between open and closed systems, also called photobioreactors (PBRs). The first ones rely on the outer environmental conditions, resulting in a more sustainable usage of natural resources, while in the seconds the conditions needed to ensure the growth are provided by artificial means, with contamination risks significantly reduced; in addition to this, depending on the equipment apparatus, they can be classified in tubular, column, and flat plate (Zuccaro et al., 2020).

1.5.2.1 Open ponds

Open tanks for biomass cultivation purposes can be characterized by different shapes, such as the circular one, representing the oldest large scale culture system, or the raceway one, the most currently used configuration, presented in figure 1.7. As a matter of fact, globally more than 80% of total biomass production is generated in open ponds, even if closed PBRs are constantly gaining much more attention, with a projected increased demand starting from 2024 (*Algae Fuel Market - Global Industry Analysis 2023*, n.d.).

A raceway tank is usually constituted by a closed loop, due to the presence of oval-shaped recirculation channels, with a depth ranging between 0.2 and 0.5 m in order to improve light penetration, and thus reducing as much as possible self-shading issues. Concerning the construction materials, they can be made of concrete, glass fiber, or membrane (Brennan & Owende, 2010). A continuous stirred environment is then provided by a paddlewheel, which ensures homogenization of the culture, prevention of thermal stratification, a more facilitated removal of oxygen generated by photosynthesis, and contributes to reduce furthermore the risk of photoinhibiton by self-shading. The major issues that affect the effectiveness of such systems mostly rely on the environment (Zuccaro et al., 2020). Indeed, there is a high risk of culture contamination, thus making such configuration not suitable for axenic cultivation purposes, and the sunlight provides a non-reliable light source to the biomass, inducing potential growth deviations with respect to design specifications. Furthermore, the huge amount of water that is requested by such systems represents another drawback that has to be

considered during an environmental and economic feasibility assessment (R. N. Singh & Sharma, 2012).

Figure 1.7. *Cultivation of Spirulina on a pilot scale in open ponds* **(Costa & de Morais, 2014)**.

1.5.2.2 Column photobioreactors

This particular category of PBRs is constituted by cylindrical equipment, that can be arranged in several configurations, based on the number of cylinders that are put in parallel. This strategy is needed to increase the surface to volume ratio of the system, solving possible shading effects that can compromise the entire quality of the cultivation. Furthermore, considering the structural features of such equipment, the radius should not exceed 0.2 m to reduce problems related to light availability in the inner regions of the bioreactor, while the height of the column cannot be greater than 4 m, in order to ensure stability to the structure itself (Zuccaro et al., 2020).

Performances and related biomass productivities are strictly related to the abovementioned geometrical features, as well as to other operating aspects: not only the light intensity represents a crucial parameter, but also the mixing efficiency that can be achieved within the reaction environment. Indeed, a mixing system helps reduce mutual shading and potential sedimentation of microalgal cells, but also creates a favorable environment for biomass growth, since it optimizes both mass and heat transfer. From an operative perspective, such condition is provided by means of a proper aeration system, and based on this, column PBRs can be classified in bubble column and airlift reactors (Zuccaro et al., 2020). With reference to

figure 1.8, the latter one allows for better mixing characteristics, due to the more complex design: bubbles of air are injected through a sparger into a draft tube, inducing the recirculation of the liquid culture through the reactor downcomers (Nitin Thukral, 2015).

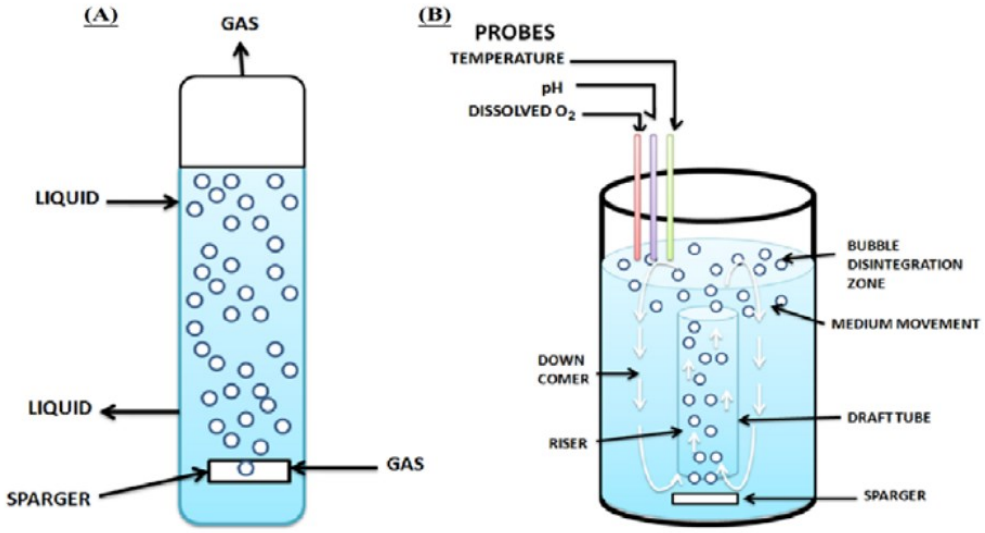

Figure 1.8. *Bubble column PBR (A) and Airlift PBR (B)* (Nitin Thukral, 2015).

Bubble size distribution is an important aspect during the equipment design, especially for the airlift PBR, as the size of the gas bubbles affect the downcomer recirculation velocity of the liquid (Pawar, 2016).

1.5.2.3 Flat-panel photobioreactors

The flat panel PBR is characterized by a cubical shape with a minimal light path (R. N. Singh & Sharma, 2012). From what concerns construction materials, usually glass or polycarbonate is implemented, in order to have surfaces that are transparent to light. Main source of light comes from artificial lamps, placed as to provide an even radiation distribution. Agitation comes both from air bubbling through spargers and/or from the implementation of a proper mechanical stirring system (R. N. Singh & Sharma, 2012).

The major advantages comprise high ratio of illuminated surface-to-area-volume, low mechanical force on cells, low energy consumption, and a high gas-liquid mass transfer, which avoids significant accumulation of oxygen within the reactor. On the contrary, fouling and cells sedimentation on the equipment walls represents a disadvantageous peculiarity, as well as difficulties on scale-up processes, due to the increase in hydrostatic pressure as the volume increases (Zhang, 2015). An equipment schematization is reported in figure 1.9 below.

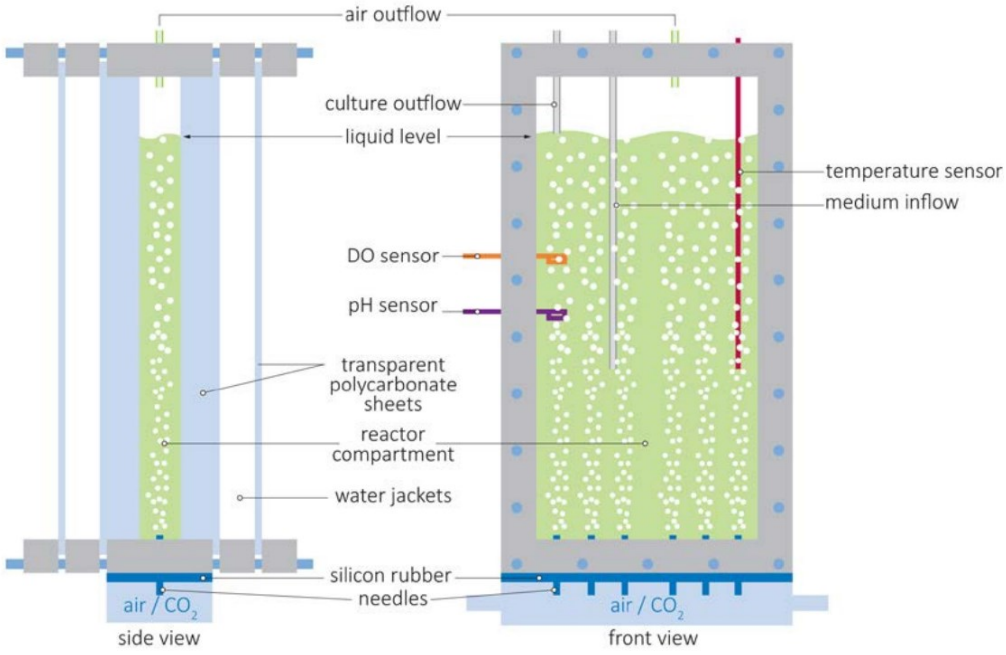

Figure 1.9. *Flat panel PBR schematization* **(**R. N. Singh & Sharma, 2012**)**.

1.5.3 Continuous cultivation systems

Nowadays, industrial bioprocesses aimed at producing microalgal biomass are mainly batch-oriented, since this technology is quite spread and known as reliable for the purpose. Anyway, it has to be acknowledged that a constant biomass productivity condition cannot be achieved, due to the nature of the reaction setting. Indeed, along the reaction time, the availability of nutrients tends to decrease as they are progressively consumed by the biomass itself, thus limiting the rate at which microbes can develop. In order to overcome such issue, researchers focus their attention on the possibility of moving microalgal cultivation to continuous systems; this ensures a more steadiness condition with respect to biomass quality and productivity, and a more sensitive system with respect to changes in the operation parameters, such as flowrate, light intensity, medium composition, pH etc. Concerning the flowrate, this represents an additional factor not included in batch operations, as presented in section *§ 1.5.2,* and its presence is due to the peculiar configuration that characterizes such novel cultivation system. The so-called chemostat bioreactor is characterized by a constant inlet and outlet flowrate, where the first one is represented by fresh medium, needed to supply enough nutrients for the growth, while the other is adopted for collecting the excess biomass produced within the

reactor. Such arrangement enables the assumption of steady-state condition, under which no accumulation within the reaction boundary is accepted. From the flowrate value, the biomass residence time, namely the time allowed for the biomass to remain with the reactor boundaries, can be modulated at the desired specification, thus influencing biomass yields and production of valuable compounds. At laboratory level, the influence of residence time on protein production in continuous cultivation in PBRs was assessed in several works: as a matter of example the study of Borella et al. (2021) discussed such effect for two cyanobacterial species, namely *Synechococcus elongatus* PCC 7942 and *Arthrospira maxima* SAG 49.88, while the one conducted by Vedana (2022) was specifically focused on *Nostoc* PCC 7120. Both provided similar results, as it was demonstrated the possibility of enhancing protein productivity to a maximum value, by just adjusting properly the residence time and preferring low values of such parameter.

Nowadays such cultivation configuration is still confined at laboratory scale, and the major bottlenecks come from the challenges arising from scale up processes, such as proper culture enlightenment, nutrients flow rate, and temperature control (Peter et al., 2022).

At the moment only few pilot plants are available and an example is a pilot plant in Japan, constituted by a set of 10 open ponds generating an overall surface of 100 m^2, in which continuous mode cultivation is implemented by using flue gases, and wastewaters as CO_2 and nutrient source, respectively (Sasongko et al., 2018). Having such enlarged scale systems allows to perform much more in-depth analysis, in order to assess operational and capital costs (Peter et al., 2022).

In terms of energy analysis, most of the power required is channeled to optimization of light distribution, proper culture mixing, and liquid-gas pumping, regardless from the PBR design (Posten, 2009). Moreover, water supply for continuous cultivation in PBRs can be a challenge to overcome in large-scale operations. Indeed, a study reports that 60% of the water consumed during microalgal cultivations in closed pilot-scale multi-tubular PBR is needed for collateral purposes, as it mainly constitutes a process utility (Martins et al., 2018).

1.6 Aim of the thesis

The reliability of cyanobacteria-based compounds, and specifically their application for the food and feed industry, depends in turn on the reliability of industrial processes, aimed at

boosting the production as much as possible to satisfy a continuously growing global demand. At the moment the majority of cyanobacteria cultivation is still confined at low scales, as several crucial bottlenecks are still unsolved. Among them, the identification of the optimal operative growth conditions covers a central role in view of biomass production and productivity assessment. So, starting from the laboratory scale, some investigations in this direction are necessary for the follow-up industrial scaling.

The aim of this thesis is to further investigate the behavior of nitrogen-fixing cyanobacteria with respect to nitrogen source and availability in medium, as well as light intensity. More specifically, the performance assessment is based on the investigation of overall culture characteristics, such as harvested biomass concentration, but also of more valuable metabolites production, for instance pigments and proteins.

From an operative perspective, the entire research process is conducted following two parallel paths: the experimental and the computational one.

The former is mainly based on experimental data collection for continuous cultivations of a particular nitrogen-fixing cyanobacterium, namely *Nostoc PCC 7120*, to assess the abovementioned effects due to variations in the operative conditions. Additionally, this evaluation stage comprises also the cultivation of this species in a pilot scale batch configuration, in order to analyze its growth performances in a larger reactor with respect to the ones usually adopted within the laboratory context.

On the other hand, the computational part is focused on modelling and simulating growth performances of two different species, namely *Anabaena* PCC 7122 and *Nostoc* PCC 7120, under nitrogen-fixing condition, understanding how vegetative and heterocystous cell population is changing with respect to the different operative conditions. The major novelty under the implemented model regards the introduction of the Droop kinetics, based on the mathematical concept of nitrogen quota.

Chapter 2

Experimental materials and methods

In this chapter, a further explanation concerning the experimental setup is provided. First of all, the species under study is presented. After that, the chapter defines various techniques implemented for cultivation purposes, along with the operating aspects involved. With respect to the latter, an in-depth overview concerning different cultivation media adopted is also presented, to understand sources and concentration of available nitrogen. From what concerns monitoring and performance analysis of cultures, the most relevant analytical techniques adopted are then highlighted.

2.1 *Nostoc* PCC 7120

The species involved in the experimental campaign is *Nostoc* PCC 7120, acquired from the Pasteur Culture of Cyanobacteria (PCC), located in Paris, France. This cyanobacterium is a filamentous diazotrophic species, capable of fixing atmospheric nitrogen for its growth and maintenance under conditions of nitrogen depletion in reactive form within the growing environment. Usually, it is considered as the reference species while assessing nitrogen-fixation process. The microorganism is kept under axenic conditions in a flask filled with $BG11_0$ medium, maintained in a thermostatic incubator at 24°C at 50 μmol m^{-2} s^{-1}. All the pre-inocula derived from that flask are then maintained in the same conditions, with the only differences concerning light intensity, around 100 μmol m^{-2} s^{-1}, and gaseous supply, through an internal bubbling system providing air enriched in CO_2 (5% v/v).

Figure 2.1. *Nostoc PCC 7120 under optical microscope*

2.2 Cultivation methods

As presented in section *§1.6,* along the experimental campaign *Nostoc* PCC 7120 was cultivated using different cultivation setups, aimed at investigating several growth aspects of this cyanobacterial species.

2.2.1 Continuous cultivation systems

The choice of continuously cultivating the species fits with the first aim of the thesis, turn to further analyze its behavior with respect to variation in operating conditions, such as nitrogen availability and source, as well as light intensity. Indeed, a continuous cultivation system represents the best option available for assessing variation in biomass production and productivity with respect to cultivation parameters, due to the peculiar steady state condition that is characterized by.

Moving to the structural aspects of the experimental apparatus, the photobioreactor resembles a flat panel photobioreactor, with a rectangular shape thus to provide an operative volume of 200 ml, as well as a sufficiently small thickness, of about 0.035 m, in order to produce a narrow path for light and reduce as much as possible self-shading phenomena. Light is allowed to pass through the reactor by means of two transparent polycarbonate plates. Internally, a mixing system is integrated through a magnetic stirrer, along with a continuous air enriched in CO_2 (5% v/v) bubbling arrangement, supplied by a pipe with a 0.2 μm filter at the beginning to prevent contaminations. These additional features are needed to provide a condition of homogeneity within the culture environment, allowing to approximate the reactor as a CSTR

system. Having such approximation is of crucial importance, since it permits to significantly reduce the complexity of the model mathematics. As a continuous system, inlet and outlet streams are present and a constant flowrate of fresh culture medium is provided, avoiding nutrient limitation, namely the most relevant disadvantage of batch systems. This is done by means of a peristaltic pump, whose speed is adjusted based on the desired flowrate through the photobioreactor. More specifically, during the whole experimental campaign, such parameter was kept constant at 184 ml day^{-1} on average, thus providing a culture residence time of approximately 1 day. Then, an overflow stream is placed at the side of the system, to collect the excess culture in an external tank and keep constant the volume inside the reactor. Since the system resembles a CSTR, the outlet stream characteristics reflect the ones inside the PBR.

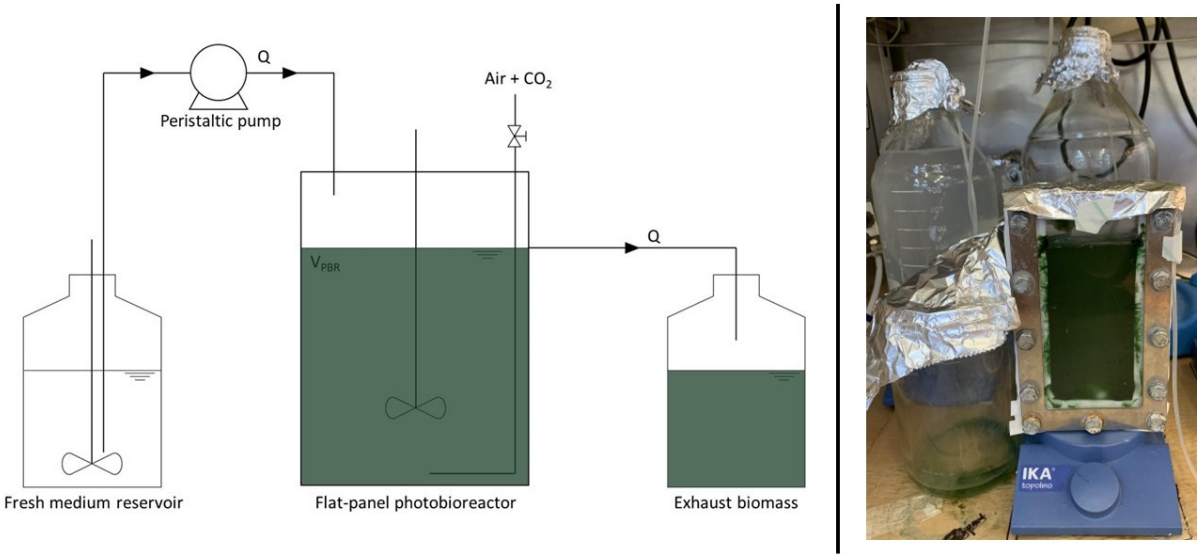

Figure 2.2. *Schematization of the continuous CSTR apparatus (left side). Actual experimental setup, with details of fresh medium supplies, flat panel PBR and outlet collecting system (right side).*

Along with the inlet flowrate, other operating parameters have to be set and controlled properly during the cultivation process. First of all, the pH is control by the bubbling system previously mentioned: the presence of additional CO_2 (5% v/v) ensures not only that the biomass is capable of carrying on all the metabolic processes needed for its growth (i.e. photosynthesis), but also the pH maintenance within the culture environment at optimum levels, around 7.5 and 8. Indeed, the CO_2 dissolved in water interacts with sodium bicarbonate molecules in culture medium to form a pH buffering system. Temperature is maintained constant inside a

thermostatic incubator at 24 °C. Constant continuous light intensity is provided by a white LED CF GROW lamp (model CXB3590-X1 supplied by CREE LED).

2.2.1.1 Light intensity

The LED lamp applied for continuous cultivation provides a continuous light within the 400-700 nm visible spectrum, according to the photosynthetic active radiation (PAR), suitable for photosynthesis. Light intensity was adjusted at the desired specification and measurements of such value were performed through a photoradiometer (HD 2102.1 from Delta OHM). Table 2.1. summarizes the conditions tested with respect to the investigated light intensities.

Table 2.1. *Investigated light intensities. The conditions marked with an asterisk refers to the work of Vedana, 2022.*

Tested condition	Light intensity [µmol m^{-2} s^{-1}]
7	100
8	300
9	400
1,2,3,4*,5*,6	550
10	1000

2.2.1.2 Medium composition: nitrogen source and availability

Nitrogen can be provided through air bubbles as molecular dinitrogen N_2 while working under diazotrophic conditions, or directly within the culture medium, in form of nitrate or ammonium. In the first case, the cyanobacterium was cultivated in $BG11_0$ medium, that reflects the composition of the standard medium BG11 (Rippka et al., 1979) except for the absence of inorganic nitrogen sources, so sodium nitrate is not supplied, and ammonium ferric citrate is replaced by iron (III) chloride. The $BG11_0$ medium composition has been further modified according to *Nostoc* sp. needs and to avoid potential nutrients limitations. In the medium used for continuous cultivation, nutrient concentration is double ($BG11_0$ 2X) compared to the standard composition, except for phosphorus whose concentration is 4-times higher. Moreover, HEPES has been replaced with sodium bicarbonate ($NaHCO_3$), in order to keep the pH ranging between 7.5 and 8, optimal for *Nostoc* sp. growth. The amount of sodium

bicarbonate has been defined according to *Nostoc* sp. needs in a previous master thesis (Vedana, 2022) and found to be equal to 250 mg L^{-1}.

Table 2.2. *$BG11_0$ 2X medium composition.*

Component	Concentration [mg L^{-1}]
$Na_2Mg\ EDTA$	2
$FeCl_3 \cdot 6H_2O$	12.43
Citric acid	12
$CaCl_2 \cdot 2H_2O$	0.1
$MgSO_4 \cdot 2H_2O$	150
$K_2HPO_4 \cdot 3H_2O$	122
H_3BO_3	5.72
$MnCl_2 \cdot 4H_2O$	3.62
$ZnSO_4 \cdot 7H_2O$	0.444
$CuSO_4 \cdot 5H_2O$	0.158
$NaMoO_4 \cdot 2H_2O$	0.782
$NaHCO_3$	250

Biomass performances with respect to nitrogen availability were investigated under diazotrophic conditions by modifying the quantity of nitrogen available in the gaseous stream bubbled within the reaction environment, so as a variation on the amount of dissolved nitrogen available in the culture environment can be perceived. Practically, such modulation was achieved by mixing the air enriched in CO_2 stream with a pure Argon stream in a t-shaped mixer, to obtain a mixture with the desired composition, expressed in volumetric fractions of the starting gaseous lines. The evaluation of the proper mixture composition was done with the aid of a bubble flowmeter.

Table 2.3. *Experimental conditions for air bubbling composition. The conditions marked with an asterisk refers to the work of Vedana, 2022.*

Tested condition	Inlet gaseous stream	N_2 concentration [% v/v]	CO_2 concentration [% v/v]	Dissolved nitrogen in medium [mg L^{-1}]
1,2,3,4*,7,8,9,10	Air enriched in CO_2	75	5.0	13.3
5*	50% Ar – 50% air mixture	40	2.5	6.7
6	60% Ar – 40% air mixture	30	2.0	5.3

On the other hand, experiments were conducted also in presence of an available reactive form of nitrogen in the culture medium (BG11). Table 2.4 summarizes tested conditions.

Table 2.4. *Modified BG11 medium with respect to nitrogen source and concentration.*

Tested condition	Nitrogen source in BG11 medium	Component concentration [mg L^{-1}]	Equivalent nitrogen concentration [mg L^{-1}]
1	$NaNO_3$	2685	442.2
2	$NaNO_3$	811	133.5
3	$NaNO_3$	362	59.7

From an operative perspective, all the media were prepared with a similar procedure: all components were mixed with deionized water and then sterilized in autoclave at 121°C for 20 minutes.

2.2.1.3 Summary of the investigated conditions

Table 2.5. *Investigated conditions summary. The conditions marked with an asterisk refers to the work of Vedana, 2022.*

	Tested condition	Diazotrophic conditions	Culture medium	Nitrogen source	Nitrogen concentration in medium [mg L^{-1}]	Light intensity [µmol m^{-2} s^{-1}]
Nitrogen source and concentration	1	*No*	BG11 2X	$NaNO_3$	442.2	550
	2	*No*	BG11 2X	$NaNO_3$	133.5	550
	3	*No*	BG11 2X	$NaNO_3$	59.7	550
	4*	*Yes*	$BG11_0$ 2X	N_2	13.3	550
	5*	*Yes*	$BG11_0$ 2X	N_2	6.7	550
	6	*Yes*	$BG11_0$ 2X	N_2	5.3	550
Light intensity	7	*Yes*	$BG11_0$ 2X	N_2	13.3	100
	8	*Yes*	$BG11_0$ 2X	N_2	13.3	300
	9	*Yes*	$BG11_0$ 2X	N_2	13.3	400
	4*	*Yes*	$BG11_0$ 2X	N_2	13.3	550
	10	*Yes*	$BG11_0$ 2X	N_2	13.3	1000

Concerning the other operative parameters, such as temperature, pH, and residence time, since their effects on biomass production and productivity were not investigated, are not reported in this summary table. Indeed, their values were kept constant along the entire experimental campaign, as previously stated in section *§ 2.2.1*.

2.2.2 Batch cultivation systems

In this work, biomass growth under batch cultivation regimes was also performed, with the aim to assess the cyanobacterium capability of adapting its growth performances in larger scales with respect to the ones usually characterizing the laboratory context. This might be useful to take a further step towards a potential industrial applicability.

More specifically, the batch cultivation was carried out in a Lgem® Lab-275 tubular glass photobioreactor. This pilot reactor is characterized by an overall capacity of 275 L: the available working volume is equal to 180 L, determined with respect to the liquid phase capacity, namely composed by biomass and culture medium together, which can reach up to 235 L also considering an additional air flow that can be injected within the system. From a geometrical point of view, it is characterized by a 65 m tubular helix, made of borosilicate glass, arranged in 12 total windings in order to optimize the available space, as well as heat and light usage. Such arrangement offers a total volume of 202 L. The remaining is occupied by the 77 L circulation vessel needed at the end of the helix for biomass collection.

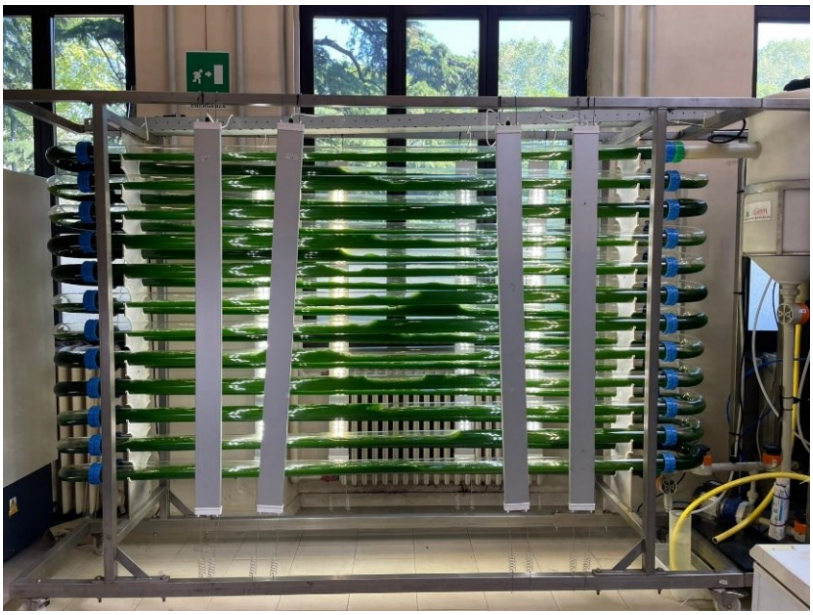

Figure 2.3. *Lgem® Lab-275 pilot batch reactor.*

Within the reactor, the culture continuous recirculation and mixing is provided by both air and liquid flow. First of all, an adjustable air flow can be injected, sustained by a diaphragm pump. The desired inlet air flowrate can be manually set within the range of 1-10 L min^{-1} through a bubble flowmeter. Secondly, the apparatus is also equipped with a Magnadrive® liquid circulation pump, to further increase mixing in the culture environment.

Culture enlightenment is provided by a set of 4 dimmable LED lamps on both reactor sides, whose light intensities can be regulated at the desired values, namely 450 µmol m^{-2} s^{-1}. Such installation is also equipped with a temperature and pH sensor.

The continuous control and setting of these operative parameters are entrusted to the software APEXfusion®. As regards pH, the installed control system is capable to maintain the measured value within a desired interval, thanks to CO_2-injection on demand. By comparing the pH setpoint value with the reactor actual one, a solenoid valve opening is continuously adjusted to modulate the inlet CO_2 flowrate in the system within the 0.5-5 L min^{-1} range, thus contrasting the occurring potential pH changes.

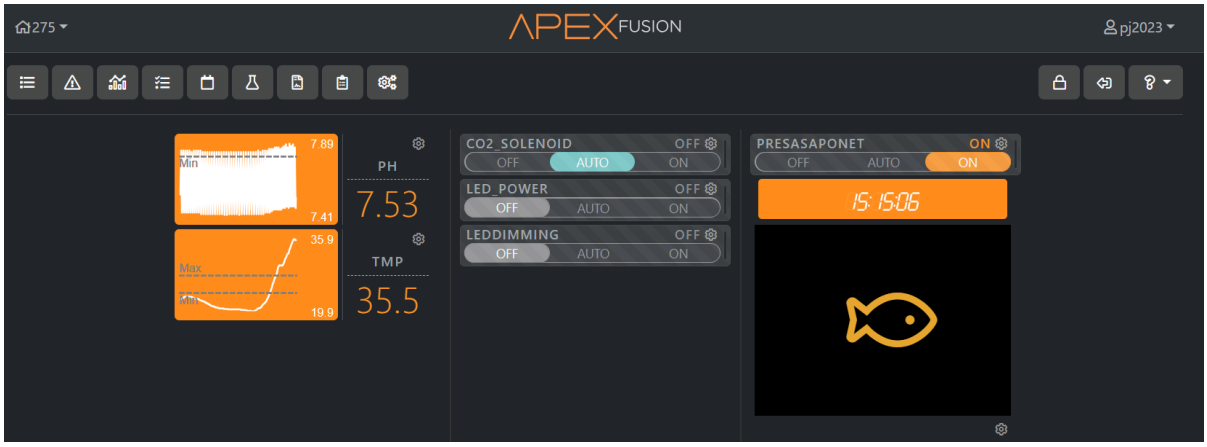

Figure 2.4. *APEXfusion® control panel.*

2.3 Culture analysis methods

The following section deepens in the description of all the techniques applied in monitoring biomass cultures performances along the various tested conditions.

2.3.1 Routine measurements: pH and OD

Measurements of pH and optical density (OD) are usually needed for daily monitoring the culture conditions. As already mentioned in section *§1.4.1.3,* optimal environment pH values range between 7.5 and 8, due to the optimum rates at which metabolic activities are carried out. According to this statement, monitoring pH can thus be a relevant aspect to consider aimed at assessing the culture quality. For the purpose, daily cultivation samples are tested with a portable pH-meter (Hanna HI 991002). Whenever a variation with respect to the optimal range occurs, the air enriched in CO_2 stream entering the reactor is manually adjusted in order to properly counteract the occurring pH variation.

Moreover, the daily sample also undergoes optical density measurements. From a theoretical perspective, the rationale behind them is to allow evaluation of biomass concentration based on the sample absorbance (A), which are directly proportional according to the Beer-Lambert law:

$$A = \varepsilon \cdot C \cdot l \tag{2.1}$$

where C represents the sample concentration, l the optical path covered by the incident light, and ε the molar attenuation coefficient, a specific constant value depending on the substance under investigation, assuming the measured absorbance to be within a 0-1 range. The measurement is performed by means of the Shimadzu® UV-1900 spectrophotometer. Whitin the instrument, two cuvettes with an optical path l of 1 cm are inserted in two distinct slots: one contains the blank, usually the culture medium, and the other one is for the sample. A light beam characterized by a user-defined wavelength of 750 nm is doubled, in order to reach both the blank and the sample of interest. Before measurements, samples have been properly diluted with culture medium to keep their absorbance within the 0-1 interval, where the Beer-Lambert law is consistent. The actual sample concentration resulted from the multiplication of the absorbance value and the dilution factor adopted. The 750nm-wavelenght is set to check solely

the diffraction of light due to suspended cells and to avoid interference from background absorption by pigments, since chlorophyll does not absorb at this wavelength.

2.3.2 Dry weight

The dry weight (DW) measurement allows to determine biomass concentration, usually expressed in terms of mass per liter of culture [g L^{-1}]. Compared to the optical density measurement performed as a fast and reliable detection method, this is much more rigorous, and it usually provides more accurate information regarding the sample concentration. Dry weight has been evaluated daily during batch cultivation and only when steady-state conditions are achieved in continuous mode, identified through a stabilization in the OD culture values. A nitrocellulose filter with pores 0.45 μm width has to be firstly dried to remove humidity, by placing it in a oven at 105 °C for at least 10 minutes, and the filter tare is determined by a precision balance (Atilon Acculab Sartorius Group®). The filter is then used for retaining the biomass coming from a known-volume sample that has to be investigated, through filtration with a vacuum pump. Again, the treated filter follows a drying phase in the oven, which takes at least 2 hours, and then its gross weight is evaluated. The biomass concentration as dry weight is then calculated through the equation (2.2). The filtered sample is also collected and stored under refrigerated conditions (-18°C) for later analysis.

$$DW = \frac{filter\ gross\ weight\ [g] - filter\ tare[g]}{sample\ volume\ [L]} \tag{2.2}$$

2.3.3 Heterocysts count and concentration

Along with the dry weight protocol, this measurement has been performed with the same frequencies highlighted in section *§2.3.2*, according to the cultivation mode. The evaluation of heterocysts population within a sample is done by a direct method, involving an optical microscope and a Bürker chamber.

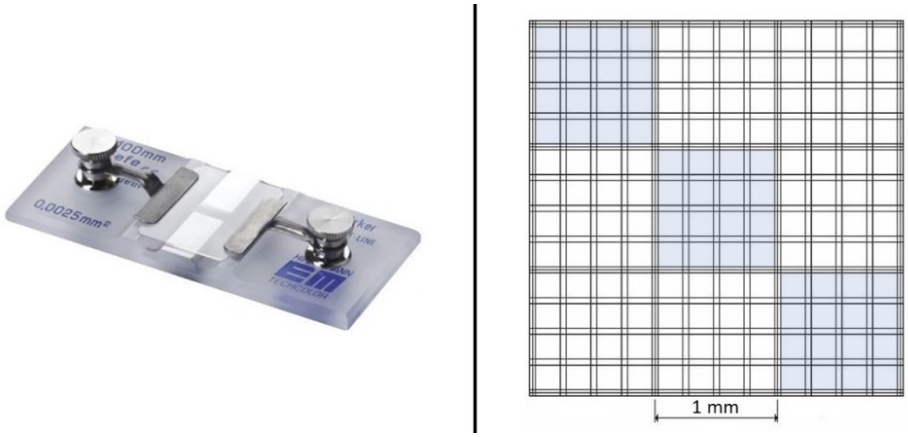

Figure 2.5. *Bürker chamber (left) and grid detail (right).*

The latter is characterized by a 9 squares grid (1 mm^2 each), divided by a triple line. Each square is in turn subdivided into 16 smaller squares (0.0025 mm^2 each) by double lines. After injecting 20 µL of the sample in the counting chamber, heterocysts number within each $1mm^2$-square along the main diagonal is determined. In order to have a rigorous approach, it is important to keep the obtained value under 100 through eventual preliminary sample dilutions, to avoid operator errors during the counting phase.

The actual heterocyst concentration is then derived starting from equation (2.3), in which D stands for the proper dilution factor eventually applied, while 10^4 represents the characteristic Bürker chamber volumetric coefficient; as its capacity is of 0.1 µL, such factor helps to express cells concentration with respect to 1 mL of culture.

$$\frac{Heterocysts}{mL} = \left(\frac{\sum Heterocysts\ per\ square}{3}\right) \cdot D \cdot 10^4 \tag{2.3}$$

After that, the value thus retrieved is used in equation (2.4), as it is multiplied by two corrective factors. The first one, namely 1.35, represents the product between heterocysts volume and density, in order to provide the conversion from cells to weight concentration. On a practical basis, it was retrieved through the manipulation of experimental data referred to several works conducted on heterocystous cyanobacteria (Bulgac, 2021; Walsby, 2007). The second factor is only needed to adjust the units of measurements in the form reported.

$$C_H\ [g_H\ L^{-1}] = \frac{Heterocysts}{mL} \cdot 1.35 \cdot 10^{-7} \tag{2.4}$$

2.4 Analytic measurements

During the various tested conditions, several features concerning cultivation quality were assessed. First of all, biomass composition was analyzed in depth through measurements of pigments, phycobiliproteins content, along with the identification of nitrogen and phosphorous amounts retained in biomass. From a nutritional perspective, the protein content was also assessed. In the end, nitrogen and phosphorous consumption were also monitored during the experiments, in order to check whether nutrients limitation conditions possibly arise.

As stated in section *§2.3.2,* the rationale under the collection of such samples follows the typology of cultivation method adopted: under continuous conditions they are gathered only during the stationary phase, while during a batch cultivation the collection becomes daily.

All the analyses were carried out in analytical double.

2.4.1 Pigments extraction and quantification

The sample extraction is performed on 1 mL of culture with a known DW value. It goes under centrifugation for 10 minutes at 13500 rpm, in order to separate biomass from supernatant, which has to be later removed. The remaining pellet is resuspended in 1 mL of Dimethylformamide (DMF), which is capable of extracting pigments out of biomass. Due to their photosensitivity, any further manipulation must be conducted away from light as much as possible. Samples can then be stored under refrigerated conditions, namely at -18°C, for at least a day, in order to complete pigments extraction phase.

To quantify the pigments content, another centrifugation at 13500 rpm for 10 minutes is needed, to separate biomass from supernatant, containing the components under investigation. Indeed, the latter is picked up, eventually diluted with additional DMF, and analyzed at the spectrophotometer, in order to reconstruct its absorption spectrum within the wavelength interval 350-750 nm. Quartz cuvettes are used for this purpose.

It is possible to derive chlorophyll *a* (Chl *a*) and carotenoids (Car) concentrations from absorbance data at specific wavelenghts according to the following equations (Wellburn, 1994):

$$Chl\ a\ [\mu g\ mL^{-1}] = (abs_{664} - abs_{750}) \cdot D \cdot \varepsilon \cdot \frac{V_{DMF}}{V_{sample}} \tag{2.5}$$

$$Car\ [\mu g\ mL^{-1}] = [(abs_{461} - abs_{750}) - (abs_{664} - abs_{750}) \cdot\ 0.04] \cdot D \cdot \varepsilon \cdot \frac{V_{DMF}}{V_{sample}} \qquad (2.6)$$

with D as the eventual dilution factor used, V_{sample} and V_{DMF} for the sample and DMF volume used for the entire analysis respectively, and ε for the specific pigment molar extinction coefficient, equal to 11.92 for chlorophyll *a* and 4 for carotenoids.

2.4.2 Phycobiliproteins extraction and quantification

Phycocyanin (PC), Allophycocyanin (APC) and phycoerythrin (PE) content for the investigated conditions was also studied. The extraction procedure is performed on 5 mL of culture, which are centrifugated for 8 minutes at 7500 rpm, in order to separate biomass from the supernatant, that is subsequently removed. Biomass pellet is resuspended in 1 mL of deionized water. Starting from that, phycobiliproteins extraction is achieved by means of 3 cycles of freezing at -18°C and unfreezing at ambient temperature, which allows breakage of microorganism cells. At the end of the third cycle, the sample is centrifugated again for 8 minutes at 7500 rpm, and the supernatant is picked up and transferred into a quartz cuvette for its absorption spectrum analysis at the spectrophotometer, within the wavelength range of 350-750. It is recommended to eventually dilute the samples to keep the absorbance spectra within the interval 0-1.

The corresponding phycobiliproteins quantification is obtained through the following equations (Bennett & Bogobad, 1973):

$$PC\ [g\ L^{-1}] = \frac{[(abs_{615} - abs_{750}) - 0.474(abs_{652} - abs_{750})]}{5.34} \cdot D \cdot \frac{V_{H2O}}{V_{sample}} \qquad (2.7)$$

$$APC\ [g\ L^{-1}] = \frac{[(abs_{652} - abs_{750}) - 0.208(abs_{615} - abs_{750})]}{5.09} \cdot D \cdot \frac{V_{H2O}}{V_{sample}} \qquad (2.8)$$

$$PE\ [g\ L^{-1}] = \frac{[(abs_{615} - abs_{750}) - \varepsilon_{PC} \cdot PC - \varepsilon_{APC} \cdot APC]}{\varepsilon_{PE}} \cdot D \cdot \frac{V_{H2O}}{V_{sample}} \qquad (2.9)$$

with ε_{PC}, ε_{APC}, and ε_{PE} representing the molar extinction coefficients for phycobiliproteins, equal to 2.41, 0.849, and 9.62 respectively for phycocyanin, allophycocyanin and phycoerythrin.

2.4.2 Phosphorus consumption: orthophosphates analysis

The protocol applied works for the identification of orthophosphates (PO_4^{3-}) concentration in a sample through a colorimetric assay, as explained by Innamorati *et. al* in Nova Thalassia vol. 11 (1990). More specifically, it is applied for culture medium and filtered samples obtained from the various conditions, in order to then retrieve an estimate of the phosphorus amount consumed by the biomass as the difference between the two.

The reaction at the basis of such colorimetric assay involves 2 mL of sample, properly diluted, and 400 µL of a specific reactant. The latter is produced according to the following receipt, expressed for 1 mL: 500 µL of 5 N sulfuric acid mixture, 100 µL of antimony potassium tartrate (1.36 g L^{-1}), 200 µL of ammonium heptamolybdate (30 g L^{-1}), and 200 µL of ascorbic acid (54 g L^{-1}). Due to the instability of such solution, it is recommended to use it within an hour. The cause under the color variation of the analyzed sample is associated to the reaction between orthophosphate ions and molybdenum, which provides a blue reaction complex, and usually takes 10 minutes to be accomplished. In order to get the actual orthophosphates concentration, the reacted samples are analyzed with a spectrophotometer with a 705 nm light beam. The absorbance values thus obtained can be then used to extrapolate the corresponding orthophosphates concentration by means of a calibration curve, obtained with test solutions at known concentrations. To have a rigorous analysis, the absorbance value obtained out of the spectrophotometer must be comprised within the calibration curve range of applicability (Figure 2.6); if such condition is not fulfilled, the sample must be further diluted with deionized water, and the final orthophosphate concentration must consider the proper dilution factor applied.

$$PO_4^{3-}\ [mg\ L^{-1}] = 7.905 \cdot abs_{705} - 0.12 \qquad R^2 = 0.997 \tag{2.10}$$

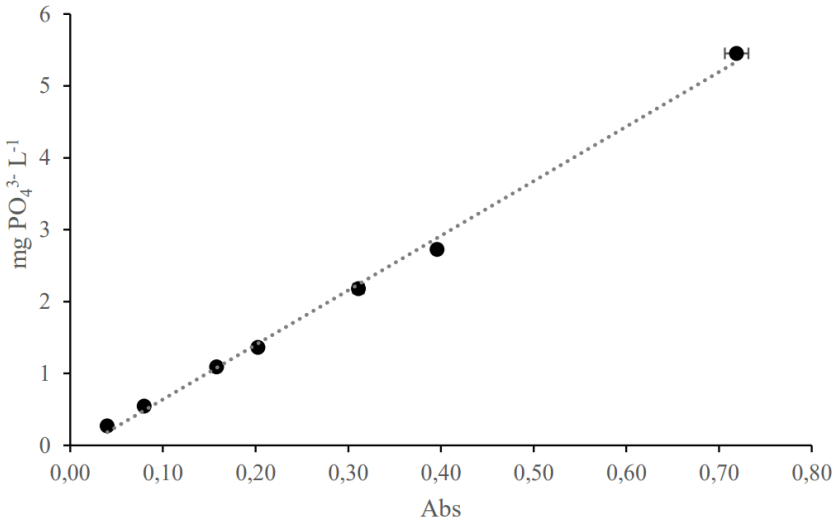

Figure 2.6. *Orthophosphate calibration curve.*

2.4.3 Phosphorus content in biomass

The evaluation of biomass phosphorus content can be carried out following the protocol developed by (Valderrama, (1981). This protocol in practice can be divided into two parts, with the first one concerning sample preparation and the following one the actual phosphorus content evaluation. The latter step is analog to the procedure explained in section *§2.4.2;* hence, this section briefly presents the preliminary part previously mentioned.

The aim is to reduce every phosphorus source into orthophosphate compounds, through acid digestion in autoclave. For this purpose, 2 mL of reagent are added to 4 mL of sample, properly diluted to have a biomass concentration equal to 150 mg L^{-1}. The reagent is composed of sodium hydroxide NaOH (9 g L^{-1}) and potassium persulfate $K_2O_8S_2$ (40 g L^{-1}). The digestion must be carried out using appropriate glass test tubes, that must be previously cleaned in acetone in order to remove every possible residue of contamination, that can alter the actual analysis outcomes. The samples are then put in autoclave at 121°C for 30 + 30 minutes, and after their cooling, it is possible to apply the orthophosphates protocol for the phosphorus content evaluation.

2.4.4 Nitrogen content assessment

Concerning investigations of nitrogen content, all samples were analyzed with the Shimadzu® TOC-LCPH instrument. From a general perspective, it is built as a total organic carbon (TOC)

analyzer, providing at the same time measures of total amount of carbon (TC) and inorganic carbon (IC); by the subtraction between such values, it is possible to derive the desired quantity. The functioning is based on the principle of catalytic oxidative combustion infrared (IR) analysis: the samples are combusted into a furnace at 680°C to form gaseous CO_2 and then moved to a non-destructive infrared analyzed (NDIR) for its quantification.

In addition to that, the instrument is also equipped with a proper apparatus for the identification of nitrogen content within an investigated liquid sample (TN), through a chemiluminescence analysis.

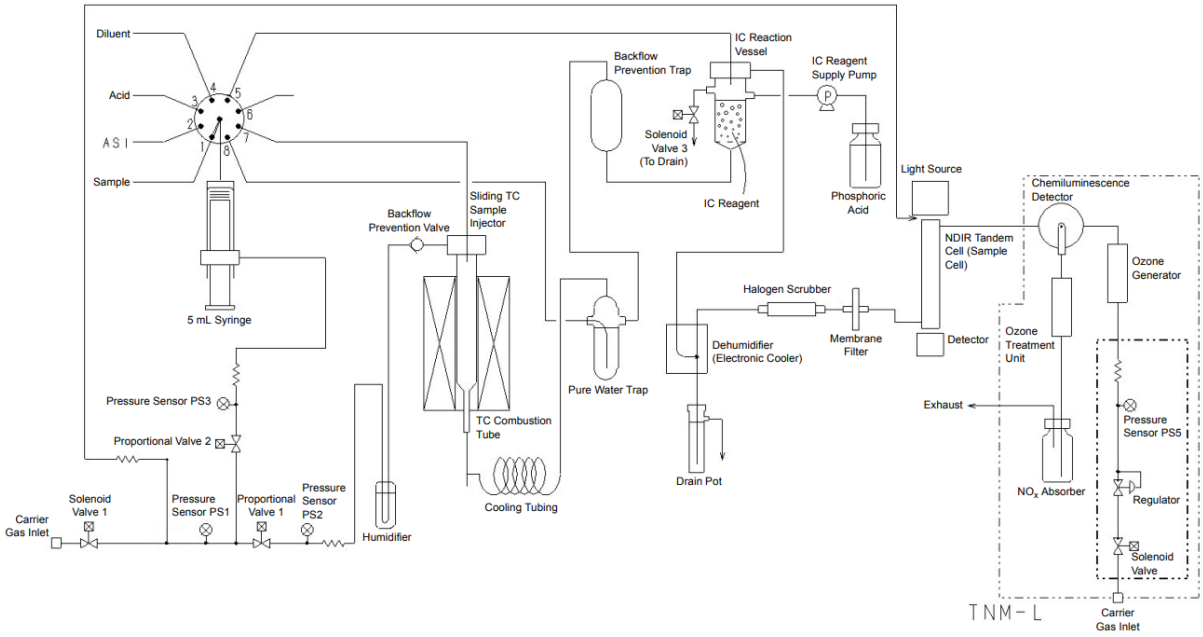

Figure 2.7. *Instrument functioning flowsheet (Shimadzu®).*

More specifically, the liquid sample is picked up by the depressurization generated from a mechanical syringe and subsequently sent to the furnace. Differently from the TOC analysis, this requires more severe conditions, as it reaches approximately 720 °C, to convert all possible nitrogen sources within the aqueous medium into gaseous nitrogen monoxide NO. Then, the gas stream goes to the specific TNM-L section of the instrument, which is in charge of its quantification by means of a chemiluminescence detector. Here, a flux of ozone enters in contact with the sampled gas thus generating the following reactions:

$$O_3 + NO \rightarrow NO_2^* + O_2 \qquad (2.11)$$

$$NO_2^* \rightarrow NO_2 + hv\ (\approx 700\ nm) \tag{2.12}$$

The molecules of NO_2^* produced by (2.11), from that excited state, tend to go back to their fundamental state by emitting electromagnetic radiations in the UV spectrum, subsequently captured by the abovementioned detector, capable of correlating their intensities with the actual NO concentration of the investigated sample.

The hardware part of the instrument comes along with also a software counterpart, namely TOC-L Sample Table Editor, to which the control of the analyzer is entrusted. From this platform, it is possible to check all the mechanical parts of the instrument, to verify the proper functioning and schedule potential maintenance interventions, as well as define experimental campaigns and run them. Regardless from the typology of analysis that is intended to perform, the instrument provides the results in terms of areas, generated through the detection of a potential disturbance provided by the sample itself from a starting baseline condition. To retrieve the desired concentration value, expressed in [mg L^{-1}], calibration curves for each typology of analysis are needed. Even if results extrapolation outside their boundaries is permissible, it is advisable to provide to the analyzer samples with coherent concentrations, in order to fit the calibration lines. So, proper preliminary dilutions may be necessary for such purpose.

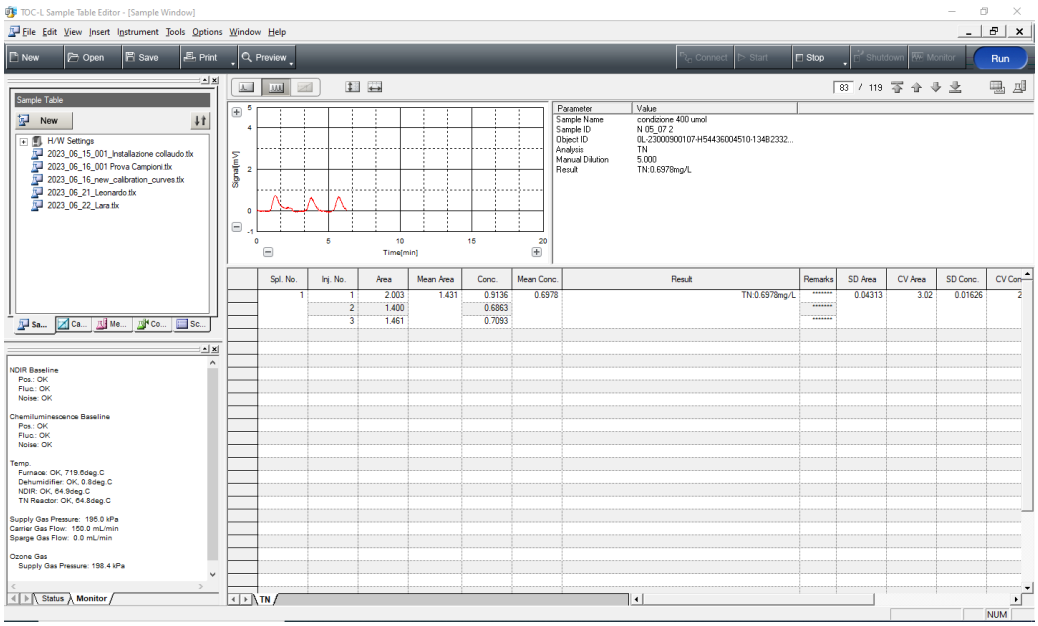

Figure 2.8. *TOC-L Sample Table editor panel (Shimadzu®).*

2.4.5 Protein content quantification

Protein content measurements are based on a specific protocol for cyanobacteria, aimed at extracting and purifying macromolecules of interest from the sampled biomass (Ivleva & Golden, 2007). The final quantification is ensured by a colorimetric analysis at the spectrophotometer.

2 mL of the desired culture are picked up and centrifugated at 13500 rpm for 10 minutes, in order to separate biomass from the culture medium, which has to be then removed. The sampled biomass undergoes another washing step, by adding 2 mL of phosphate-buffered saline (PBS) solution and lately centrifugating again at 13500 rpm for 10 minutes. At the end of the centrifugation cycle, the supernatant is removed, and biomass resuspended in 200 µL of PBS. The entire preparation procedure ends with storage under refrigerated conditions, namely at -80°C, for at least 24 hours before the analysis.

The first step for protein extraction is concerns the induction of heat stress condition to partially break cells, by putting frozen biomass into a 37 °C thermostatic bath. From this point on, it is recommended to work in ice, as the extracted proteins can degrade at ambient temperatures. Starting from the initial 200 µL of the prepared sample, 40 µL of a stock solution of phenylmethanesulfonyl fluoride (PMSF) 10 mM, and 200 µL of a lysis buffer solution are added: the first significantly increases the stability of the extracted proteins, while the second is the main responsible for protein extraction. The lysis buffer solution is constituted by dithiothreitol (DTT), ethylenediaminetetraacetic acid (EDTA), and Triton X-100, a non-ionic detergent. Furthermore, to facilitate the process of protein extraction, a quantity of glass spheres proportional to the amount of biomass under exam is added, and then mixed all together in a vortex. More specifically, this passage is organized in 10 total cycles, each one of them characterized by a 30 s agitation step, and 30 s of rest in ice, to avoid overheating conditions that can damage extracted proteins. A dilution step with further PBS solution can be also needed at this point, in order to fit within the calibration curve boundaries, and after that, a centrifugation at 1500 rpm for 1 min helps separating biomass and glass spheres from a green supernatant, standing for a raw cellular extract. The prepared solution is then tested with bicinchonimic acid (BCA) assay: 50 µL are picked up to react with 1 mL of a specific reactant. The reactive solution is composed, in volumetric fractions, by 1/50 of copper sulfate and 49/50 of BCA. From a reaction mechanism point of view, proteins reduce cupric ions Cu^{2+} to cuprous

ions Cu^{+}, which can subsequently interact with BCA and induce the characteristic purple coloration. The reaction is performed in thermostatic bath at 60°C for 15 minutes, and hereafter samples absorbance is tested with respect to a 562 nm light beam. From the calibration curve (Figure 2.9), developed by means of bovine serum albumin (BSA) solutions at known concentrations, it is possible to correlate the measured absorbance with the corresponding protein content. If a dilution was previously performed, the concentration must be at the end multiplied by the proper dilution factor.

$$BSA\ [\mu g\ mL^{-1}] = 1144.2 \cdot abs_{562} - 85.12 \qquad R^2 = 0.998 \tag{2.13}$$

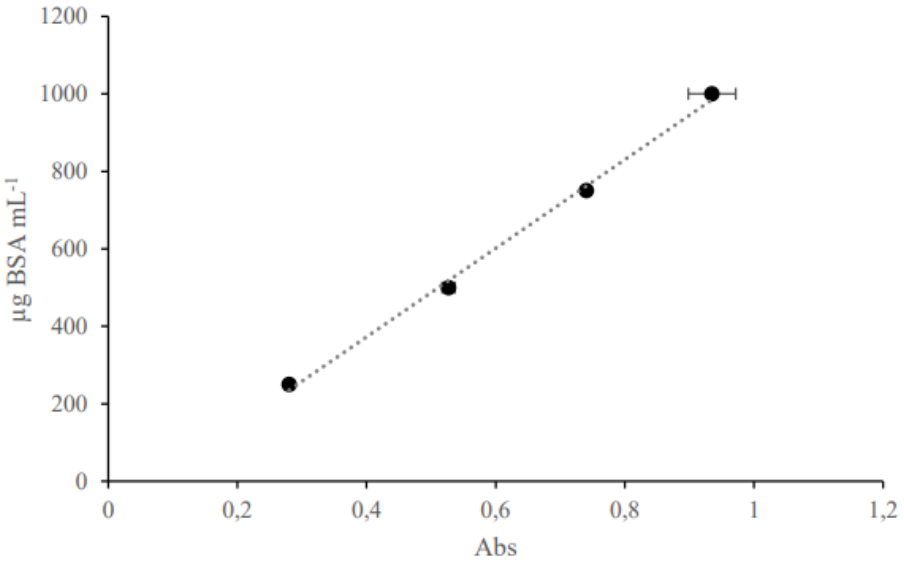

Figure 2.9. *BSA assay calibration curve.*

2.5 Statistical Analysis

In order to check the presence of statistically significant differences between the mean values of experimental data collected, the ANOVA and the Tukey's tests were applied. An important assumption linked to the test applicability regards variances among tested conditions, that must be statistically equal; whenever this was not verified, the Kruskal-Wallis test, analogous to the ANOVA for cases with unequal variances, has been implemented.

For both tests, a value equal to 0.05 was fixed as reference p-value, and performed through the aid of MINITAB® Statistical Software.

Chapter 3

Predictive model overview

One of the pillars for a successful scale up of a biomass cultivation system for industrial purposes is represented by a predictive mathematical model, aimed at forecasting the outcomes of the culture based on the input operative conditions. With respect to this subject, features like the accuracy as well as the level of detail obtained from such a model becomes relevant aspects to tackle during its development. The model presented in this chapter, accounting for the growth of nitrogen-fixing cyanobacteria *Anabaena* PCC 7122 and *Nostoc* PCC 7120, in order to satisfy the previously mentioned requests embeds the description of several phenomena occurring during culture growth. Indeed, its potentiality relies on the predictive description of both types of cells behavior within the growing environment: vegetative cells growth based on nutrients availability and differentiation process for heterocysts generation. This higher level of detail is allowed by the presence of the Droop kinetics, novelty of the model itself, introducing the concept of limiting nutrient quota. From a chronological perspective, computational efforts for describing the dynamics of heterocystous nitrogen-fixing cyanobacteria have been already made, as stated in the reference literature (Grover et al., 2019). However, also due to the different approach used for developing the corresponding mass balances, namely in terms of carbon and nitrogen exchanged between the species cells, no experimental data were available for evaluating its performances, leaving it purely theoretical. For this reason, the novel approach explained in this chapter is capable of providing simulated results that can be lately compared with the experimental evidence collected for the species under investigation.

3.1 Microbial kinetics comparison: Droop and Monod models

Describing microbial kinetics within a culture environment relies on the possibility of accurately describing the rate at which the species under exam is developing. From a

mathematical perspective, in order to furnish a consistent variable, the specific biomass growth rate μ must be introduced, namely the rate normalized with respect to biomass. Indeed, under circumstances where resources and space are unlimited, the rate of change of population (biomass in this case) is proportional to its own size (Wang et al., 2022):

$$\frac{dX}{dt} = \mu X \tag{3.1}$$

with X standing for biomass concentration in the culture environment. It has also to be acknowledged that, with respect to nutrients availability, the microbe capability of growing can differ: the larger the available concentration, the higher the specific growth rate achieved. Obviously, this correlation has a physical limit, namely the maximum specific growth rate μ_{max}, above which is not possible to register any further increase. Mathematically speaking, in 1942 Monod introduces a kinetic model capable of simultaneously accounting these aspects:

$$\mu = \mu_{max} \frac{S}{K_S + S} \tag{3.2}$$

where *S* represents the available nutrient concentration, and K_S is a specific constant with the same dimension, representing the substrate concentration allowing for a specific growth rate half with respect to the maximum one (Monod, 1942).

Due to its simplicity, the Monod model for microbial growth represents the most popular model embedded in the majority of biomass culture simulations.

The major limitation is embedded in a fundamental postulate of such model, assuming that the instantaneous change of biomass must be in constant proportion with the one in substrate (Droop, 1968), as expressed in the following equation:

$$\frac{dX}{dS} = -Y \tag{3.3}$$

and Y as the yield coefficient. The direct implication of the statement above is a constant chemical cell composition, later refuted (Ketchum, 1939). Indeed, during the experiments conducted with the algal species *Phaeodactylum tricornutum* with respect to phosphorus uptake, he experienced the phenomenon of luxury uptake: the microorganism was capable of acquiring and releasing phosphorus in a controlled environment before cell replication (Kuenzler & Ketchum, 1962). Under this condition, Monod model becomes unreliable in many cases, as the growth is not directly relatable to the nutrient concentration in medium.

To overcome this limitation, in 1968 Droop proposed its own model, introducing the concept of internal nutrient quota Q, namely the amount of nutrient of interest retained within the cell itself:

$$\mu = \mu_{max}\left(1 - \frac{Q_{min}}{Q}\right) \tag{3.4}$$

with Q_{min} as the minimum cell quota required for the basic cell structure (Droop, 1983).

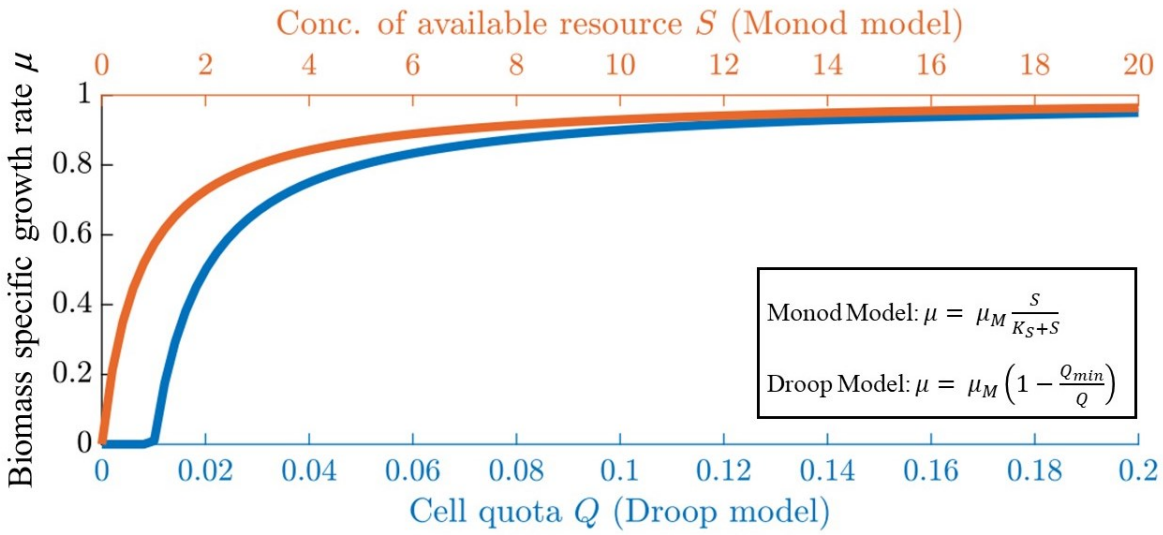

Figure 3.1. Droop and Monod model trends in comparison. For the graphical representation, $\boldsymbol{\mu_M}$ was set equal to 1, $\boldsymbol{K_S}$ equal to 0.75, and $\boldsymbol{Q_{min}}$ equal to 0.01. Adapted from Wang et al., 2022.

From a graphical perspective, the trends obtained by the different models are significantly different when the reference nutrient availability in culture medium is scarce, expressed by the substrate concentration S in the Monod form and by the nutrient quota Q in the Droop equation, respectively. When moving to greater nutrients concentrations, such difference tends to diminish, showing a similar asymptotical dynamic (Wang et al., 2022).

3.2 Model equations general structure

From a general viewpoint, with respect to the various phenomena that have to be modelled, it is possible to present the peculiar terms characterizing each equation.

First, the mass balances setting up has to be accomplished, as it follows:

$$Acc = In - Out + Gen/Cons \tag{3.5}$$

In such an equation, each term has a physical meaning and can be subsequently formulated according to the subject of the balance itself. The first term, Acc, represents the accumulation term, namely the amount of matter retained within the boundaries of the selected reference system. It is usually expressed per units of space or time, with respect to the nature of the phenomenon described, and it is thus mathematically described by a time or spatial derivative. In and Out are the input and output terms, respectively, and they are present whenever a physical flow of matter is going in, or out, the system. According to such definition, they are usually expressed as flowrates (amount of a substance passing per unit of time). In the end, the $Gen/Cons$ term accounts for eventual contributions in generating or consuming the substance covered by the balance. Starting from this form, several assumptions concerning the system peculiarities can be introduced, in order to modify the overall aspect of equation (3.5).

In accordance with the experiments performed in this work to support the model development, a chemostat reactor is considered as reference balance boundaries, and so the general shape must be accordingly remodeled. The constant flowrate characterizing this configuration implies reconsidering the previously defined accumulation term, with no expected changes with respect to the temporal coordinate. Moreover, the presence of a mixing system, ensuring homogeneity within the bioreactor, simplifies the latter as a continuously-stirred tank reactor (CSTR). The derived mathematical simplification on the mass balance concerns once more the accumulation term, with no changes with respect to any spatial coordinate allowed. To sum up, the absence of any variation with respect to both spatial and time coordinates allows to set the accumulation term Acc equal to zero. This leads to significantly reduce the complexity, as the balance degenerates in an algebraic equation. The material balance basic form is reported below:

$$0 = In - Out + Gen/Cons \tag{3.6}$$

additionally, the input term when assessing biomass can be set to zero, since the inlet flow is made of fresh medium, as stated in section *§1.5.3*.

Deeping in the details of the model, all the phenomena simultaneously modeled are introduced below. Along with vegetative cells growth within the reaction environment, the differentiation

of heterocysts from the previous ones represents the second important phenomenon to be simulated, considering the metabolism of cyanobacterial species under study. Since, as expressed in section §3.1, the model novelty regards the introduction of Droop kinetics based on nutrient quota, its behavior represents another variable to track in order to assess the overall simulation quality. Indeed, the experimental campaign was also focused on assessing the effect of nitrogen availability. All other nutrients were provided in excess to avoid growth limiting conditions, and so the quota is evaluated with respect to nitrogen only. In the end, the last phenomenon of interest concerns availability of nitrogen in medium, in order to see, from another perspective, nitrogen accumulation in biomass.

Each phenomenon is described by the correspondent equations, which are further explained in the following sections and all together contribute to constitute the overall model, composed by four nonlinear algebraic equations.

3.2.1. Vegetative cells growth

The first model equation presented accounts for the description of vegetative cells concentration C_V within a chemostat bioreactor. Considering the balance general structure depicted in section *§3.2*, it is possible to decline it for such specific elements, obtaining the following shape:

$$0 = -Out + Gen/Con \tag{3.7}$$

noticing that the input biomass term is absent, following the rationale in section *§3.2*.

The output term (Out) defines the overflow stream collecting the excess biomass at a specific concentration outside the reactor. From the mathematical perspective, the term has the dimension of a concentration ($g_V\ L^{-1}$), and is characterized by a minus sign, reflecting that the biomass is leaving the reference boundaries.

$$Out\ [g_V\ L^{-1}] = C_V \tag{3.8}$$

The other term in the mass balance ($Gen/Cons$) accounts simultaneously for the possible vegetative cell generation and consumption contributions, as presented in equation (3.9):

$$Gen/Cons\ [g_V\ L^{-1}] = \left(\mu_{max}\left(1-\frac{Q_{N,min}}{Q_N}\right)f(I) - k_{V\to H}\frac{Q_{N,max}-Q_N}{Q_{N,max}-Q_{N,min}} - \mu_{e,V}\right)C_V\tau \quad (3.9)$$

The multiplication of bracketed term by the residence time τ (d) brings the same dimension of the previous output contribution, in order to obtain a dimensionally consistent equation. Moving to the details of the various terms in equation (3.9), the first one on the left represents the actual vegetative cells generation rate r_V: it describes the velocity at which, within a chemostat configuration, the vegetative cells concentration is varying.

$$r_V\ [g_V\ L^{-1}s^{-1}] = \left(\mu_{max}\left(1-\frac{Q_{N,min}}{Q_N}\right)f(I)\right)C_V \quad (3.10)$$

Such term is characterized by the presence of two contributions, namely the one derived from Droop kinetics (Droop, 1983), and the light dependency $f(I)$. Specifically for the latter, the effect of light on vegetative cells growth can be described by a modified Haldane model (Bernard & Rémond, 2012):

$$f(I)\ [adim] = \frac{1}{L}\int_0^L \frac{I(z)}{I(z)+K_I\left(\frac{I(z)}{I_{opt}}-1\right)^2}dz \quad (3.11)$$

with L (m) as the reactor depth, I_{opt} (µmol m^{-2} s^{-1}) as the optimum light intensity for biomass growth rate, and K_I (µmol m^{-2} s^{-1}) the half-saturation constant, specific for each microbial species. $I(z)$ instead describes the trend of light availability with respect to the reactor depth coordinate z and dependent on biomass concentration C_X (g$_X$ L^{-1}), defined as the sum of vegetative and heterocyst cells. Such relationship is mathematically described by the Beer-Lambert law.

$$I(z)\ [\mu mol\ m^{-2}\ s^{-1}] = I_0 \cdot \exp\left(-k_a \cdot C_X \cdot z\right) \quad (3.12)$$

It must be remarked that the obtained trend is also dependent on the microbial species assessed, through the presence of the biomass absorption coefficient k_a (m^{-2} g^{-1}), and on the incident light intensity I_0 (µmol m^{-2} s^{-1}).

Recalling back equation (3.9), the last contribution that has to be investigated regards the potential vegetative cells consumption: from a physical point of view, it must comprise maintenance energy expenses $\mu_{e,V}$ (d^{-1}), and the rate of conversion into heterocysts $r_{V\to H}$ (d^{-1}),

according to their metabolism (Grover et al., 2019). This last term is described in equation (3.13).

$$r_{V\to H} = k_{V\to H}\frac{Q_{N,max} - Q_N}{Q_{N,max} - Q_{N,min}} \tag{3.13}$$

The dependency on the internal nitrogen quota Q_N ($g_N\ g_X^{-1}$) is considered through the corrective factor multiplying the differentiation constant $k_{V\to H}$ (d^{-1}) (Grover et al., 2019). Such term is bounded between 0 and 1, as the nitrogen quota is bounded between a minim $Q_{N,min}$, and a maximum $Q_{N,max}$ value: when Q_N reaches the minimum, the rate is maximum due to the correction factor equal to 1, while when it reaches the maximum, the rate goes to 0 as the factor drops to 0.

3.2.2 Heterocysts differentiation

The second model equation is aimed at describing the development of heterocyst cells concentration C_H from vegetative one by differentiation, as it represents the only metabolic allowable way. In a completely analogous way with respect to what has been said for vegetative cells, the starting mass balance structure is the one presented in equation (3.7), and the presentation of each term is carried out following the same rationale as before.

The term Out considers again the physical presence of the overflow stream, it has the dimension of a concentration ($g_H\ L^{-1}$), and is characterized by a minus sign, since it is leaving the bioreactor.

$$Out\ [g_H\ L^{-1}] = C_H \tag{3.14}$$

Moving then to the $Gen/Cons$ term, the heterocysts mass balance comprises only a contribution of generation, as the consumption one, namely described by the maintenance energy, is embedded within vegetative cells from which they derive. Such term is presented in equation (3.15) below.

$$Gen/Cons\ [g_H\ L^{-1}] = +\left(k_{V\to H}Y_{H/V}C_V\frac{Q_{N,max} - Q_N}{Q_{N,max} - Q_{N,min}}\right)\tau \tag{3.15}$$

The additional variable $Y_{H/V}$ represents the yield of heterocysts with respect to vegetative cells ($g_H\ g_V^{-1}$) (Grover et al., 2019). Also in this case, the growth in heterocysts concentration is

depending on the available nitrogen quota, by the correction factor presented in *§3.2.1* (Grover et al., 2019): when it reaches the maximum quota, the differentiation rate drops to 0, while when the minimum quota is reached, the rate goes to the maximum allowable value.
Again, the multiplication of the bracketed term by τ is necessary to bring consistency in the balance terms units.

3.2.3 Nitrogen quota quantification

To include the Droop kinetics in the model and derive the value corresponding to the vegetative and heterocyst concentrations within the chemostat environment, an equation describing the nitrogen quota in biomass has to be added. Contrary to the two equations described so far, this one is built with respect to a different reference system. Indeed, as the quota by definition constitutes an inner cell property, balance boundaries are set in correspondence to the cell ones. As a consequence, both input and output terms are removed from the mass balance, which thus accounts only for the generation and consumption term, reported in equation (3.16).

$$0 = +Gen/Cons \tag{3.16}$$

This term can be expressed by two contributions: one specifically for the quota generation Gen, and the other one for its progressive consumption $Cons$.
The first introduced contribution is the quota build up and it describes the uptake velocity of dissolved nitrogen in medium through biomass fixation ρ_{NF} (Grover et al., 2019).
In the equation (3.17), the maximum nitrogen uptake rate ρ_{NF}^{max} ($g_N\ g_H^{-1}\ d^{-1}$) is corrected by two factors. The first one, namely $\frac{C_N}{KN+C_N}$, is directly taken from Monod dynamics to correlate such process with the availability of dissolved nitrogen in medium (Monod, 1942). Along with the available nitrogen concentration C_N ($g_N\ L^{-1}$), the ratio also presents the half-saturation constant for nitrogen uptake K_N ($g_N\ L^{-1}$). The second factor is the same presented in sections *§3.2.1* and *§3.2.2*, which sets a correlation between the nutrient uptake and the amount already fixed within biomass: as the quota tends to the maximum value, the correction terms induce the drop of such rate to zero, while when it reaches the minimum one, the correction effect is negligible and thus the rate is maximum. Finally, since the nitrogen quota refers to the total biomass (C_X), the $\frac{C_H}{C_X}$ term is introduced to refer the nitrogen fixation to the cellular

subpopulation responsible for the process itself, namely the heterocysts. In this way, the entire term is expressed in the units of measurement reported in equation (3.17).

$$Gen = \rho_{NF}[g_N\ g_H^{-1}\ d^{-1}\ ] = \rho_{NF}^{max}\frac{C_N}{K_N + C_N}\frac{C_H}{C_X}\frac{Q_{N,max} - Q_N}{Q_{N,max} - Q_{N,min}} \tag{3.17}$$

Moving to the second term as consumption contribution, it describes the progressive reduction in the previously fixed nitrogen content due to biomass growth, and for that it is anticipated by a minus sign. As highlighted in the section *§1.5.1.4* for nutrient role in microbial growth, nitrogen represents a macronutrient essential for several metabolic activities, and the model equation focuses on the nitrogen expenses required for building vegetative cells, excluding the ones lately converted into heterocysts. This term is quite similar to the one described in equation (3.9) regarding vegetative cells mass balance:

$$Cons\ [g_N\ g_H^{-1}\ d^{-1}\ ] = \left(\mu_{max}\left(1 - \frac{Q_{N,min}}{Q_N}\right)f(I) - k_{V\to H}\frac{Q_{N,max} - Q_N}{Q_{N,max} - Q_{N,min}} - \mu_{e,V}\right)Q_N \tag{3.18}$$

3.2.4 Nitrogen content in medium

The last model equation assesses the resulting nitrogen concentration achievable within the culture medium. In this case, the balance structure for a CSTR configuration includes all the input, output, and generation/consumption terms.

Starting from the input term, it is represented by the following equation:

$$In\ [g_N\ L^{-1}\ d^{-1}] = \frac{C_N^{sat}}{\tau} \tag{3.19}$$

where C_N^{sat}($g_N\ L^{-1}$) is the inlet nitrogen concentration provided in the culture. Since the model is designed for biomass behavior under nitrogen fixation condition, no reactive forms of nitrogen are added in the medium. So, the previously mentioned variable C_N^{sat} stands for the saturation concentration of molecular nitrogen achievable in the inlet medium in equilibrium with air.

The output term, instead, is presented in equation (3.20), and it is characterized by a structure similar to the input one:

$$Out\ [g_N\ L^{-1}\ d^{-1}] = \frac{C_N}{\tau} \tag{3.20}$$

with C_N ($g_N\,L^{-1}$) as the output nitrogen concentration in medium.

In the end, the $Gen/Cons$ accounts for two distinct phenomena simultaneously. The first one, aimed at describing the increase in available nitrogen concentration, considers its solubilization in the medium aqueous solution. According to Henry's law, the gradient in concentration $C_N^{sat} - C_N$ is the process driving force, and k_{La} (d^{-1}) is the volumetric mass transfer coefficient specific for the system. The second phenomenon consists of the reduction of available nitrogen in medium due to nitrogen fixation performed by heterocysts. Mathematically, it is similar to the term in equation (3.17), with the only difference that the factor $\frac{C_H}{C_X}$ is here substituted by C_H in order to maintain consistency among the dimensions of the various contributions.

The overall shape of such $Gen/Cons$ is reported in equation (3.21).

$$Gen/Cons\ [g_N\ L^{-1}\ d^{-1}] = +\ k_{La}(C_N^{sat} - C_N) - \rho_{NF}^{max}\frac{C_N}{KN+C_N}C_H\frac{Q_{N,max}-Q_N}{Q_{N,max}-Q_{N,min}} \qquad (3.21)$$

3.3 Predictive model summary

Below, all the equations previously presented along section *§3.2* and constituting the developed model are summarized, in order to provide a general overview in its entirely.

Vegetative cells growth:

$$-C_V + \left(\mu_{max}\left(1-\frac{Q_{N,min}}{Q_N}\right)f(I) - k_{V\to H}\frac{Q_{N,max}-Q_N}{Q_{N,max}-Q_{N,min}} - \mu_{e,V}\right)C_V\tau = 0 \qquad (3.22)$$

Heterocysts differentiation:

$$-C_H + \left(k_{V\to H}Y_{H/V}C_V\frac{Q_{N,max}-Q_N}{Q_{N,max}-Q_{N,min}}\right)\tau = 0 \qquad (3.23)$$

Nitrogen quota quantification:

$$\rho_{NF}^{max}\frac{C_N}{K_N+C_N}\frac{C_H}{C_X}\frac{Q_{N,max}-Q_N}{Q_{N,max}-Q_{N,min}} - \left(\mu_{max}\left(1-\frac{Q_{N,min}}{Q_N}\right)f(I)) - k_{V\to H}\frac{Q_{N,max}-Q_N}{Q_{N,max}-Q_{N,min}} - \mu_{e,V}\right)Q_N = 0 \qquad (3.24)$$

Nitrogen content in medium:

$$\frac{C_N^{sat}}{\tau} - \frac{C_N}{\tau} + k_{La}(C_N^{sat} - C_N) - \rho_{NF}^{max}\frac{C_N}{K_N+C_N}C_H\frac{Q_{N,max}-Q_N}{Q_{N,max}-Q_{N,min}} = 0 \qquad (3.25)$$

The model thus presented is a four non-linear equations system and four different unknown variables can be underlined: C_V, C_H, Q_N, and C_N. This allows to have a system characterized by

a number of degrees of freedom equal to 0: such value is by definition obtained as the difference between the number of available equations and the number of unknowns to be determined. According to this feature, the system itself can be defined as exactly specified, namely a system capable, once solved, of providing a single exact solution. Even if the theory brings to such a conclusion, actually the system resolution is quite challenging. Indeed, the model complexity does not really depend on the mathematical structure of the equations, but relies in the presence of several unknown parameters, whose values are necessary to be determined.

3.4 Unknown model parameters and optimization routine

As just introduced, along with the unknown variables characterizing the model, there is also the presence of additional parameters, whose values have to be defined, as they are specific for each investigated species (Grover et al., 2019). These parameters are summarized in table 3.1.

Table 3.1. *Predictive model unknown parameters.*

Parameter	Units of measurement	Definition
$\boldsymbol{Q_{N,min}}$	$g_N\, g_X^{-1}$	Minimum nitrogen quota
$\boldsymbol{k_{V\rightarrow H}}$	d^{-1}	Differentiation constant
$\boldsymbol{\rho_{NF}^{max}}$	$g_N\, g_H^{-1}\, d^{-1}$	Maximum nitrogen fixation rate
$\boldsymbol{Y_{H/V}}$	$g_H\, g_V^{-1}$	Yield heterocyst – vegetative cells
$\boldsymbol{\mu_{e,V}}$	d^{-1}	Vegetative cells maintenance energy

The major problem connected to these unknown parameters is related to the lack of reliability of the resulting model outcomes. Indeed, based on the obtained numbers, a wide range of potential suitable solutions can be retrieved. In order to reduce as much as possible such issue, it is fundamental to find, along with the investigated variables, the correct values also for these introduced parameters. In practice, this is done by fitting them to experimental data, so that the parameters values obtained are such as to simulate the experimental data as reliably as possible. Such approach highlights the relevant part played by experimental campaigns while assessing

a mathematical model, as they are mandatory preliminary steps for a successful model development.

The system equation resolution and the simultaneous model parameters fitting were entrusted by means of MATLAB® scripts, due to the overall problem complexity. Moreover, with respect to the latter problem task, it is relevant to present the implemented optimization routine such that it was possible to accomplish the desired objective. In other words, an optimization routine is used to determine the optimal solution for a particular problem. Specifically for the case under study, the optimal solution, in the form of a vector containing the assessed parameter values $\boldsymbol{p}$, must be the one capable of reducing as much as possible an objective function, developed in the following way:

$$OF = \sum_{i=1}^{n} \left(err_{rel,i}\right)^2 = \sum_{i=1}^{n} \left(\frac{y_i - f(x_i, \boldsymbol{p})}{f(x_i, \boldsymbol{p})}\right)^2 \tag{3.26}$$

As presented in equation (3.26), the objective function implemented is based on the least squares optimization approach, where the final aim is to minimize as much as possible the summation resulted from the squared errors built from experimental y_i and computational data $f(x_i, \boldsymbol{p})$. The errors are calculated using the independent variables x_i and fitted model parameters. From a theoretical perspective, the actual algorithm is usually furnished with absolute errors, namely as their simple difference. Since here the optimization problem involves equations, whose independent variables are characterized by significant differences in terms of order of magnitude, to equalize their weights and provide an algorithm capable of simultaneously fitting accurately data for all the available equations, the introduction of relative errors within the objective function turned out to be effective for this purpose.

In the end, the selection of the suitable vector of fitted parameters was not only entrusted to the objective function minimization, but it was also supported by the evaluation of the determination coefficients R^2, one for each independent variable. In statistics, it provides a measure of how well observed outcomes are replicated by the model, based on the proportion of total variation of outcomes explained by the model (Heinisch, 1962). Such coefficients evaluation is performed according to equation (3.27).

$$R^2 = 1 - \frac{SS_{res}}{SS_{tot}} \tag{3.27}$$

Concerning the term at the numerator, namely SS_{res}, it represents the residuals sum of squares, and basically defined as the sum among the squared residuals, as presented in equation (3.28).

$$SS_{res} = \sum_{i=1}^{n} \left(err_{abs,i}\right)^2 = \sum_{i=1}^{n} (y_i - f(x_i, \boldsymbol{p}))^2 \tag{3.28}$$

The term at the denominator, SS_{tot}, representing the total sum of squares, is proportional to the variance of the data, as evaluated according to equation below:

$$SS_{tot} = \sum_{i=1}^{n} (y_i - \bar{y})^2 \tag{3.29}$$

with $\bar{y}$ as the mean of observed data.

$$\bar{y} = \frac{1}{n} \sum_{i=1}^{n} y_i \tag{3.30}$$

Such coefficients usually ranges between 0 and 1: as the values gets closer to 1, the reliability of the model, in terms of both independent variables and fitted parameters values, becomes more solid.

Chapter 4

Computational results for *Anabaena* PCC 7122 species

As the experimental results for *Anabaena* PCC 7122, a filamentous heterocystic nitrogen-fixing cyanobacterium, were already discussed in previous master thesis works (Bulgac, 2021; Borella, 2017), this chapter will focus only on the computational results regarding the predictive model application on such experimental data.

First of all, a general overview of the available data is provided, with the identification of all the known additional model parameters for such species, retrieved by means of laboratory observations. After that, the computational results obtained are presented: along with the simulated data, also the fitted model parameters introduced in section *§3.4* are reported, and critically discussed.

4.1 Experimental data overview

The data collected along the two previously quoted works comprises the assessment of such species behavior, cultivated under continuous conditions in flat panel chemostat bioreactors, with respect to different residence times and to fixed light conditions. The results obtained are reported in terms of vegetative cell and heterocyst concentrations. Additionally, since the species is capable of fixing molecular dinitrogen, the behavior assessment was conducted also by analyzing the nitrogen content embedded in biomass along the various tested conditions. Below, all the data collected are summarized and grouped in specific sections with respect to the tested continuous light intensity, namely 190, 350, and 550 μmol m^{-2} s^{-1} provided by a LED PAR lamp.

4.1.1 Species behavior at 190 µmol m^{-2} s^{-1}

The investigation of *Anabaena* PCC 7122 behavior at 190 µmol m^{-2} s^{-1} at different residence times was conducted during the master thesis work of Borella, 2017. The obtained results are summed up in table 4.1.

Table 4.1. *Experimental results for Anabaena PCC 7122 in response to different residence times at 190 µmol m^{-2} s^{-1}* (Borella, 2017).

Residence time [d]	Vegetative cells concentration [g_V L^{-1}]		Heterocystous cells concentration [g_H L^{-1}]		Nitrogen quota in biomass [g_N g_X^{-1}]	
	Mean	Std. dev	Mean	Std. dev	Mean	Std. dev
1.3	0.429	0.082	0.041	0.008	0.058	0.004
1.6	0.620	0.067	0.090	0.008	0.064	0.006
2.5	0.814	0.062	0.106	0.014	0.074	0.009
2.9	0.732	0.078	0.118	0.013	0.057	0.008
3.7	0.823	0.043	0.137	0.015	0.061	0.002
4.6	0.958	0.076	0.172	0.012	0.074	0.012

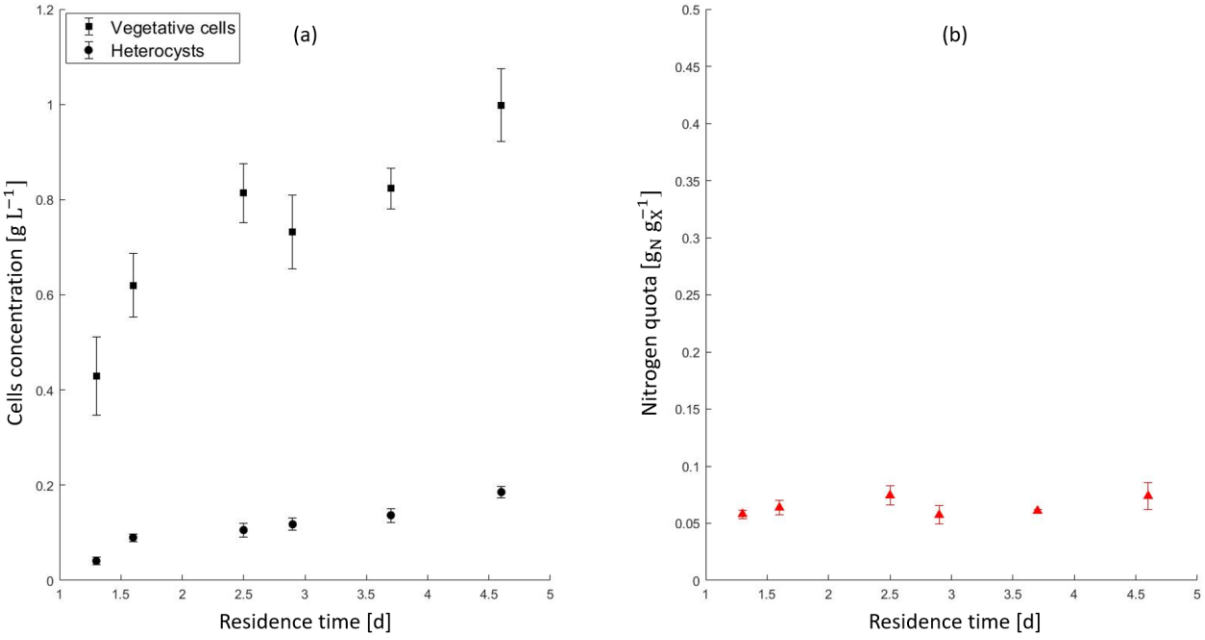

Figure 4.1. *Experimental cell concentration (a) and nitrogen quota (b) trends over residence time for Anabaena PCC 7122 at 190 µmol m^{-2} s^{-1}* (Borella, 2017).

4.1.2 Species behavior at 350 µmol m^{-2} s^{-1}

The species performances under an incident light intensity of 350 µmol m^{-2} s^{-1} were studied in the work of Bulgac, 2021, and the results presented in table 4.2 and figure 4.2.

Table 4.2. *Experimental results for Anabaena PCC 7122 in response to different residence times at 350 µmol m^{-2} s^{-1}* (Bulgac, 2021).

Residence time [d]	**Vegetative cells concentration [g_V L^{-1}]**		**Heterocystous cells concentration [g_H L^{-1}]**		**Nitrogen quota in biomass [g_N g_X^{-1}]**	
	Mean	Std. dev	Mean	Std. dev	Mean	Std. dev
0.8	0.366	0.048	0.092	0.023	0.051	0.004
1.5	0.572	0.098	0.102	0.027	0.064	0.009
2.3	0.767	0.046	0.139	0.030	0.074	0.005
3.0	1.070	0.081	0.139	0.007	0.062	0.009

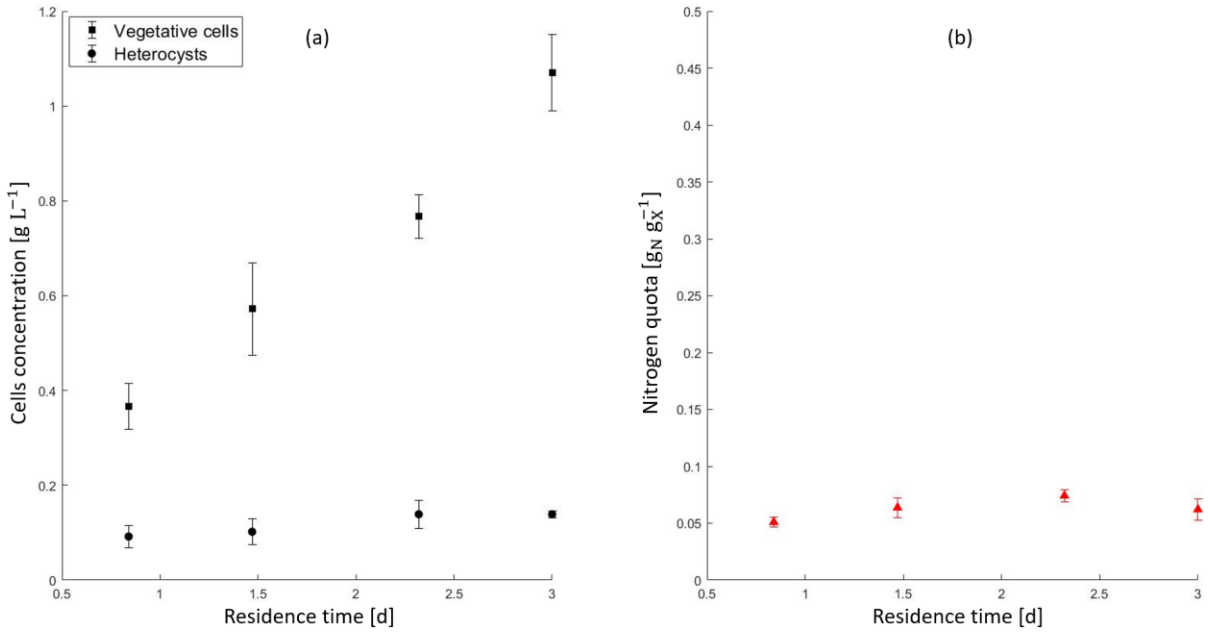

Figure 4.2. *Experimental cell concentration (a) and nitrogen quota (b) trends over residence time for Anabaena PCC 7122 at 350 µmol m^{-2} s^{-1}* (Bulgac, 2021).

4.1.3 Species behavior at 550 µmol m^{-2} s^{-1}

In the end, the last dataset is reported in table 4.4 and illustrated in figure 4.4 below. In this case, biomass was continuously cultivated at an incident light intensity of 550 µmol m^{-2} s^{-1}, thus obtaining the following results with respect to different residence times for vegetative cells and heterocysts, as well as for nitrogen quota (Bulgac, 2021).

Table 4.4. *Experimental results for Anabaena PCC 7122 in response to different residence times at 550 µmol m^{-2} s^{-1}* (Bulgac, 2021).

Residence time [d]	**Vegetative cells concentration [g_V L^{-1}]**		**Heterocystous cells concentration [g_H L^{-1}]**		**Nitrogen quota in biomass [g_N g_X^{-1}]**	
	Mean	Std. dev	Mean	Std. dev	Mean	Std. dev
0.8	0.507	0.205	0.102	0.043	0.057	0.008
1.5	0.869	0.081	0.166	0.031	0.067	0.005
2.3	1.038	0.122	0.150	0.046	0.062	0.009
3.0	1.312	0.074	0.192	0.036	0.071	0.001

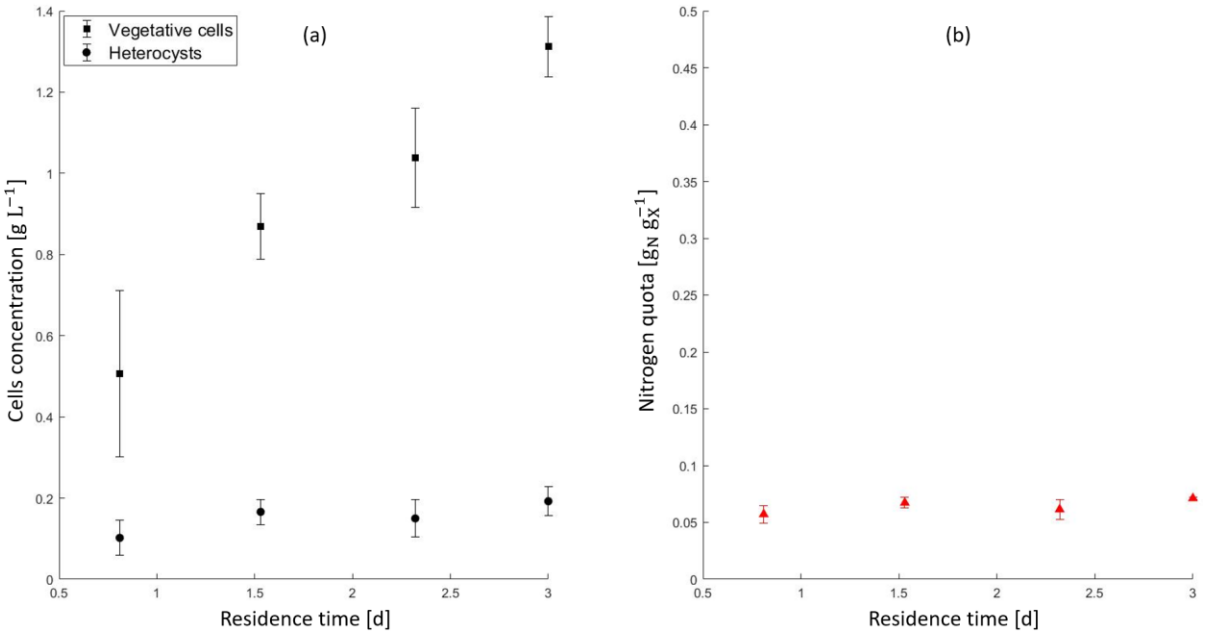

Figure 4.4. *Experimental cell concentration (a) and nitrogen quota (b) trends over residence time for Anabaena PCC 7122 at 550 µmol m^{-2} s^{-1}* (Bulgac, 2021).

4.2 Additional model parameters identification

In order to reduce the computational complexity associated with the model system resolution as much as possible, it is necessary to preliminary saturate some unknown parameters with experimentally-derived values from previous works. This procedure allows then to come up with a model characterized by the set of still unknown parameters listed in section *§3.4,* for which the fitting procedure must be applied. The parameters derived with such rationale are listed in table 4.5.

Table 4.5. *Experimentally derived model parameters* (Bulgac, 2021)*,* (Borella, 2017)*,* (Grandi, 2018)*.*

Parameter	Value	Units of measurement	Definition
I_{opt}	270	μmol m^{-2} s^{-1}	Optimum light intensity
K_I	97	μmol m^{-2} s^{-1}	Modified-Haldane model half saturation constant
K_N	0.0029	g_N L^{-1}	Monod model half saturation constant
μ_{max}	8.22	d^{-1}	Maximum specific biomass growth rate
k_{La}	123.36	d^{-1}	Volumetric mass transfer coefficient
k_a	0.145	m^{-2} g^{-1}	Biomass light absorption coefficient

Concerning the first four parameters, already presented along section *§3.2*, respirometric tests represent a valuable tool in assessing their values for the specific species under study. Indeed, such experimental protocol is based on the possibility to measure oxygen production and consumption rate by a microalgal culture under controlled conditions, in order to retrieve all the kinetic parameters connected to nutrient, temperature, and light intensity influence (Sforza et al., 2019).

Moving to the volumetric mass transfer coefficient, as presented in section *§3.2.4*, it is needed while investigating the amount of nitrogen able to move from the gaseous phase within the air bubbles to the liquid medium phase, thus providing the actual nitrogen concentration available to biomass. Moreover, it is an important parameter to account for while scaling up an aerated bioreactor (Aroniada et al., 2020). The adopted method is the so-called static gassing-out technique: dissolved oxygen is firstly removed from the liquid phase by bubbling an inert gas, until its concentration drops to zero, and then is reintroduced in order to measure its new

content increase. The measurements are usually done by means of an oxygen probe (Cerri et al., 2016).

In the end, the biomass light absorption coefficient, namely k_a, modulates the amount of photons absorbed by a certain biomass concentration starting from a known incident light intensity. The mathematical relationship under such phenomenon is reported in equation (3.12), which is useful to extrapolate the desired parameter value. Indeed, through the logarithmic linearization of this equation, is possible to linearly correlate light intensity with corresponding biomass concentration, through k_a as its slope.

4.3 Modeling results

4.3.1 Fitted model parameters

With the rationale expressed in section *§3.4*, the parameters still unknown were fitted based on the experimental data collected. For such operation, datasets at 190 and at 550 μmol m^{-2} s^{-1} were combined in order to enlarge as much as possible the amount of data on which running the optimization routine. As a general rule, the starting guessed parameters were set unbounded, with some particular exceptions regarding $Q_{N,min}$ and $Y_{H/V}$, for which consistent lower and upper bounds were fixed. Indeed, for the $Q_{N,min}$ parameter a constraint was introduced, as its fitted value must not overcome the 4% threshold. The selection of this value reflects critical considerations based on the experimental evidence accumulated so far. In addition, such value is reasonable when compared with the literature, even if the interspecies variability must be considered (Barbera et al., 2022). In the case of $Y_{H/V}$, the parameter was constrained between 0 and 0.99, as by definition it represents a yield. The resulting values are listed in table 4.6.

Table 4.6. *Fitted model parameters values.*

Parameter	Value	Units of measurement	Definition
$Q_{N,min}$	0.009	$g_N\ g_X^{-1}$	Minimum nitrogen quota
$k_{V\rightarrow H}$	3.067	d^{-1}	Differentiation constant
ρ_{NF}^{max}	0.990	$g_N\ g_H^{-1}\ d^{-1}$	Maximum nitrogen fixation rate
$Y_{H/V}$	0.086	$g_H\ g_V^{-1}$	Yield heterocyst – vegetative cells
$\mu_{e,V}$	1.015	d^{-1}	Vegetative cells maintenance energy

From a graphical perspective, the fitting quality obtained through such fitted parameters, is captured in figure 4.5.

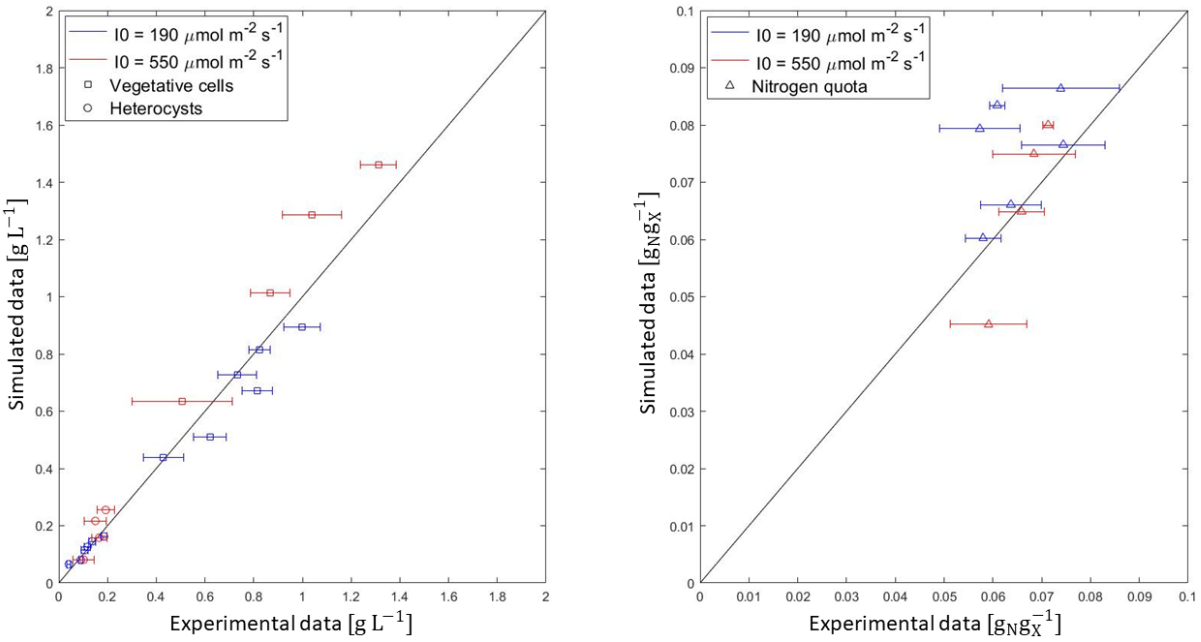

Figure 4.5. *Parity plots for simulated and experimental data.*

4.3.2 Model validation and $Q_{N,max}$ sensitivity analysis

While developing a predictive model, once the unknown parameters are fitted, it is important to investigate their goodness. This is usually done through a validation procedure, aimed at assessing the model quality on different datasets with respect to the ones previously implemented in the fitting routine. For this purpose, experimental data for the species behavior at 350 μmol m^{-2} s^{-1} with respect to different residence times was taken into account. At a computational level, this is achieved by running the simulation with all the parameters already

fixed, and by just solving simultaneously the model equations in section *§3.3.* Even if the CSTR configuration used as reference suggests a set of nonlinear algebraic equations, its conventional resolution with fsolve function in MATLAB® lead to some numerical issues. Therefore, such system was solved dynamically using *ode23s* function, and the corresponding steady-state solutions at different residence times selected.

It has to be acknowledged that the entire fitting process in section *§4.3.1* was carried out by using a value equal to 0.1 $g_N\ g_X^{-1}$ for the maximum nitrogen quota. As for $Q_{N,min}$, this value has to be considered as an initial guess, empirically derived from the experimental evidence. Moreover, its irrelevance with respect to the retrieved fitted parameters array through has been ascertained. The identification of the most accurate value for such term was performed by means of a sensitivity analysis embedded into the material balances resolution routine. The parameter was allowed to range between 0.08 and 0.12 $g_N\ g_X^{-1}$, and used for the model resolution. Then, the identification of the most suitable value for $Q_{N,max}$ was done by comparing the resulting correlation coefficients, evaluated for each dataset separately.

Table 4.7. *Derived correlation coefficients for each dataset as sensitivity analysis results for* $\boldsymbol{Q_{N,max}}$.

Light intensity $[\mu mol\ m^{-2}\ s^{-1}]$	$Q_{N,max}$ *value* $[g_N\ g_X^{-1}]$				
	0.08	*0.09*	*0.10*	*0.11*	*0.12*
190	0.9776	0.9757	0.9702	0.9642	0.9567
350	0.8965	0.8990	0.9021	0.9054	0.9087
550	0.9515	0.9540	0.9569	0.9598	0.9625
Average	**0.9419**	**0.9426**	**0.9430**	**0.9431**	**0.9426**

The reported averages, evaluated as the means of all the datasets correlation coefficients at a specific $Q_{N,max}$ value, shows 0.11 $g_N\ g_X^{-1}$ as the suitable value in order to provide the most reliable model with respect to the experimental data collected.

In the end, according to the set of fitted parameters in section *§4.3.1* and the resulted value for $Q_{N,max}$, the model extrapolates the behavior of vegetative cells, heterocysts, and nitrogen quota with respect to different simulated residence times. In the following figures such trends are

reported for each assessed light intensity, also compared with the data collected out of the experimental campaigns.

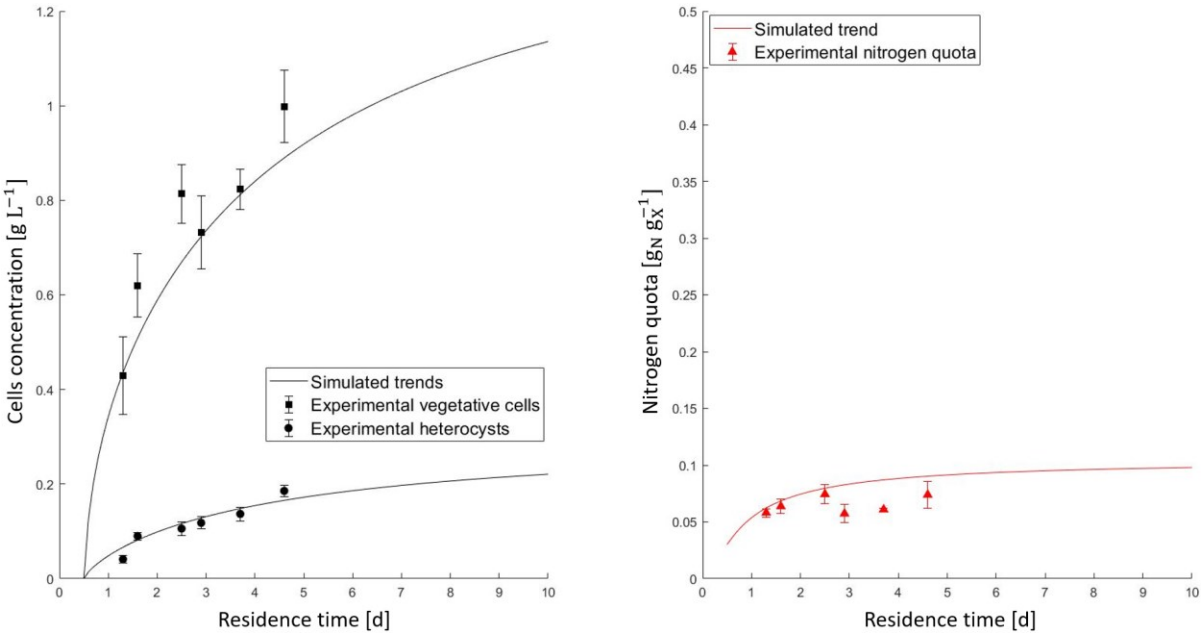

Figure 4.6. *Computational results for Anabaena PCC 7122 at 190 µmol m^{-2} s^{-1}.*

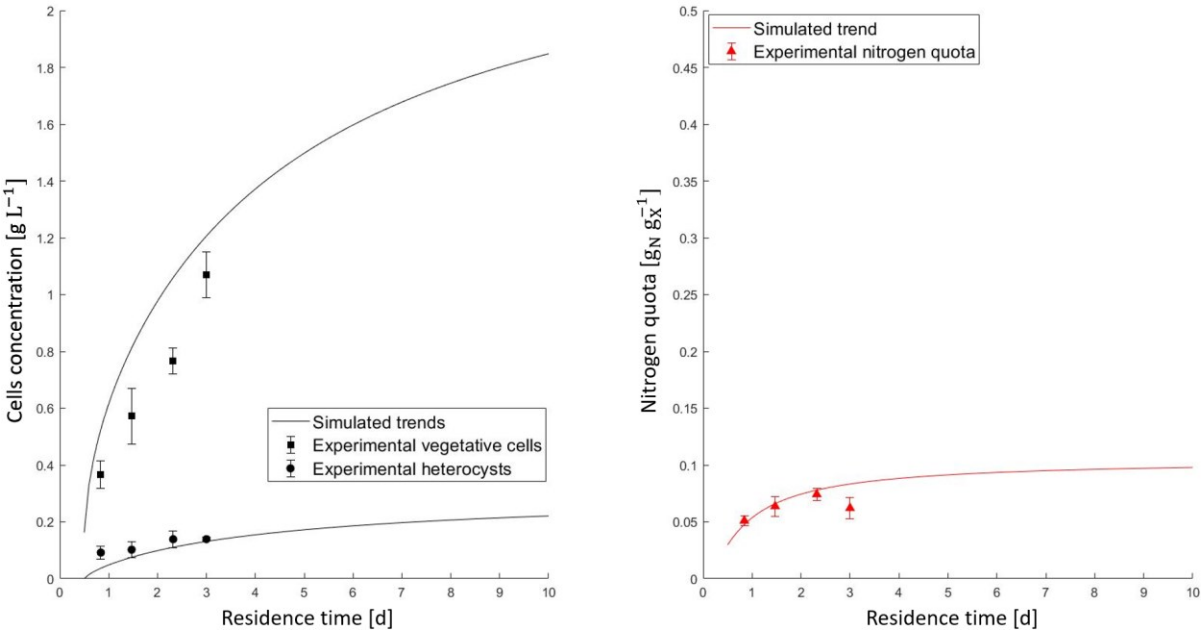

Figure 4.7. *Computational results for Anabaena PCC 7122 at 350 µmol m^{-2} s^{-1}.*

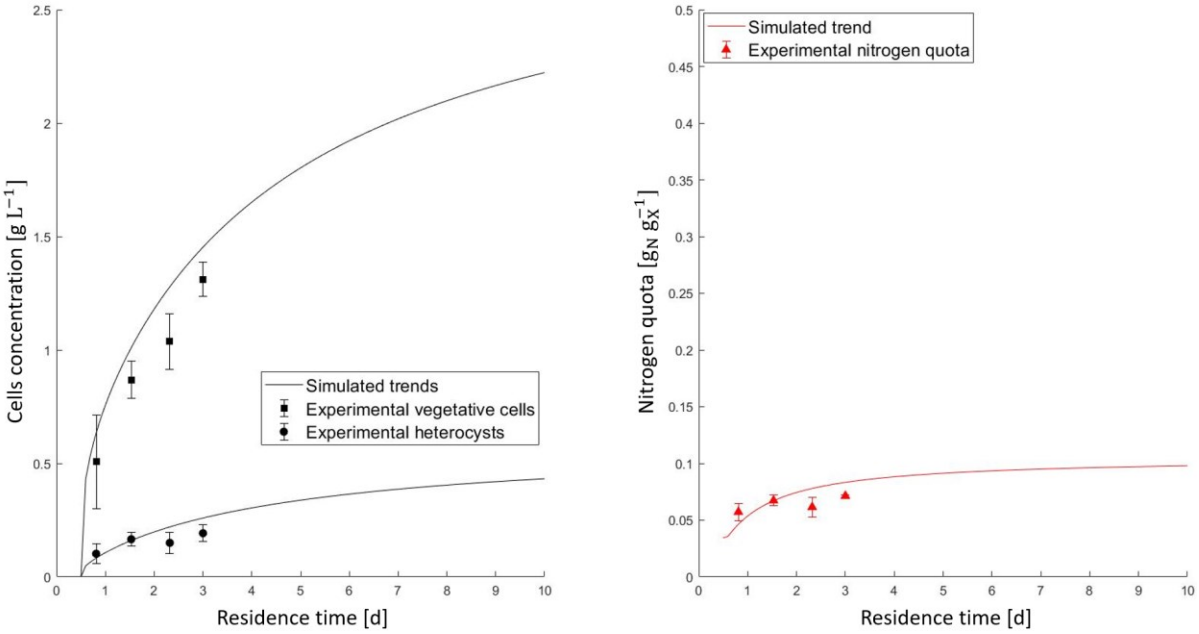

Figure 4.8. *Computational results for Anabaena PCC 7122 at 550 µmol m^{-2} s^{-1}.*

From a qualitative perspective, for each plotted independent variable is possible to perceive an asymptotical trend: starting from a general increase at low residence times, while at higher values no further variations are expected. This outcome may be due to the intrinsic nature of the culture system, which tends to be progressively more similar to a batch operation as τ increases. Therefore, under the latter mentioned conditions, a reduction of fresh medium supply becomes more evident, and in turn this negatively affect the availability of nutrients required for metabolism and, ultimately, for biomass growth.

Specifically for the vegetative cells concentration, this behavior can be explained by the initial rapid increase in nitrogen quota, allowing a biomass build up at a faster rate. Then, the stabilization of the embedded limiting nutrient at higher residence times induces a progressive slowdown. At this point, due to upper bound provided by $Q_{N,max}$, limiting the total nutrient expendable for biomass growth, and the maintenance contribution, no longer variations with respect any residence time value are expected.

Similarly, the discussion can be extended to heterocystous cells: an initial rapid accumulation of heterocysts can be pointed out, according to the variation in nitrogen quota, and then a stabilization for higher residence times occurs, due to a reduced need for nitrogen fixation. From a biological perspective, since vegetative cells tends to stabilize, the only reason to fix

molecular dinitrogen may be only for maintenance purposes, and so an accumulation of such differentiated cells is not further needed.

Moreover, it is important to highlight the different shapes of the same asymptotical trends described so far for vegetative and heterocystous cells. This represents a great achievement with respect to the earlier stages of the model development, where the two simulated trends were almost identical and thus preventing a satisfying fitting for heterocysts experimental data. For this specific issue, the introduction of a differentiation constant $k_{V\rightarrow H}$ directly dependent on the variations in nitrogen quota represents the turning point of the entire modelling process, as reported in the work of Grover et al., 2019.

It is also necessary to make some considerations regarding the values for the model parameters in tables 4.6 and 4.7, specifically derived through the computational approach presented earlier. Starting from $Q_{N,max}$, the 0.11 $g_N\ g_X^{-1}$ obtained does not only meet the numerical aspect of the problem, but it also accommodates the biological level. In general terms, the assessment of model parameters values also from the latter perspective covers an important role in the overall development, since it is important to remember the practical application to which such model is aimed at. Indeed, for the specific case of the maximum nitrogen quota, the corresponding value satisfies both levels, as it provides a good quality of the overall simulation, if compared to the collected experimental data, as well as a reasonable value with respect to the experimental evidence in this regard, as supported by the literature. As a matter of reference, the study conducted by (Barbera et al., 2022), highlights reasonable nitrogen quota values within the interval 8-16%, making the computational derived parameter completely aligned. Moving then the discussion towards the other parameters, the comparison is drawn with respect to the work of (Grover et al., 2019), since the development of this model is based on the framework provided by that study. Values in hand, it is possible to state the significant difference between the two sets of parameters values. However, it is important also to contextualize the situation, explaining how such set was derived in the reference work. As explained in the paper, and stated at the beginning of Chapter 3, the model was generated to theoretically simulate population and nutrient dynamics for nitrogen-fixing cyanobacteria. About that, the theoretical frame in which that model fits precludes the possibility of working with actual experimental data for actual species, implying in response the necessity of applying other strategies for the derivation of such parameters. According to this rationale, such

derivation process was conducted with a numerical-oriented approach, by namely using one-at-a-time sensitivity analysis, in which each parameter was varied in turn with the others fixed (Grover et al., 2019).In the end, the final values selection was done aiming at producing as realistic as possible behaviors: as a matter of example, the differentiation rate constant $k_{V\rightarrow H}$ was adjusted to produce a realistic proportion of heterocyst biomass of approximately 10%, and the bounds for nitrogen quota, namely $Q_{N,max}$ and $Q_{N,min}$, for a realistic C:N ratio around 6 (Grover et al., 2019) . In light of this, it is reasonable to have fitted model parameters not aligned with the ones provided in the reference work, resulting from the different rationale applied.

Despite this, the model thus developed provides a reasonable explanation for the biological behavior of such species, also according to the experimental evidence. Obviously, its strength lies in the simultaneous potential implementation for other microalgal species. In line with this rationale, the model was also adopted for modelling the behavior of another nitrogen-fixing cyanobacterium, namely *Nostoc* PCC 7120, using experimental data collected during this master thesis work.

Chapter 5

Experimental and computational results for *Nostoc* PCC 7120 species

Nostoc PCC 7120 represents the reference species of this master thesis. Its behavior was assessed both at experimental level and at computational level, by the implementation of the predictive model described in *§Chapter 3*. Indeed, this chapter is aimed at presenting the obtained results regarding both investigated aspects. The experimental data acquired during this work are presented along with the ones previously gathered in Vedana (2022). The discussion offered in this chapter can be articulated in three different sections, according to the selected operating variable for assessing biomass growth.

The first one focuses on the effect of residence time. This section is computationally oriented, as such dataset is used for model validation purposes. The aim is to check whether the model validated for *Anabaena* PCC 7122 can be extended also for other filamentous heterocystic nitrogen-fixing cyanobacteria.

Then, the focus is moved on to the experimental campaigns, aimed at assessing the effects of operating variables on cyanobacterial continuous cultivation systems; more specifically, the discussion is firstly directed towards the effect of light intensity, and ultimately towards the one related to nitrogen availability in medium.

5.1 Effect of residence time

With the same rationale applied for *Anabaena* PCC 7122 in previous chapter, the predictive model so far developed is applied also for *Nostoc* PCC 7120 species, according to the experimental data collected at different residence times (Vedana, 2022).

5.1.1 Experimental data overview

The experimental data assessing *Nostoc* PCC 7120 were collected in continuous 200 mL flat panel photobioreactors. Different residence times were evaluated by adjusting the proper flowrate through the reactor, thus obtaining the experimental values of 0.8, 1.1, 2.2, and 3.7 days.

Similarly to what stated in section *§2.2.1,* all the operating parameters except for the residence time, were fixed: temperature was maintained at 24 °C in a thermostatic incubator, pH set between 7.5 and 8 with the auxiliary of the pH buffering system provided by the air enriched in CO_2 (5% v/v) bubbling combined with $NaHCO_3$ in culture medium, and a light intensity of 550 μmol m^{-2} s^{-1} was continuously furnished with a PAR lamp.

Table 5.1. *Experimental results for Nostoc PCC 7120 in response to different residence times at 550 μmol m^{-2} s^{-1}* (Vedana, 2022).

Residence time [d]	Vegetative cells concentration [g_V L^{-1}]		Heterocystous cells concentration [g_H L^{-1}]		Nitrogen quota in biomass [g_N g_X^{-1}]	
	Mean	Std. dev	Mean	Std. dev	Mean	Std. dev
0.8	0.416	0.068	0.147	0.020	0.094	0.001
1.1	0.796	0.108	0.262	0.086	0.093	0.004
2.2	1.319	0.300	0.235	0.080	0.080	0.008
3.7	1.539	0.049	0.292	0.009	0.094	0.000

5.1.2 Model fitting results

As the model applied for such species is the same used for *Anabaena* PCC 7122, the assessment of the correlated model parameters values remain the first issue to tackle. Depending on their typology and nature, either experimentally or computationally driven, the evaluation procedures followed are the same explained along *§Chapter 4.* Moreover, concerning the experimentally derived ones, most of the parameters were retrieved in a previous work (Vedana, 2022), while μ_{max} and k_a values were assessed in this master thesis. In table 5.2 all the resulting values are listed.

Table 5.2. *Model parameters for Nostoc PCC 7120 species.*

Experimentally derived model parameters			
Parameter	*Value*	*Units of measurement*	*Definition*
$\boldsymbol{I_{opt}}$	376.60	μmol m^{-2} s^{-1}	Optimum light intensity
$\boldsymbol{K_I}$	93.95	μmol m^{-2} s^{-1}	Modified-Haldane model half saturation constant
$\boldsymbol{K_N}$	0.0029	g_N L^{-1}	Monod model half saturation constant
$\boldsymbol{\mu_{max}}$	5.176	d^{-1}	Maximum specific biomass growth rate
$\boldsymbol{k_{La}}$	123.36	d^{-1}	Volumetric mass transfer coefficient
$\boldsymbol{k_a}$	0.110	m^{-2} g^{-1}	Biomass light absorption coefficient
Fitted model parameters			
Parameter	*Value*	*Units of measurement*	*Definition*
$\boldsymbol{Q_{N,min}}$	0.0321	g_N g_X^{-1}	Minimum nitrogen quota
$\boldsymbol{k_{V\rightarrow H}}$	4.7166	d^{-1}	Differentiation constant
$\boldsymbol{\rho_{NF}^{max}}$	9.9978	g_N g_H^{-1} d^{-1}	Maximum nitrogen fixation rate
$\boldsymbol{Y_{H/V}}$	0.9896	g_H g_V^{-1}	Yield heterocyst – vegetative cells
$\boldsymbol{\mu_{e,V}}$	0.8270	d^{-1}	Vegetative cells maintenance energy
Final $\boldsymbol{Q_{N,max}}$ value			
Parameter value			*Overall dataset R^2 coefficient*
0.095			0.9606

According to the parameters thus retrieved, the model is capable of providing microalgal culture outcomes with respect to residence time values. In graphical terms, this leads to the following trends for vegetative cells and heterocysts concentration, as well as nitrogen quota.

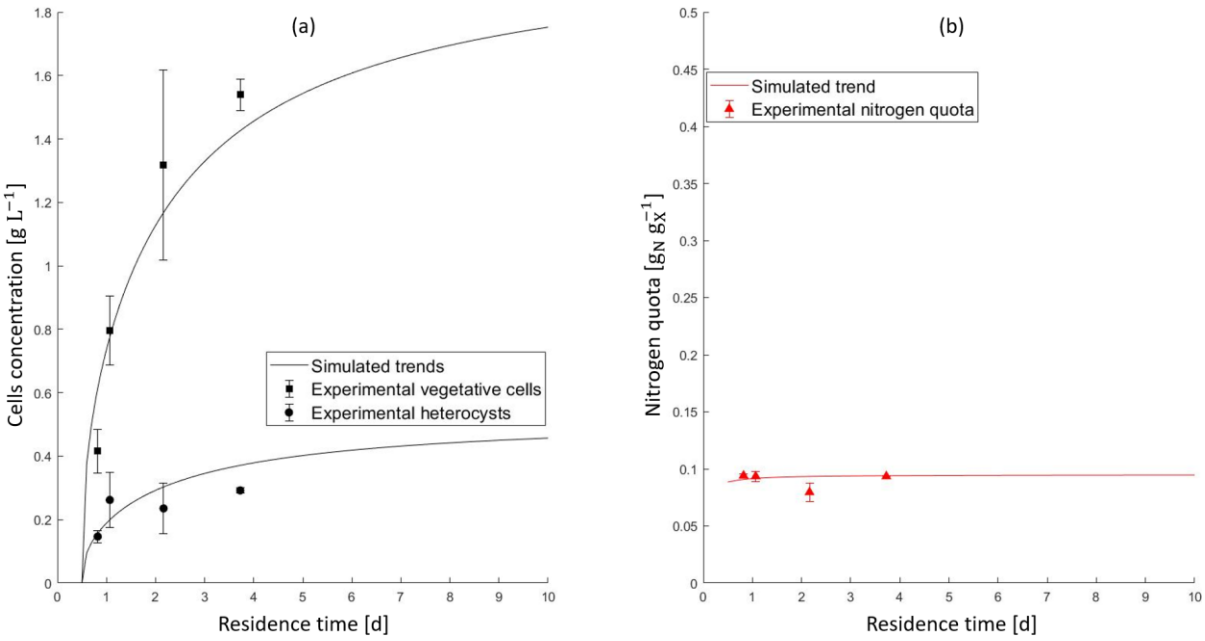

Figure 5.1. *Simulated behavior of Nostoc PCC 7120 cellular concentration (a) and nitrogen quota (b) with respect to the residence time.*

In addition, in order to graphically capture the correlation coefficient reported in table 5.2, aimed at showing the overall fitting quality provided by the model thus developed, reference can be made to figure 5.2.

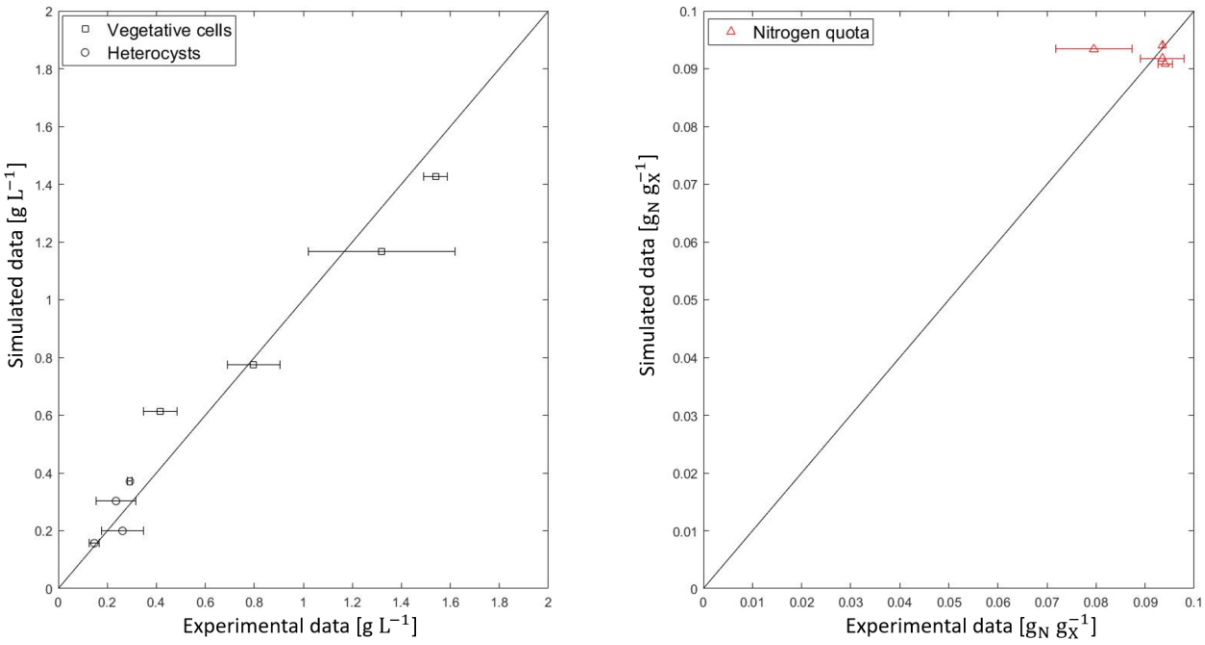

Figure 5.2. *Parity plots for simulated and experimental data.*

From the trends thus obtained, it is possible to state that *Nostoc* sp., compared to *Anabaena* sp. (presented in *§Chapter4*), responds in similar way with respect to the assessed operating parameter in continuous cultivation at fixed light intensity of 550 μmol m^{-2} s^{-1} (Figure 5.1a). But it is also possible to point out a peculiar difference concerning the way in which the two species acquire nitrogen from the outer environment (Figure 5.1b). Even if the computational approach provided a slightly higher value for *Anabaena* PCC 7122 maximum nitrogen quota, namely 0.11 g_N $g_X^{-1,}$ as compared to the 0.095 g_N g_X^{-1} value retrieved for *Nostoc* PCC 7120, the latter is capable of performing nitrogen-fixation more efficiently. Indeed, it can be highlighted when comparing the maximum nitrogen fixation rate, reaching almost 10 g_N g_H^{-1} d^{-1} for *Nostoc* PCC 7120, almost 10 times greater than the 0.99 g_N g_H^{-1} d^{-1} derived for *Anabaena* PCC 7122. Such result is in accordance with the experimental evidence reported in several studies (Do Nascimento et al., 2015; Trentin et al., 2023).

Consequently, this metabolic feature is reflected in vegetative cell and heterocysts concentration at different residence times: as nitrogen is acquired more rapidly in *Nostoc* PCC 7120 at lower operating parameter values, it is possible to perceive an increase in biomass concentration, as sum of vegetative cells and heterocysts. These considerations can also be achieved by comparing simulated species productivities with respect to the residence time, as reported in figure 5.3. From a theoretical perspective, biomass productivity is evaluated through equation (5.1).

$$P_X\ [g_X\ L^{-1}\ d^{-1}] = \frac{C_X}{\tau} \tag{5.1}$$

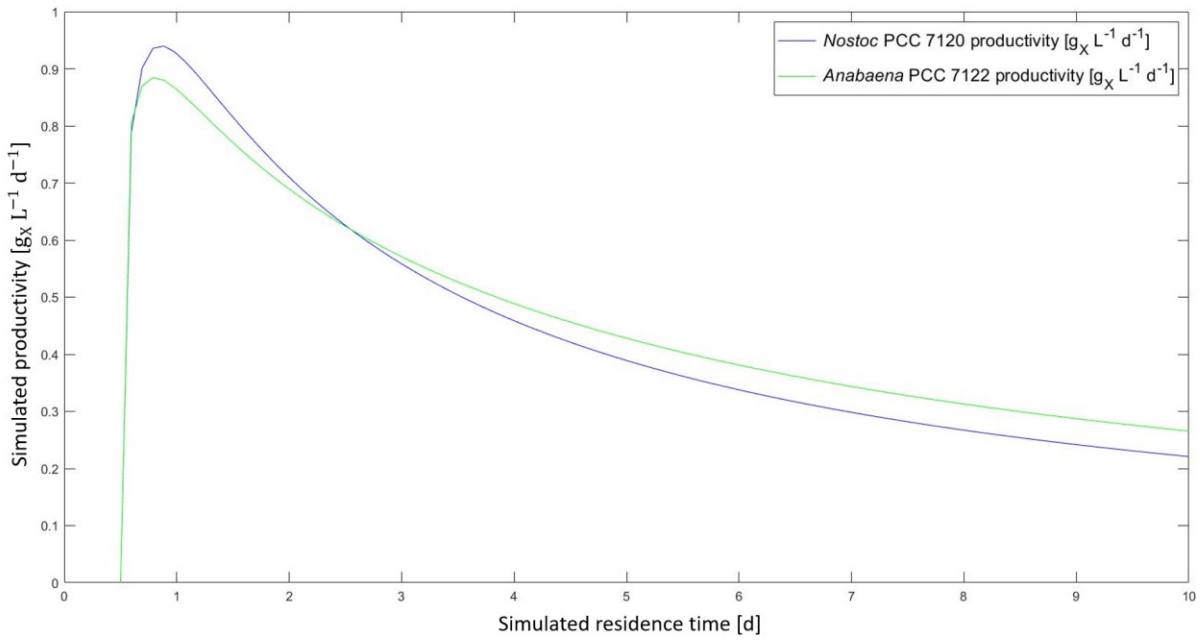

Figure 5.3. *Simulated biomass productivities for both cyanobacterial species.*

In general terms, a similar trend can be pointed out for both species, with the presence of a peak in productivity corresponding to a residence time value approximately equal to 1. More specifically, *Nostoc* PCC 7120 achieves a maximal productivity equal to 0.94 g_X L^{-1} d^{-1} contrarily to *Anabaena* PCC 7122 with 0.88 g_X L^{-1} d^{-1}, thus implying higher performance for the first cyanobacterium with respect to the second, if exploiting lower residence times for their continuous cultivation. On the other hand, moving at higher τ values *Anabaena* prevails, with a slightly higher productivity. Nevertheless, in this region productivities are generally lower, and so this may not be relevant for a potential industrial application. Despite that, the differences in the computationally derived productivity values for the two species under study just presented are quite minimal. The reason has to be found in a deeper understanding of the nitrogen fixation process; as already discussed in §*Chapter 1,* since this metabolic process is strictly correlated to the biomass build up, similar productivities may imply similar rates at which both species are fixing nitrogen. This theoretical evidence can also be sustained from a computational perspective: in figure 5.4 the two simulated rates are compared with respect to a set of simulated residence times, thus showing similar values along the illustrated trends.

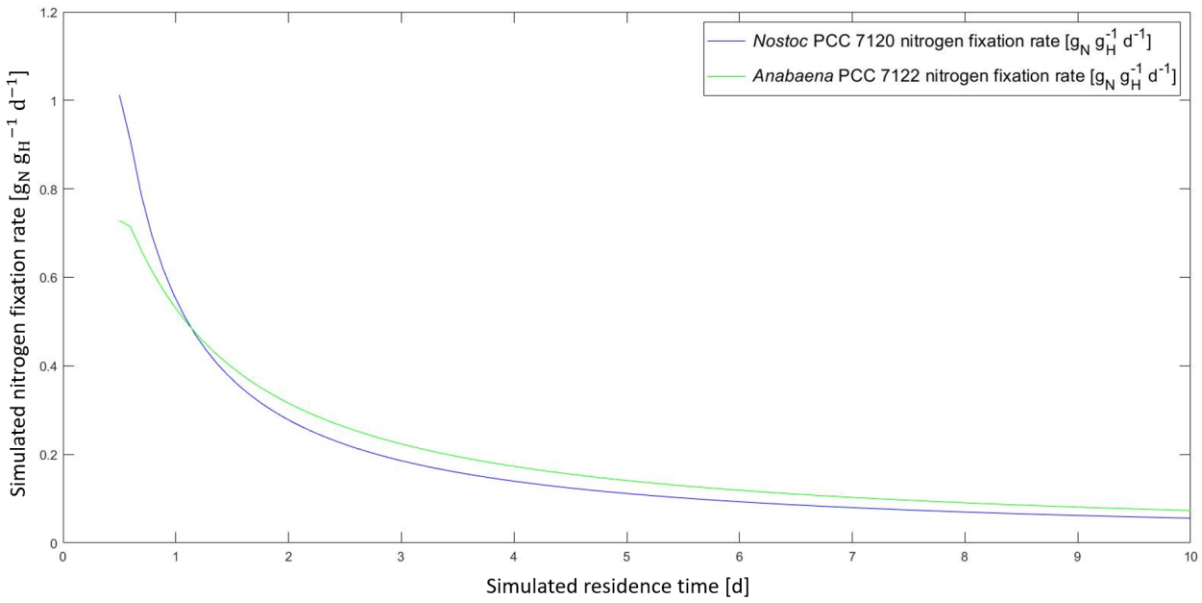

Figure 5.4. *Simulated nitrogen fixation rates for both cyanobacterial species.*

From a mathematical perspective, as previously explained in *§Chapter 3*, the rate of such process is derived according to equation (5.2):

$$\rho_{NF}\ [g_N\ {g_H}^{-1}\ d^{-1}] = \rho_{NF,max}\frac{Q_{N,max} - Q_N}{Q_{N,max} - Q_{N,min}} \tag{5.2}$$

where the maximum rate is corrected by the factor comprising all the nitrogen quota constraints. In light of this, the only way to ensure this phenomenon, despite the differences previously highlighted in the species-specific values, is to have significant differences in the actual nitrogen quota values between the two species. More specifically, it can be concluded that *Nostoc* PCC 7120 is characterized by higher amounts of stored nitrogen with respect to *Anabaena* PCC 7122, which then implies a higher content of nitrogen-based compounds embedded within the former species, favoring its subsequent industrial exploitation. From a mathematical perspective, this peculiarity can also be highlighted by comparing the corresponding nitrogen productivities for the two different species, which has to be intended as the actual amount of fixed nitrogen in biomass. Its evaluation follows equation (5.3).

$$P_N\ [mg_N\ L^{-1}\ d^{-1}] = P_X \cdot Q_N \tag{5.3}$$

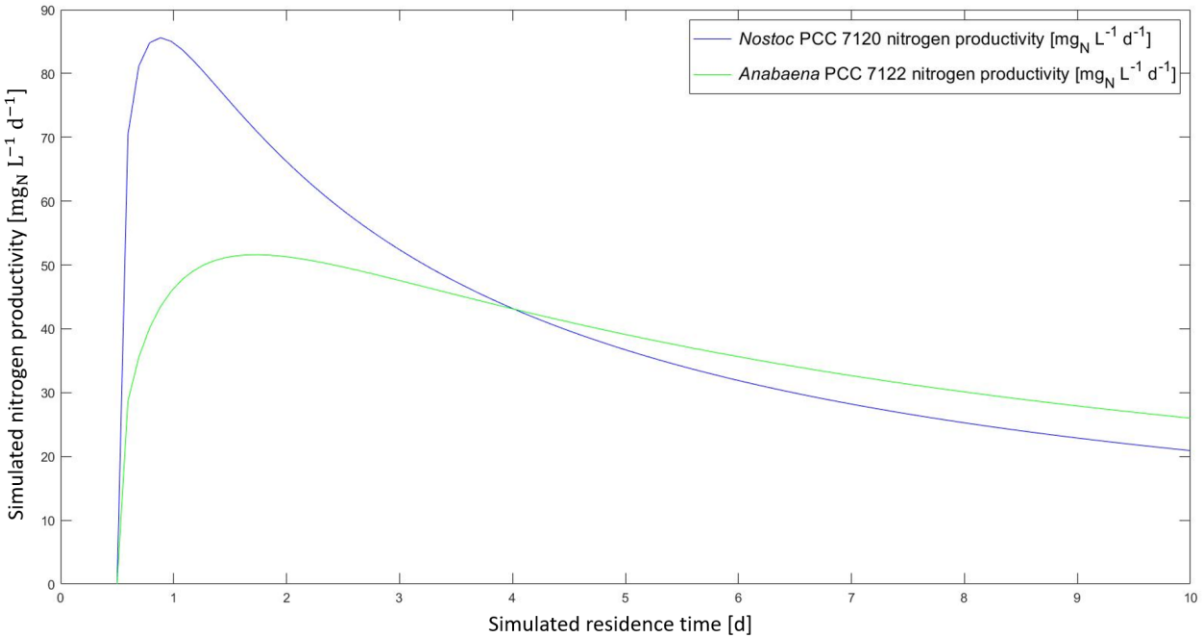

Figure 5.4: *Simulated nitrogen productivities for both cyanobacterial species.*

As clearly shown in figure 5.4, at τ approximately equal to 1 is possible to point out a higher productivity in *Nostoc* sp. than in *Anabaena* sp., noticing that higher values for such variable corresponds to higher internal nitrogen quota values. This result is also supported by the experimental evidence in Trentin et al. (2023).

5.2 Effect of light intensity

As already discussed in section *§1.5.1.2*, light is a crucial operating variable for assessing algae cultivation performances, in view of an adequate production on a larger scale. According to this, the effect of light intensity was assessed on continuous cultivation of *Nostoc* PCC 7120, both in terms of biomass production performances and embedded valuable compounds. From an operative perspective, the study was conducted assessing different values of light intensity, namely 100, 300, 400 and 1000 µmol m^{-2} s^{-1}, with the addition of an intermediate condition at 550 µmol m^{-2} s^{-1} taken from Vedana, 2022 in order to enlarge as much as possible the dataset dimension on which to base the discussion. Moreover, since continuous culture systems were implemented, a residence time equal to 1 day was fixed for all the tested conditions. This section focuses on getting more information about the behavior of the studied species, to also support the predictive model validation.

5.2.1 Biomass production

With respect to harvested biomass, the resulting trend at different tested light intensities is presented in figure 5.5.

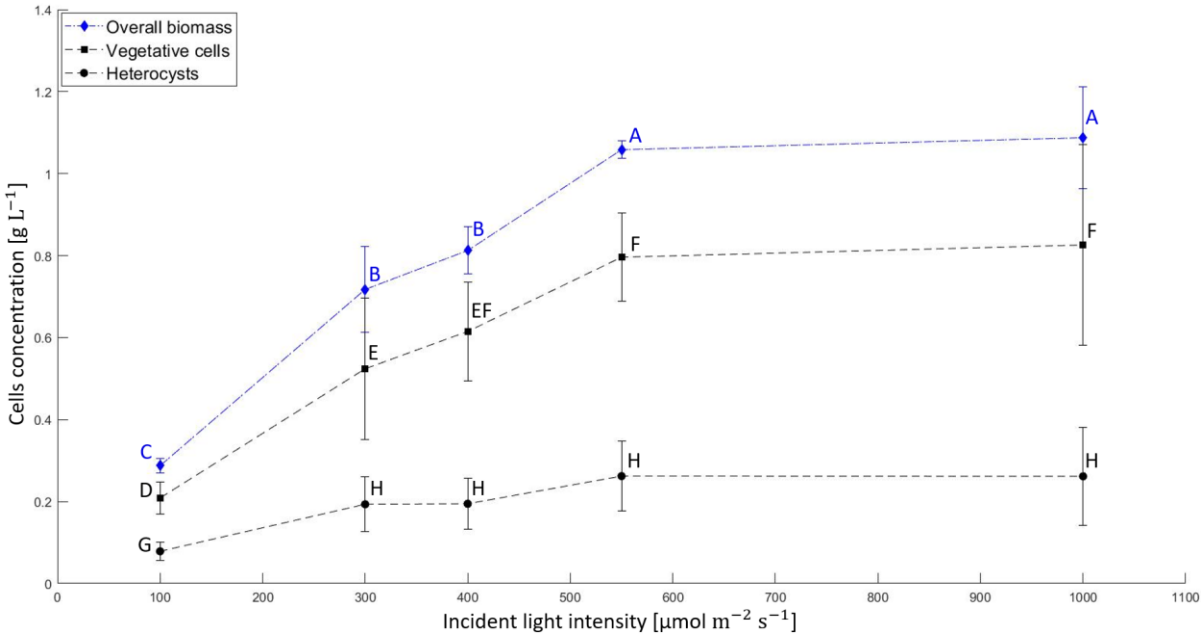

Figure 5.5. *Nostoc PCC 7120 experimental behavior with respect to different incident light intensities. Means that do not share a letter are significantly different.*

The illustrated overall biomass trend can be divided into two parts. The first one, within the range 100-300 µmol m^{-2} s^{-1}, shows a linear profile, where increasing biomass concentration can be favored by higher light intensity. Above 300 µmol m^{-2} s^{-1}, the increase in biomass tends to slow down, reaching a plateau at 1.07 ± 0.08 g L^{-1} between 600 and 1000 µmol m^{-2} s^{-1}. From a biological perspective, this may be due to photosaturation, namely a condition in which photosynthesis is not further stimulated, as the amount of photons provided is such that it saturates all antenna systems (Béchet et al., 2013). Although higher light intensities have not been investigated, it is possible to hypothesize a potential reduction in overall biomass production in those conditions, due to photoinhibition conditions arising as a result of cellular photodamaging (Razzak et al., 2013). The results so far presented are in accordance with evidence in literature, aimed at assessing the effect of light intensity on continuous microalgal cultivation. As a matter of example, it is possible to mention the works by Sforza et al. (2014) on *Scenedesmus obliquus* 276.7, a green microalga, and the one by Borella (2017), conducted on cyanobacterium *Anabaena* PCC 7122.

In addition, figure 5.5 also reports the trends of both vegetative cells and heterocysts at the different light intensities. For vegetative cells, the trend is almost equal to the one just discussed. Indeed, as vegetative cells in heterocystous cyanobacteria represents photosynthetic sites, this typology is more susceptible to changes in incident light conditions. On the contrary, heterocysts seems not to be as affected by light intensity as vegetative cells, due to their rapid stabilization at 0.23 ± 0.07 g_H L^{-1} in concentration, starting from 300 µmol m^{-2} s^{-1}.

Table 5.3. *Experimental results for Nostoc PCC 7120 in response to different light intensities. Means that do not share a letter are significantly different. The condition marked with an asterisk refers to the work of Vedana, 2022.*

Tested condition	Light intensity [µmol m^{-2} s^{-1}]	Biomass concentration [g_X L^{-1}]		Vegetative cells concentration [g_V L^{-1}]		Heterocysts concentration [g_H L^{-1}]		Productivity [g_X L^{-1} d^{-1}]	
		Mean	Std. dev	Mean	Std. dev	Mean	Std. dev	Mean	Std. dev
7	100	0.288^{C}	0.017	0.209^{D}	0.039	0.079^{G}	0.022	0.270^{I}	0.016
8	300	0.718^{B}	0.104	0.524^{E}	0.172	0.194^{H}	0.067	0.661^{J}	0.096
9	400	0.813^{B}	0.057	0.615^{EF}	0.120	0.197^{H}	0.063	0.745^{J}	0.053
4*	550	1.058^{A}	0.022	0.796^{F}	0.108	0.262^{H}	0.086	0.991^{K}	0.020
10	1000	1.088^{A}	0.124	0.826^{F}	0.244	0.262^{H}	0.120	0.992^{K}	0.113

Along with production, biomass productivity also represents in general a performance indicator to be studied while modulating the operating parameters, and the resulting values are grouped in table 5.3. Moreover, as all the experiments were conducted exploiting the same residence time, the resulting trend is similar to the one illustrated in previous section concerning biomass concentration, with a maximum in productivity around 0.99 g_X L^{-1} d^{-1} between 550 and 1000 µmol m^{-2} s^{-1}. This suggests that productivity can also be negatively affected while moving to higher light intensities, again due to photosaturation and subsequently photo inhibition phenomena arising. These considerations are also sustained by the discussion provided by Sforza et al. (2014), where an identical response of *Scenedesmus obliquus* 276.7 productivity over incident light intensities was pointed out. In addition, from an operational perspective, it must be remembered that the light intensity does not only impact culture performances, but also the whole process economics; as it increases, also the related operative

costs tend inevitably to arise, compromising the overall feasibility of the latter. Consequently, preferring intermediate values of such parameter can be successful for the overall process outcomes.

Obviously, the light intensity response can also be described from a biological perspective, namely by assessing cyanobacterial photosynthetic performances with respect to the operating parameter under study. This can be done by looking at potential variations in pigments and phycobiliproteins content, remembering that the identification of optimal growth conditions does not only depend on the obtained biomass concentration, but also on the optimization of valuable compounds production.

5.2.3 Valuable compounds production

Starting from the analysis on overall pigments content in figure 5.6, the results collected show a quite steady value within the interval 100-550 µmol m^{-2} s^{-1}, while a general decrease at higher light intensities, such as 1000 µmol m^{-2} s^{-1}. The reason behind this trend is probably due to the incipient photo inhibition condition at the highest tested light intensity. Indeed, as light becomes more available, an increased concentration of pigments results not to be necessary, due to the ease in photons collection (Alves De Oliveira et al., 2014).

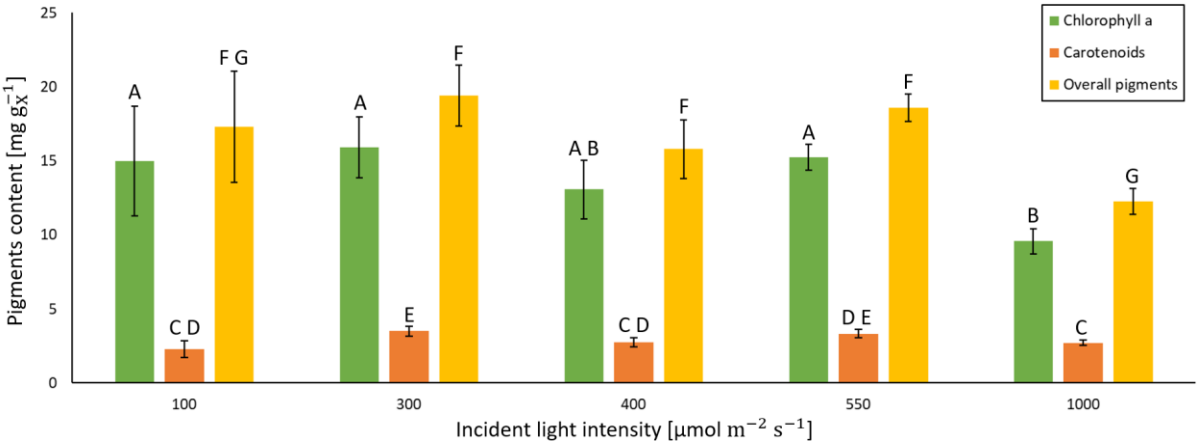

Figure 5.6. *Nostoc PCC 7120 experimental pigments content with respect to assessed light intensities. Means that do not share a letter are significantly different.*

Although this result can be considered sufficient to confirm a reduced photosynthetic activity at stronger enlightenment conditions, another important aspect that has to be considered for

such purpose is represented by the relative variation in chlorophyll *a* and carotenoids content within biomass (chl a/car), presented in figure 5.7.

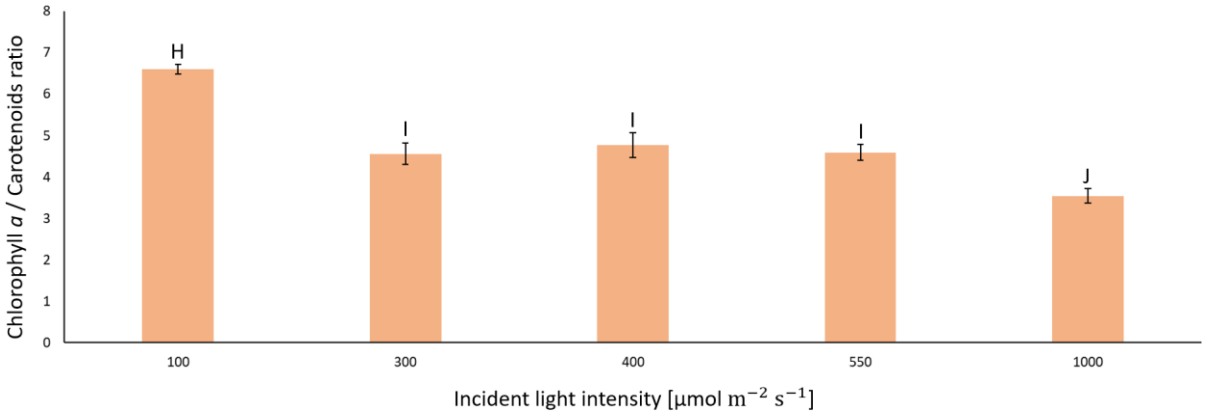

Figure 5.7. *Nostoc PCC 7120 experimental chla/car ratio with respect to assessed light intensities. Means that do not share a letter are significantly different.*

From the plot it is possible to perceive a progressive decrease in chl a/car ratio as the incident light intensity used for cultivation is increased. Indeed, *Nostoc* PCC 7120, as other photosynthetic organisms, responds to an overlight stress condition by rapidly decreasing the chlorophyll *a* content to reduce its capability of collecting photons, while keeping almost unchanged the carotenoids content. Specifically for the latter pigment typology, the degradative response with respect to the assessed light intensity seems to be less marked, which do not only serve for the photons collection process, but also act as a protective defense through their antioxidant activity (Alves De Oliveira et al., 2014; Riethman et al., 1988).

Table 5.4. *Nostoc PCC 7120 pigments content with respect to light intensities. Means that do not share a letter are significantly different. The condition marked with an asterisk refers to the work of Vedana, 2022.*

Tested condition	Light intensity [µmol m^{-2} s^{-1}]	Chlorophyll *a* content [mg gx^{-1}]		Carotenoids content [mg gx^{-1}]		Total content [mg gx^{-1}]		Chla/Car ratio [ ]	
		Mean	Std. dev	Mean	Std. dev	Mean	Std. dev	Mean	Std. dev
7	100	15.0^{A}	3.7	2.3^{CD}	0.6	17.3^{FG}	3.7	6.6^{H}	0.1
8	300	15.9^{A}	2.0	3.5^{E}	0.4	19.4^{F}	2.1	4.6^{I}	0.3
9	400	13.1^{AB}	2.0	2.7^{CD}	0.3	15.8^{F}	2.0	4.7^{I}	0.3
4*	550	15.2^{A}	0.9	3.3^{DE}	0.3	18.6^{F}	0.9	4.6^{I}	0.2
10	1000	9.6^{B}	0.8	2.7^{C}	0.2	12.3^{G}	0.9	3.5^{J}	0.2

Similarly to what stated for pigments content, phycobiliproteins responds in a completely analogous way with respect to a change in light intensity conditions. Indeed, as illustrated in figure 5.8 an overall decrease can be observed at 1000 µmol m^{-2} s^{-1}, as a biological adaptation in order to prevent absorption of radiation in excess (Alves De Oliveira et al., 2014). In addition to this, the interesting aspect of such behavior is related to the relative variations occurring among these different typologies of proteins, specifically for phycocyanin and allophycocyanin, in the various tested conditions. In fact, while the allophycocyanin content seems not to be influenced by the incident light intensity, a sudden reduction in phycocyanin content occurs at 1000 µmol m^{-2} s^{-1}.

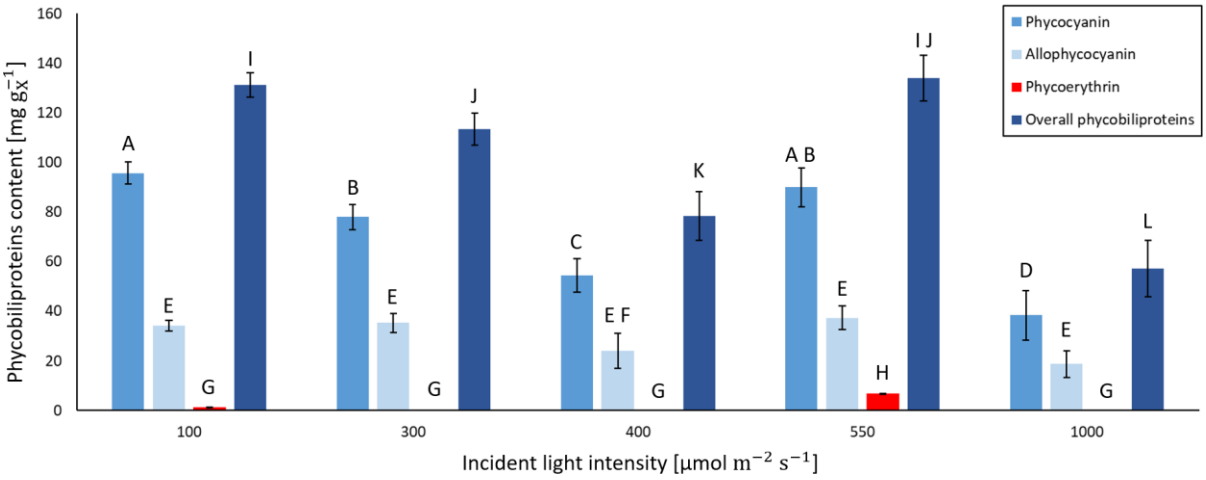

Figure 5.8. *Nostoc PCC 7120 experimental phycobiliproteins content with respect to assessed light intensities. Means that do not share a letter are significantly different.*

The explanation may be linked to the phycobilisomes structure itself, in which allophycocyanin represents the internal framework, while phycocyanin the external elongations (Assunção et al., 2022): as the latter is primarily involved in photons collection, its dismantle allows biomass to survive also under these unfavorable conditions. For this reason, having a constant allophycocyanin content in biomass implies a constant amount of phycobilisomes, relegating the light intensity effect only to their internal composition.

Table 5.5. *Nostoc PCC 7120 phycobiliproteins content with respect to light intensities. Means that do not share a letter are significantly different. The condition marked with an asterisk refers to the work of Vedana, 2022.*

Tested condition	Light intensity [µmol m^{-2} s^{-1}]	Phycocyanin content [mg gx^{-1}]		Allophycocyanin content [mg gx^{-1}]		Phycoerythrin content [mg gx^{-1}]		Total content [mg gx^{-1}]	
		Mean	Std. dev	Mean	Std. dev	Mean	Std. dev	Mean	Std. dev
7	100	95.7 ^{A}	4.5	34.2 ^{E}	2.1	1.3 ^{G}	0.0	131.2 ^{I}	5.0
8	300	78.0 ^{B}	5.0	35.3 ^{E}	4.0	0.1 ^{G}	0.0	113.4 ^{J}	6.4
9	400	54.4 ^{C}	6.8	24.0 ^{EF}	7.1	0.0 ^{G}	0.0	78.5 ^{K}	9.8
4*	550	89.9 ^{AB}	7.8	37.3 ^{E}	4.8	6.7 ^{H}	0.0	134.0 ^{IJ}	9.1
10	1000	38.4 ^{D}	9.9	18.8 ^{E}	5.4	0.0 ^{G}	0.0	57.1 ^{L}	11.3

To conclude, based on the considerations provided so far with respect to both biomass and corresponding internal compounds production, an intermediate light intensity equal to 550

μmol m^{-2} s^{-1} may be considered suitable for a performing cultivation of such cyanobacterial species, as formerly demonstrated in other studies conducted on the same species (Loreto et al., 2003).

5.3 Effect of nitrogen source and availability

Since nitrogen represents an important macronutrient to ensure biomass growth, second in content only to carbon, the assessment of species behavior with respect to its availability represents a very interesting aspect to face while investigating optimal growth conditions. This is especially relevant for the cultivation of nitrogen-fixing microorganisms, which can grow by consuming molecular dinitrogen or reactive forms of nitrogen, as nitrate or ammonium. From the process perspective, it is important to investigate if the nitrogen source has an effect and which is the microorganism kinetic based on such nutrient. A detailed explanation concerning the operational setup adopted is described in section *§2.2.1.2*.

The results can be discussed on several levels: the resulted behavior may not be only analyzed with respect to the harvested biomass concentration, but the discussion can be deepened moving to potential variations in the internal production of valuable compounds that can be potentially extracted and used for various purposes, as presented in *§Chapter 1*.

5.3.1 Biomass production

The experimental results collected according to such rationale are presented in figure 5.9. More in detail, along with the overall biomass concentration, the trends are articulated with respect to both vegetative and heterocystous cells.

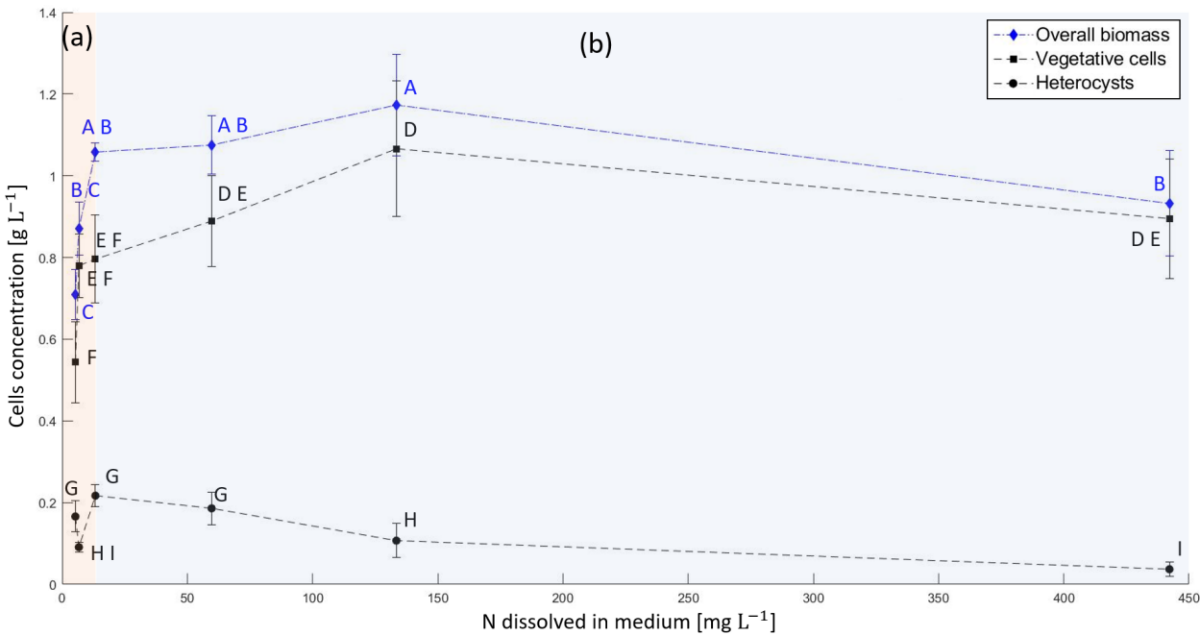

Figure 5.9. *Nostoc PCC 7120 cells experimental behavior with respect to the nitrogen concentration available within the culture medium under diazotrophic (a) and non-diazotrophic (b) conditions. Means that do not share a letter are significantly different. Lines are just eye guides.*

The biomass concentration with respect to the availability of nitrogen in solution can be described in accordance with the classical trend provided by Monod kinetics (Monod, 1942). Starting from the lower tested nitrogen concentration, approximately 5.3 mg L^{-1}, a limiting condition arises, which compromises species performances and thus the derived harvested concentration. Such experimental evidence is also in line with what stated in the work of Barbera et al. (2022), in which a 33% reduction in *Auxenochlorella protothecoides* 33.80 biomass concentration was observed when the inlet nitrogen concentration decreased from 117 mg L^{-1} to 40 mg L^{-1}. The progressive increase in nutrient concentration allows then to provide, at least at the beginning, an asymptotical response: indeed, till an available nitrogen concentration of 133 mg L^{-1}, it is possible to continuously produce biomass characterized, on average, by a concentration of 1.04 ± 0.13 g L^{-1}. Obviously, this aspect opens the door to considerations regarding process sustainability, aimed at assessing which would be the most convenient operative condition, also in optics of a larger scale production. About that, the exploitation of the cyanobacterium nitrogen fixation process may be considered as the most suitable, thanks to the lack of additional reactive nitrogen source needed within the medium, which can lead to reduced process capital costs without compromising harvested biomass

concentration. Along with the increase in costs, it is important to point out another potential disadvantage related to a further increase in available nitrogen. Indeed, instead of making the environment favorable for microorganisms growth, higher concentrations can provide an inhibiting effect, which in turn can reduce the obtained biomass concentration. Recalling the beginning of the paragraph, accounting for the latter effect can be mathematically done by a modified Monod model, provided by Andrews and Noack (Andrews, 1968). Moreover, the theory is also sustained by experimental evidence in this regard: indeed, for *Nodularia* sp. strains, a mineral nitrogen concentration approximately equal to 350 mg L^{-1} resulted to be sufficient to trigger a considerable growth inhibition phenomenon (Sanz-Alférez & del Campo, 1994).

Considering the peculiar cyanobacterial cells differentiation process, the experimental trends for vegetative cells and heterocysts can be discussed. Without dwelling too much on the first, as their behavior resembles the overall biomass trend, some interesting considerations can be depicted instead for heterocysts. The dependency of heterocysts with respect to nitrogen fixing and non-nitrogen fixing conditions is well known: since their differentiation is favored under nitrogen depletion conditions, as also reported in section *§1.2,* an external addition of nitrogen reactive sources can inhibit their presence (Garcia-Pichel, 2009; K. Kumar et al., 2010). Deepening in the discussion, this work explores such phenomenon by considering the effect of modulations in nitrogen availability, both under nitrogen fixing conditions and not. According to the literature, the presence of nitrogen in the form of nitrate can reduce the differentiation process, and this inhibiting effect becoming more evident as nitrate concentration increases, as also reported in the corresponding plot in figure 5.9. In addition, while working under nitrogen fixing conditions, similar conclusions can be traced. Starting from the maximum allowable nutrient concentration, namely 13.3 mg L^{-1} due to equilibrium between air and liquid medium, a maximum in heterocysts concentration should be visible. After that, a progressive reduction should be evident, as the gaseous dinitrogen is diluted through argon. With respect to the experimental data reported in figure 5.9, the consequent statistical analysis enters in conflicts with the description just provided, probably due to the lack of precision characterizing the direct method used for heterocysts count. Straddling between the experiments conducted in nitrogen fixation and not, namely the one at 13.3 mg L^{-1} with air enriched in CO_2 and the one at 133 mg L^{-1} by adding $NaNO_3$ in a modified BG11, the statistics does not show any

significant variation in heterocysts concentrations. According to the previous discussion, this may seem counterintuitive, as the presence of an additional nitrogen reactive source should produce a significant effect on the available heterocysts. This could be due to the supportive phenomenon offered by the still undergoing nitrogen fixation, capable of overwhelming the little inhibitory effect furnished by this amount of nitrate.

Considering species performance with respect to nitrogen source and availability, the behavior of internal quota should also be discussed, starting from the experimental trend shown in figure 5.10. In this case, since the nutrient under investigation is assumed within biomass through different metabolic paths depending on the available source, the discussion is made separately with respect to diazotrophic and non-diazotrophic conditions.

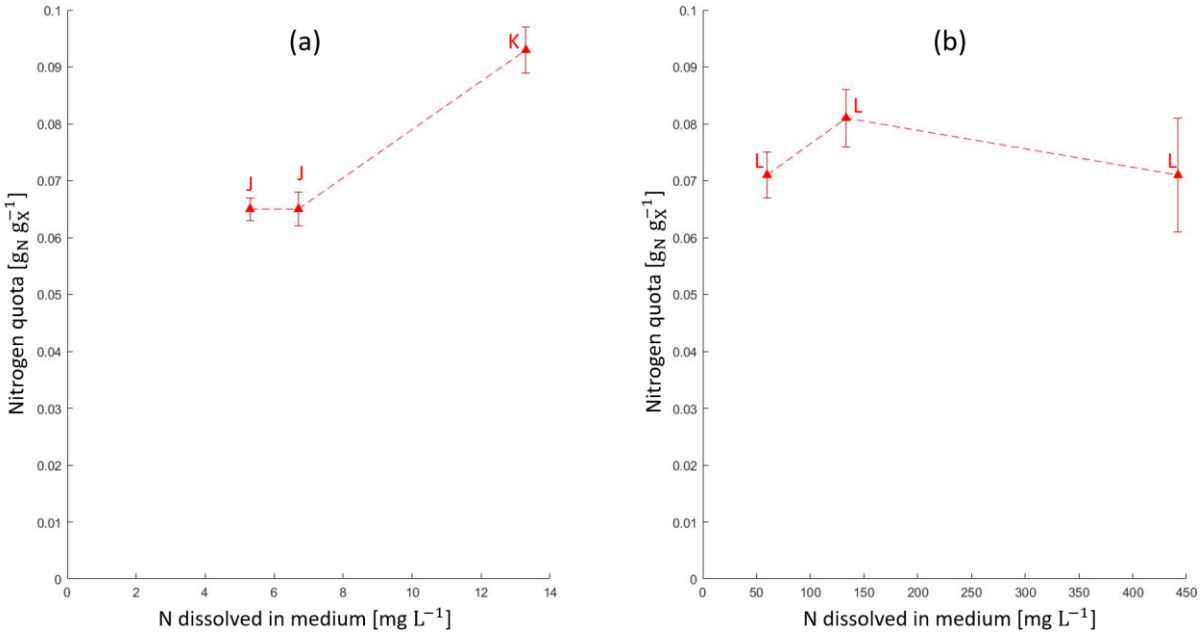

Figure 5.10. *Nostoc PCC 7120 nitrogen quota with respect to the nitrogen concentration available within the culture medium under diazotrophic (a) and non-diazotrophic (b) conditions. Means that do not share a letter are significantly different. Lines are just eye guides.*

By considering the experimental data collected under nitrogen fixing conditions, it is possible to see an increase in the amount of nitrogen that can be stocked within biomass, with a maximum obtained at condition 4*. A potential limitation in nitrogen concentration provided with the gaseous phase, as shown in the left-hand side of the plot, lowers the allowable nitrogen quota. Interestingly, the statistical analysis does not reveal any difference between the two limiting conditions, showing similar biomass performances in terms of embedded nitrogen

content. However, for the same experiments, a net variation in heterocysts concentration was derived, with the one at 5.3 mg L^{-1} of dissolved nitrogen characterized by a higher value with respect to the one at 6.7 mg L^{-1}. Such experimental evidence seems in contrast with the species biological behavior since an analogous trend is expected for both variables. Therefore, this problem can be addressed by comparing the reliability of the methods adopted for such variables identification; as the heterocysts counting method is intrinsically affected by greater error with respect to the one used for the nitrogen quota assessment, the latter derived trend results to be the more reliable. Accounting for this, it is possible to assume an overestimation for the c_H value at 5.3 mg L^{-1}. In general, this trend is also in line with the literature: about it, it is possible to make reference to the work of Barbera et al., 2022, in which a sharp decrease in *Auxenochlorella protothecoides* 33.80 internal nitrogen quota was highlighted as the result of a nutrient limitation condition.

On the contrary, moving to the internal quota behavior under non-diazotrophic conditions, the statistical analysis showed no significant differences between the collected data. This may be due to the intrinsic species behavior with respect to the presence of reactive nitrogen sources in medium: as reported in Cejudo & Paneque (1986), nitrate tends to have an inhibitory effect on this metabolic process, since it is not necessary to acquire gaseous dinitrogen. According to what stated so far, working under diazotrophic conditions represents a suitable option, as it is characterized by the highest performance in terms of nitrogen acquisition, and consequentially, of nitrogen-based valuable compounds production, as proteins.

To conclude, table 5.6 sums up all the results discussed so far.

Table 5.6. *Results for Nostoc PCC 7120 in response to different nitrogen sources and concentrations. Light orange rows refers to diazotrophic conditions, while light blue ones to non-diazotrophic. Means that do not share a letter are significantly different. The conditions marked with an asterisk refers to the work of Vedana, 2022.*

Tested condition	Available nitrogen [mg L^{-1}]	Biomass concentration [g_X L^{-1}]		Vegetative cells concentration [g_V L^{-1}]		Heterocysts concentration [g_H L^{-1}]		Nitrogen quota in biomass [g_N g_X^{-1}]	
		Mean	Std. dev	Mean	Std. dev	Mean	Std. dev	Mean	Std. dev
6	5.3	0.710^{C}	0.061	0.544^{F}	0.099	0.166^{G}	0.038	0.065^{J}	0.002
5*	6.7	0.871^{BC}	0.065	0.780^{EF}	0.078	0.091^{HI}	0.012	0.065^{J}	0.003
4*	13.3	1.058^{AB}	0.022	0.796^{EF}	0.108	0.217^{G}	0.027	0.093^{K}	0.004
3	59.7	1.075^{AB}	0.071	0.889^{DE}	0.111	0.186^{G}	0.040	0.071^{L}	0.004
2	133.5	1.173^{A}	0.124	1.066^{D}	0.166	0.107^{H}	0.042	0.081^{L}	0.005
1	442.2	0.932^{B}	0.129	0.895^{DE}	0.147	0.037^{I}	0.018	0.071^{L}	0.010

The identification of the most suitable working conditions comprises also the evaluation of those providing the optimal productivity. From a practical perspective, since the experimental residence time along all the tested conditions was set approximately equal to 1 day, derived productivities and biomass concentration values are almost identical, and so the corresponding graphical trends.

In light of this, maximum productivities are achieved within the interval 13.3÷133.5 mg L^{-1} of dissolved nitrogen, reaching approximately 1.04 ± 0.13 g L^{-1} d^{-1} on average. However, it must be remembered that within such interval nitrogen fixing and non-nitrogen fixing conditions are exploited; thus, the preference cannot fail to go to the first one, in virtue of the capital costs reduction derived by the lack of external nitrogen source within the cultivation medium adopted.

5.3.3 Valuable compounds production

The effect of nitrogen source and availability have been investigated also regarding the production of valuable compounds from *Nostoc* PCC 7120 biomass. More specifically, this work focuses on the food and feed exploitation of microalgal biomass, thus analyzing internal

production of pigments and phycobiliproteins. Notice that such discussion is divided in two parts, based on the experimental data collected. This is aimed at observing whether a potential correlation between nitrogen fixation process and valuable compounds production can be found or not.

5.3.3.1 Diazotrophic conditions

The experimental results concerning pigments production with respect to the different concentration of nitrogen available under nitrogen fixing conditions are reported in figure 5.11 and table 5.7.

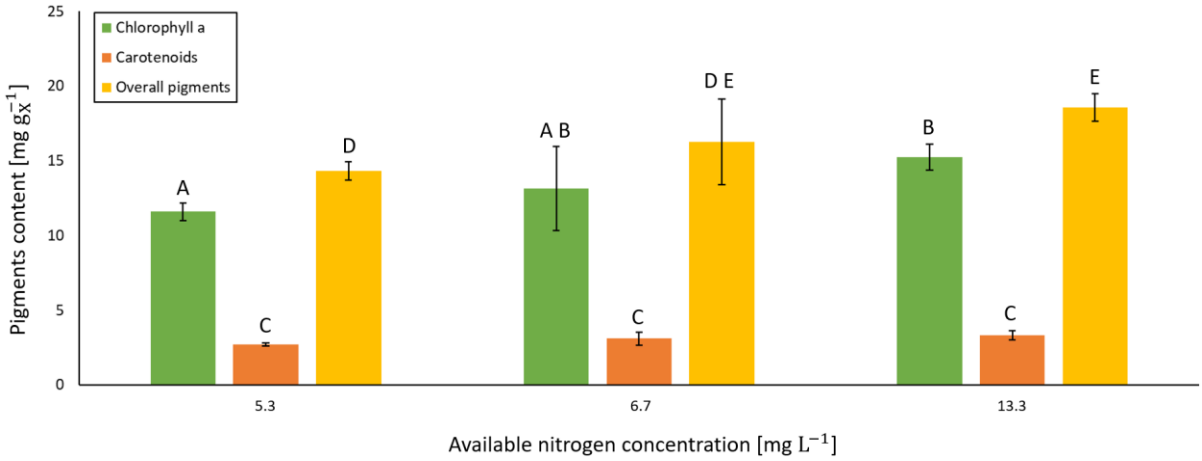

Figure 5.11. *Nostoc PCC 7120 pigments content with respect to the available nitrogen concentration. Means that do not share a letter are significantly different.*

Table 5.7. *Nostoc PCC 7120 pigments content with respect to the available nitrogen concentration. Means that do not share a letter are significantly different. The conditions denoted with an asterisk refer to the work of Vedana, 2022.*

Tested condition	**Available nitrogen [mg L^{-1}]**	**Chlorophyll *a* content [mg gx^{-1}]**		**Carotenoids content [mg gx^{-1}]**		**Total content [mg gx^{-1}]**	
		Mean	Std. dev	Mean	Std. dev	Mean	Std. dev
6	5.3	11.6 ^{A}	0.6	2.7 ^{C}	0.1	14.3 ^{D}	0.6
5*	6.7	13.1 ^{AB}	2.8	3.1 ^{C}	0.4	16.2 ^{DE}	2.9
4*	13.3	15.2 ^{B}	0.9	3.3 ^{C}	0.3	18.6 ^{E}	0.9

In general terms, considering the results provided by the statistical analysis, a slight increase in the overall pigments content can be spotted as a response to a greater nitrogen availability, mainly due to the chlorophyll *a* content. In addition, the fact that a concrete nutrient limitation condition may not have been reached with such experiments yet, does not lead to concrete outcomes and trends, such as an expected reduction in carotenoids. This assumption is also sustained by the fact that nitrogen limitation and starvation conditions can significantly decrease microalgal photosynthetic activity, and so pigments production (Pancha et al., 2014). Clearly, that conclusion was derived for microalgal species *Scenedesmus* sp. CCNM 1077, not capable of performing nitrogen fixation; thus, the resulting outcomes for *Nostoc* PCC 7120 may differ.

Moving then to phycobiliproteins, the results are shown in figure 5.12 and table 5.8 below.

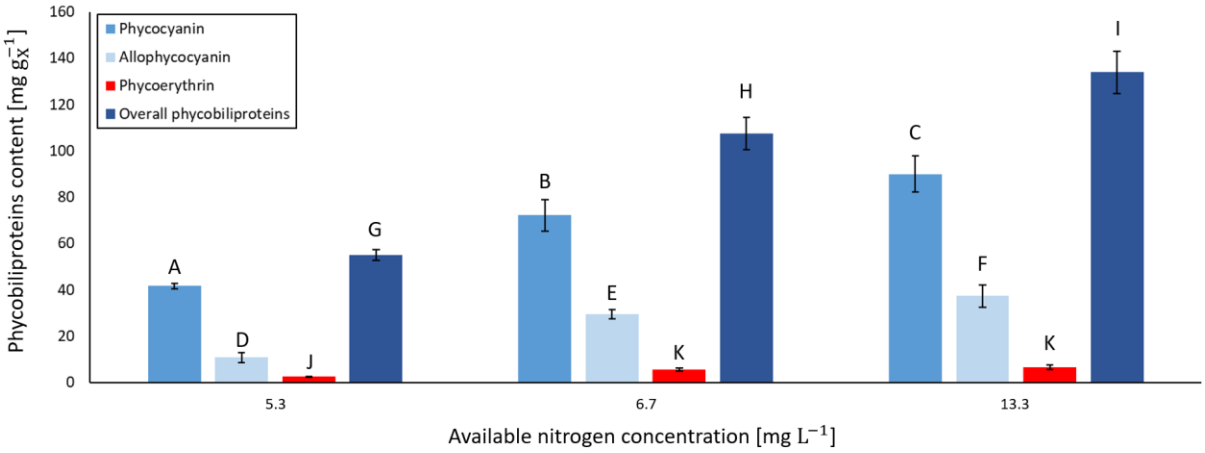

Figure 5.12. *Nostoc PCC 7120 phycobiliproteins content with respect to the available nitrogen concentration. Means that do not share a letter are significantly different.*

Table 5.8. *Nostoc PCC 7120 phycobiliproteins content with respect to the available nitrogen concentration. Means that do not share a letter are significantly different. The conditions marked with an asterisk refer to the work of Vedana, 2022.*

Tested condition	Available nitrogen [mg L^{-1}]	Phycocyanin content [mg gx^{-1}]		Allophycocyanin content [mg gx^{-1}]		Phycoerythrin content [mg gx^{-1}]		Total content [mg gx^{-1}]	
		Mean	Std. dev	Mean	Std. dev	Mean	Std. dev	Mean	Std. dev
6	5.3	41.7 ^{A}	1.1	10.7 ^{D}	2.0	2.6 ^{J}	0.1	55.0 ^{G}	2.3
5*	6.7	72.2 ^{B}	6.8	29.5 ^{E}	2.0	5.7 ^{K}	0.6	107.4 ^{H}	7.1
4*	13.3	89.9 ^{C}	7.8	37.3 ^{F}	4.8	6.7 ^{K}	1.0	133.6 ^{I}	9.2

In this case, the statistical analysis provides a clear correlation between phycobiliproteins content and available nitrogen concentration under nitrogen fixing conditions. Indeed, as the latter decreases from 13.3 mg L^{-1} to 5.3 mg L^{-1}, the total amount is reduced by almost 60%, from 133.6 ± 9.2 mg g_X^{-1} to 55.0 ± 2.3 mg g_X^{-1}, respectively. Deepening into this phenomenon, the major contribution is furnished by the phycocyanin content, namely the most abundant typology in such cyanobacterium: as the nitrogen availability diminishes, it progressively decreases, till becoming less than half the starting value obtained in condition 4*. On the other hand, even if condition 6 shows a clear overall reduction with respect to the others, allophycocyanin and phycoerythrin content seem not to be significantly affected by available nitrogen variations. From a biological perspective, this may be explained by the intrinsic placement of the different types of phycobiliproteins within the light-harvesting system (Assunção et al., 2022). Indeed, as allophycocyanin represents the core of such antenna system, the consequent dismantle to recover nitrogen in contrast to a potential limiting condition may be more difficult than doing it with phycocyanin, namely the elongations of phycobilisomes (Assunção et al., 2022). This assumption is also supported by the theory according to which under nitrogen depletion conditions phycobiliproteins can be degraded to be used as nitrogen sources (Allen & Smith, 1969).

5.3.3.2 Non-diazotrophic conditions

While assessing reactive nitrogen availability in the form of sodium nitrate within the culture medium, the obtained results concerning valuable compounds production are grouped in this section.

The results for pigments content are presented in figure 5.13 and table 5.9.

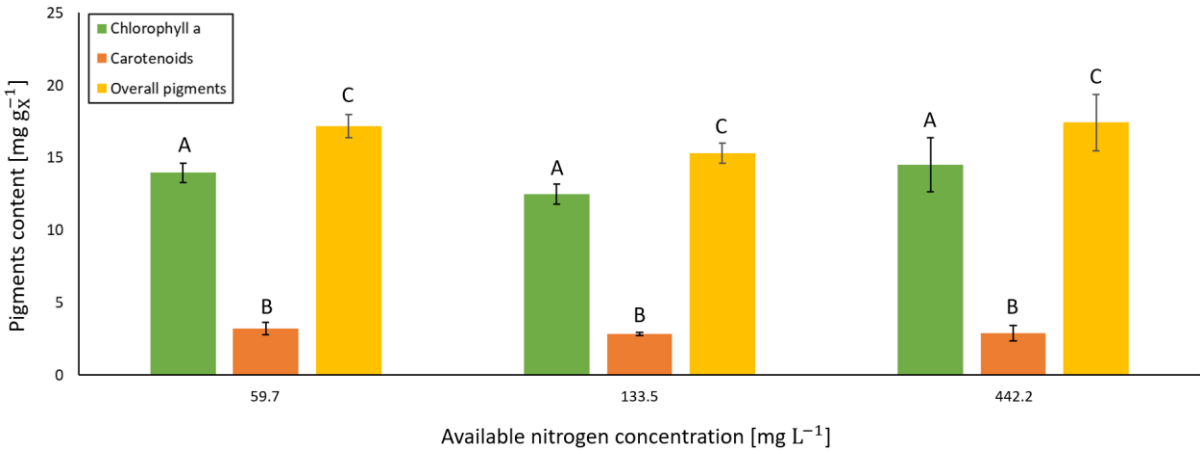

Figure 5.13. *Nostoc PCC 7120 pigments content with respect to the available nitrogen concentration (provided in the form of $NaNO_3$). Means that do not share a letter are significantly different.*

As reported by the statistical analysis, there is no significant differences in pigments production with respect to the amount of sodium nitrate provided within the culture medium, with an averaged value of 16.7 ± 1.2 mg g_X^{-1} in terms of total pigments content in biomass. It is also important to underline that such result is lined with the ones reported in the work of Rosales Loaiza et al. (2016), in which the effects of different nitrate concentrations provided in culture medium were assessed with respect to pigments production in four strains of *Nostoc* and *Anabaena*.

Moreover, if compared to the values obtained in the previous section *§5.3.4.1*, it is possible to clearly ascertain a different trend in pigments content with respect to the availability of nitrogen within cultivation medium. According to this, moving to an incipient limiting condition, namely for the data collected under diazotrophic behavior, a negative effect on such compounds can be highlighted, while larger nitrogen concentrations does not bring any significant effect.

Table 5.9. *Nostoc PCC 7120 pigments content with respect to the available nitrogen concentration (provided as $NaNO_3$). Means that do not share a letter are significantly different.*

Tested condition	Available nitrogen [mg L^{-1}]	Chlorophyll *a* content [mg gx^{-1}]		Carotenoids content [mg gx^{-1}]		Total content [mg gx^{-1}]	
		Mean	Std. dev	Mean	Std. dev	Mean	Std. dev
3	59.7	14.0 ^{A}	0.7	3.2 ^{B}	0.4	17.2 ^{C}	0.8
2	133.5	12.5 ^{A}	0.7	2.8 ^{B}	0.1	15.3 ^{C}	0.7
1	442.2	14.5 ^{A}	1.9	2.9 ^{B}	0.5	17.4 ^{C}	1.9

Similar conclusions can be made discussing sodium nitrate impact on phycobiliproteins production, as presented in figure 5.14 and table 5.10.

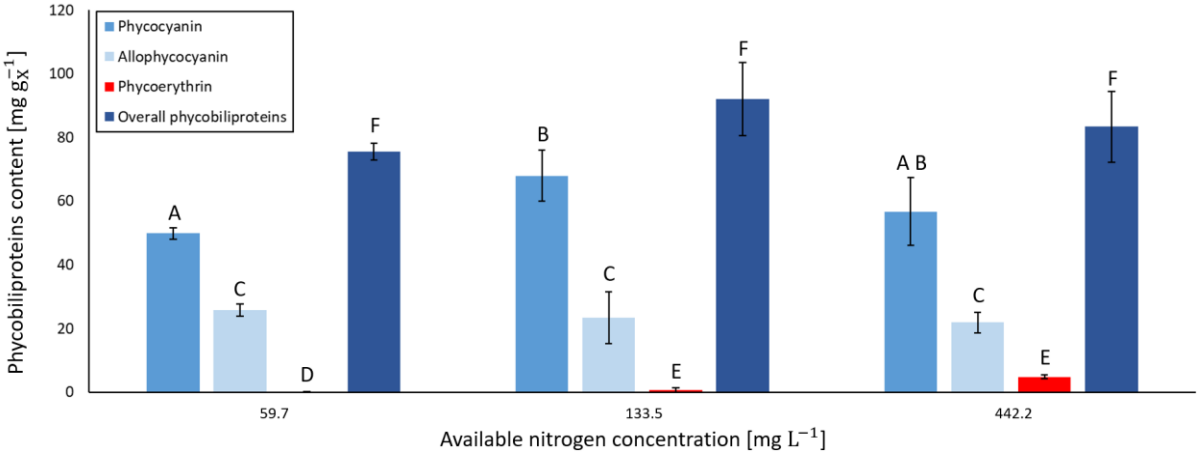

Figure 5.14. *Nostoc PCC 7120 phycobiliproteins content with respect to the available nitrogen concentration (provided in the form of $NaNO_3$). Means that do not share a letter are significantly different.*

Apart from a slight variation in phycoerythrin content, dropping to zero as a result of a reduction in nitrate supply in medium, phycobiliproteins profile remains quite steady with respect to the available nitrogen concentration, with a corresponding averaged value of 83.7 ± 8.2 mg g_X^{-1}. Interestingly, if compared to diazotrophic conditions values reported in section *§5.3.4.1*, a clear change of pace can be spotted, with a general higher production of these compounds in the latter case, except for condition 6. Indeed, the maximum production of phycobiliproteins can be spotted in condition 4*, with a value of 133.6 ± 9.2 mg g_X^{-1}. Along with that, such consideration can be then transposed to all the different individual

phycobiliproteins typologies. This peculiar species characteristic was already pointed out in a previous work, assessing specifically the production of phycocyanin in *Nostoc* (Lee et al., 2017); even if the analysis was performed in bottle-type PBRs under batch operations, also in this case a 5% increment in phycocyanin content in $BG11_0$ was obtained with respect to a cultivation in BG11, as it can be shown in this work. To confirm this, with references to table 5.10, phycocyanin content under non-diazotrophic conditions is 58.2 ± 9.1 mg g_X^{-1} on average, while the maximum is 89.9 ± 7.8 mg g_X^{-1}, as derived from diazotrophic condition 4*.

Table 5.10. *Nostoc PCC 7120 phycobiliproteins content with respect to the available nitrogen concentration (provided in the form of $NaNO_3$). Means that do not share a letter are significantly different.*

Tested condition	Available nitrogen [mg L^{-1}]	Phycocyanin content [mg g_X^{-1}]		Allophycocyanin content [mg g_X^{-1}]		Phycoerythrin content [mg g_X^{-1}]		Total content [mg g_X^{-1}]	
		Mean	Std. dev	Mean	Std. dev	Mean	Std. dev	Mean	Std. dev
3	59.7	49.9 ^{A}	1.8	25.8 ^{C}	1.9	0.0 ^{D}	0.1	75.7 ^{F}	2.6
2	133.5	68.0 ^{B}	8.0	23.3 ^{C}	8.2	0.7 ^{E}	0.8	92.0 ^{F}	11.5
1	442.2	56.8 ^{AB}	10.7	21.8 ^{C}	3.1	4.8 ^{E}	0.6	83.3 ^{F}	11.1

Again, in line with the previous discussion regarding pigments production, working under diazotrophic conditions seems to be the best option, as it can reduce capital costs related to nutrients purchase while optimizing valuable compounds production.

5.4 Batchwise cultivation results

As stated in section *§2.2.2*, *Nostoc* PCC 7120 behavior was also assessed under batch conditions in a 275-L pilot reactor. This was done to check species performances in a larger scale cultivation, with a view towards a potential process upscale. For that purpose, data regarding overall biomass, as well as vegetative cells and heterocysts cells were collected, as reported in figure 5.15.

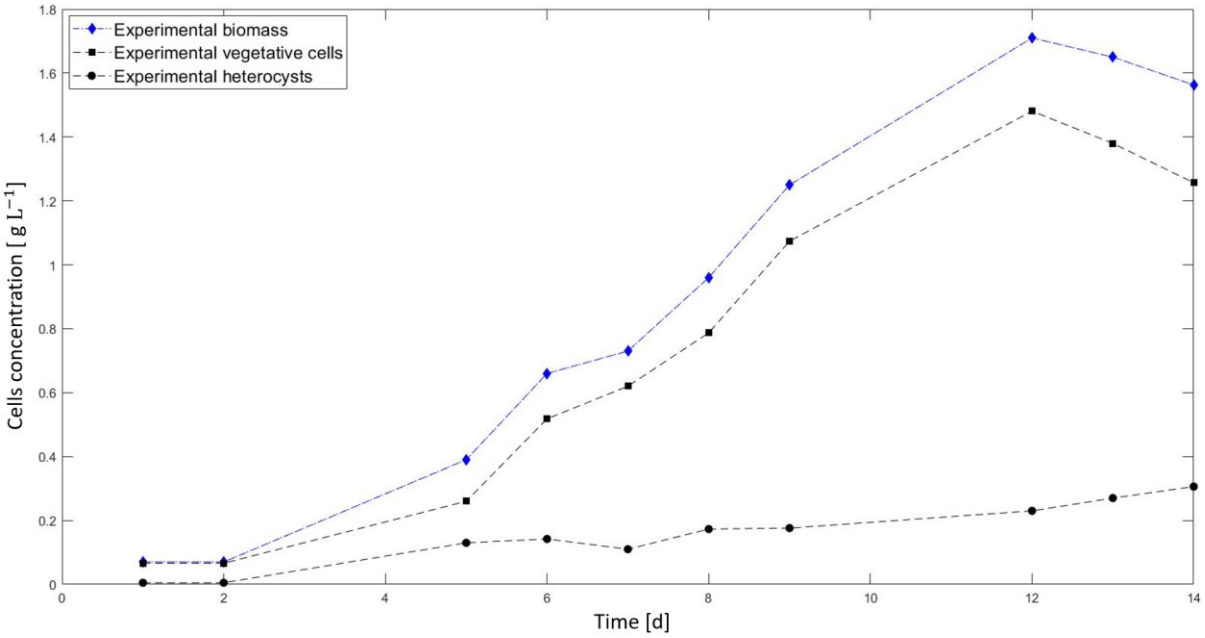

Figure 5.15. *Nostoc PCC 7120 growth curves under batch conditions.*

Specifically for the overall biomass concentration, the experimental trend thus reported resembles the theoretical batch growth curve already presented in section *§1.5.2*. It is possible to identify an initial lag phase (day 1-2), where biomass at 0.07 g L^{-1} is adapting to the growth environment, the exponential phase (day 2-12), with a rapid biomass build up, and a final stationary-death phase (day 12-14), where the species stops growing and then undergoes a progressive reduction in concentration. The experiment finished after 14 days, with a final biomass concentration equal to 1.56 g L^{-1}. Moreover, a maximum in overall biomass concentration was achieved on day 12, namely at 1.71 g L^{-1}. This result seems to be aligned with the final value of biomass concentration for *Nostoc* PCC 7120 under batch conditions reported in a previous master thesis work (Piazza, 2021), namely 1.80 ± 0.30 g L^{-1}. The data previously presented can be then manipulated in order to retrieve two performance indicators, specific for the assessed species in such system, namely its productivity P_X and maximum specific growth rate μ_{max}. For the first one, the value can be derived through equation (5.4):

$$P_X = \frac{C_{X,final} - C_{X,initial}}{n} \tag{5.4}$$

where the terms at the numerator refer to the initial and final biomass concentration within the cultivation system, while the n at the denominator represents the number of assessed days.

According to this formula, a biomass productivity equal to 106.6 mg L^{-1} d^{-1} was retrieved, value in accordance with the resulted productivity coming from the work of Piazza (2021). Concerning the maximum specific growth rate, the corresponding value can be derived through linear interpolation of biomass logarithmic trend within the exponential phase, with μ_{max} as the resulting slope, with a retrieved value equal to 0.27 d^{-1}. Also in this case, it is possible to identify the similarity with the corresponding value reported in the work of Piazza, 2021, namely 0.42 ± 0.14 d^{-1}.

In general terms, apart from a slight difference in terms of light intensity and available phosphorus concentration in medium, the resemblance between the cultivation performances reported from these two compared works becomes even more interesting if the different adopted cultivation scales are taken into account, since the values taken as comparison were obtained in 200 mL Quickfit® Drechsel bottles (Piazza, 2021). This allows to confirm the possibility of implementing *Nostoc* PCC 7120 in larger cultivation systems, in order to intensify biomass production, as well as consequent valuable extractable compounds.

With respect to the latter subject, also the investigation of valuable products stored in biomass represents a relevant aspect to tackle while tracking species growth performances. In this case, pigments and phycobiliproteins content was daily evaluated during the entire duration of the experiment, as illustrated in the following figures and tables.

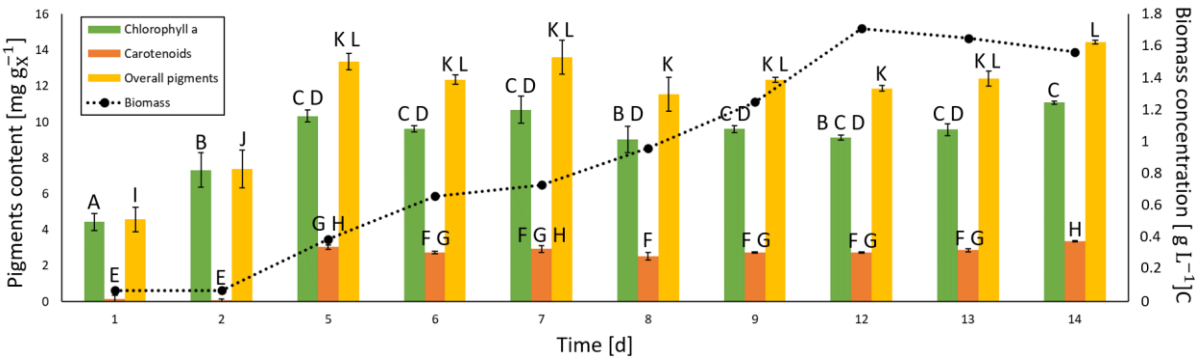

Figure 5.16. *Nostoc PCC 7120 pigments content in batch cultivation system. Means that do not share a letter are significantly different.*

Table 5.11. *Nostoc PCC 7120 pigments content in batch cultivation system. Means that do not share a letter are significantly different.*

Time [d]	Chlorophyll *a* content [mg g_X^{-1}]		Carotenoids content [mg g_X^{-1}]		Total content [mg g_X^{-1}]	
	Mean	Std. dev	Mean	Std. dev	Mean	Std. dev
1	4.4^{A}	0.5	0.1^{E}	0.2	4.6^{I}	0.7
2	7.3^{B}	1.0	0.1^{E}	0.1	7.4^{J}	1.0
5	10.3^{CD}	0.3	3.0^{GH}	0.1	13.4^{KL}	0.5
6	9.6^{CD}	0.2	2.7^{FG}	0.1	12.4^{KL}	0.3
7	10.7^{CD}	0.7	2.9^{FGH}	0.2	13.6^{KL}	0.9
8	9.0^{BD}	0.7	2.5^{F}	0.2	11.5^{K}	0.9
9	9.6^{CD}	0.2	2.7^{FG}	0.0	12.4^{KL}	0.2
12	9.1^{BCD}	0.1	2.7^{FG}	0.0	11.9^{K}	0.2
13	9.6^{CD}	0.3	2.9^{FG}	0.1	12.4^{KL}	0.4
14	11.1^{C}	0.1	3.4^{H}	0.0	14.4^{L}	0.1

Specifically for the overall pigments content in biomass, the initial increase in biomass provides a subsequent increment, which then tends to settle around 12.7 ± 1.0 mg g_X^{-1} on average. Moving then to the specific pigments typologies, namely chlorophyll *a* and carotenoids, similar trends can be highlighted, with an asymptote respectively at 9.9 ± 0.7 mg g_X^{-1} and 2.9 ± 0.3 mg g_X^{-1}. In addition, a fairly constant ratio between the two can be spotted, equal to 3.5 ± 0.1.

Moving then to phycobiliproteins content, the results are presented in figure 5.17 and table 5.12. The presence of a maximum in overall phycobiliproteins content in biomass can be perceived, between day 5 and 8 approximately, at around 9% of DW. After that, in conjunction with the last stages of a batch cultivation system, the overall content tends to progressively decrease. From a biological perspective, this can be explained by the occurrence of photoinhibition processes; indeed, as biomass tends to increase in concentration, the average amount of light available to the culture tends to diminish, thus reducing the necessity of having well developed phycobilisomes. Moreover, it is also possible to point out the peculiar trend of

phycoerythrin content, showing a maximum in the same time slot as the one previously discussed.

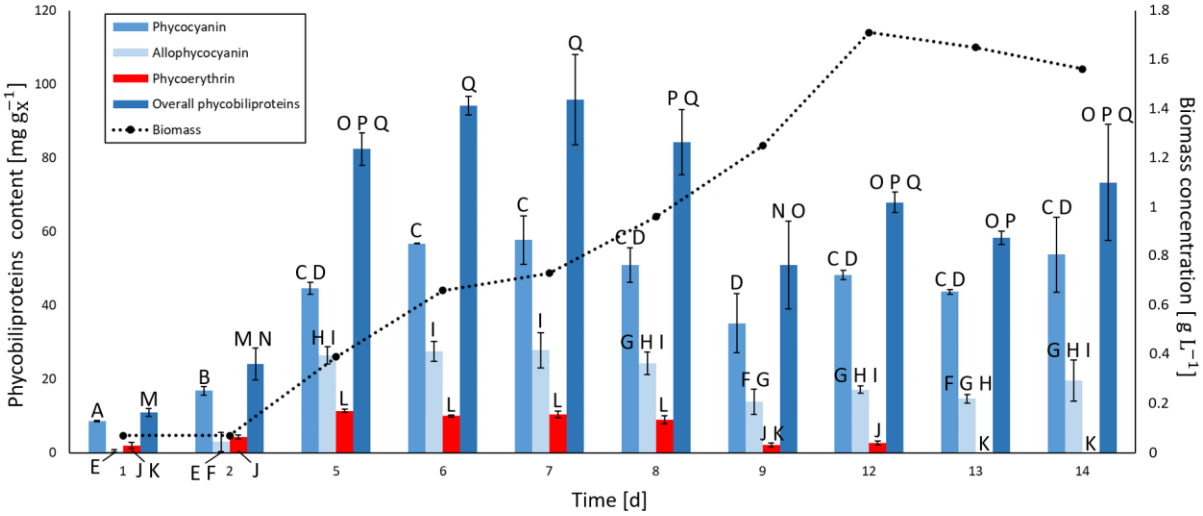

Figure 5.17. *Nostoc PCC 7120 phycobiliproteins content in batch cultivation system. Means that do not share a letter are significantly different.*

Table 5.12. *Nostoc PCC 7120 phycobiliproteins content in batch cultivation system. Means that do not share a letter are significantly different.*

Time [d]	Phycocyanin content [mg gx^{-1}]		Allophycocyanin content [mg gx^{-1}]		Phycoerythrin content [mg gx^{-1}]		Total content [mg gx^{-1}]	
	Mean	Std. dev	Mean	Std. dev	Mean	Std. dev	Mean	Std. dev
1	8.5^{A}	0.2	0.4^{E}	0.4	1.9^{JK}	0.8	10.9^{M}	1.1
2	16.8^{B}	1.2	2.9^{EF}	2.6	4.3^{J}	0.5	24.0^{MN}	4.3
5	44.6^{CD}	1.6	26.4^{HI}	2.4	11.3^{L}	0.4	82.4^{OPQ}	4.4
6	56.7^{C}	0.1	27.6^{I}	2.7	10.0^{L}	0.3	94.2^{Q}	2.5
7	57.7^{C}	6.6	27.8^{I}	4.7	10.3^{L}	0.9	95.8^{Q}	12.2
8	51.0^{CD}	4.7	24.3^{GHI}	3.0	9.0^{L}	1.0	84.2^{PQ}	8.8
9	35.1^{D}	8.0	13.8^{FG}	3.4	2.0^{JK}	0.5	50.9^{NO}	11.9
12	48.2^{CD}	1.3	17.1^{GHI}	0.9	2.6^{J}	0.5	67.9^{OPQ}	2.7
13	43.7^{CD}	0.6	14.6^{FGH}	1.2	0.0^{K}	0.0	58.3^{OP}	1.8
14	53.7^{CD}	10.2	19.5^{GHI}	5.6	0.0^{K}	0.0	73.3^{OPQ}	15.8

Based on what has been discussed so far, the time span between day 7 and 8 may represent the optimal one for collecting biomass out of the cultivation equipment. Indeed, the optimal condition should be the result of a compromise between harvested concentration and embedded valuable compounds content, aimed at maximizing as much as possible these aspects. From a processing point of view, being able to reach such condition does not simply provide higher productions, but also allows to boost economic feasibility of the latter. As a matter of example, by applying such rationale, capital and operation costs needed for downstream extraction and purification processes would result to be lower.

Conclusions

The aim of this thesis was to deepen the discussion about filamentous heterocystic nitrogen-fixing cyanobacteria, and more specifically about the potential exploitation of that peculiar metabolic process for the subsequent production of valuable compounds for the food and feed industry. Since the several advantages of a continuous CSTR configuration with respect to a batchwise one are widely known, especially in terms of biomass productivity steadiness, the investigation was first conducted in lab-scale (200 mL) chemostat photobioreactors. According to the selected configuration, a residence time equal to 1 day was fixed for all the tested conditions. In detail, the choice made allowed to assess the influence of certain operating parameters on *Nostoc* PCC 7120 cultures, such enlightenment conditions, and nutrients availability. With respect to the first aspect, the effect of light intensity provided to the culture was investigated. Based on the derived results, an optimal light intensity value was found, equal to 550 μmol m^{-2} s^{-1}, as the best compromise between culture performances and embedded valuable extractable products.

So, keeping the light intensity at the optimal value, the investigation then moved to the second operating parameter, namely the nitrogen concentration in solution, and the reason is related to the nitrogen fixation process performed by the cyanobacterial species under study. Since the literature sustains that atmospheric dinitrogen should be enough for sustaining biomass growth, the analysis was aimed at understanding the effects of its availability. First of all, under diazotrophic conditions, by diluting the air enriched in CO_2 inlet stream with argon, a progressive limitation condition was reached, with a subsequent reduction in terms of biomass concentration and corresponding stored compounds. For the same purpose, *Nostoc* PCC 7120 was also cultivated in media enriched in nitrogen, which was provided in different concentrations in form of sodium nitrate. In this case, an inhibitory effect was highlighted at higher nitrogen concentration (442.2 mg L^{-1}), providing an overall decrease in cultivation performances. In light of this, the advantage of working under conventional diazotrophic conditions was confirmed. From a cultivation perspective, this is due to the possibility of reaching a maximum not only in terms of biomass concentration and productivity but also in terms of obtainable compounds. Indeed, under an incident light intensity of 550 μmol m^{-2} s^{-1}

combined with 13.3 mg L^{-1} of dissolved nitrogen in medium, a biomass concentration equal to 1.058 ± 0.022 g L^{-1} with an overall productivity of 0.991 ± 0.020 g L^{-1} d^{-1} was obtained, characterized at the same time by a satisfying content of internal compounds, such as pigments and phycobiliproteins. With respect to pigments, an overall content equal to 18.6 ± 0.9 mg g_X^{-1} can be achieved, including chlorophyll *a* and carotenoids, respectively at 15.2 ± 0.9 and 3.3 ± 0.3 mg g_X^{-1}. Concerning phycobiliproteins then, a maximum content equal to 133.6 ± 9.2 mg g_X^{-1} was reached, mainly associated with a maximum production in phycocyanin, reaching an internal content of around 89.9 ± 7.8 mg g_X^{-1}. Besides cultivation performances, focusing on possible future industrial application, the possibility of exploiting only atmospheric dinitrogen seems to be advantageous from an economic point of view, as it would imply a significant capital costs reduction related to nitrogen-based nutrient supplying.

The last part of this experimental campaign was oriented to batch cultivation, in order to derive the main growth performance indicator of such species, namely the specific maximum growth rate μ_{max}, in a pilot scale system. For the purpose, a 275-L tubular photobioreactor was used, in order to assess the cyanobacterium behavior in cultivation scales more similar to the industrial ones. The results show the species capability of optimally adapting to a different culture environment, as for example the derived μ_{max} value, namely 0.270 d^{-1}, is comparable to the one derived in smaller scales cultivation.

To complete the discussion, a predictive mathematical model was assessed, in order to accurately describe the behavior of such microalgal category and the corresponding continuous cultivation outcomes. The major model peculiarity is represented by the possibility of describing the species growth through both typologies of cells, namely vegetative cells and heterocysts, by simultaneously characterizing the way in which nitrogen, as the limiting nutrient, is fixed within biomass. From a mathematical perspective, this step was accomplished by the introduction of the concept of nitrogen quota, implemented in the Droop kinetics for describing microbial behavior. This kind of model was already known in the literature, but only at a theoretical level, without any successful practical application. In this work, such model has been taken up and appropriately modified to adapt it to the experimental behavior of nitrogen-fixing cyanobacteria, as reported from previous experimental campaigns. From an operative perspective, one of the major bottlenecks of its theoretical version regards the values of the deriving additional model parameters: if previously these were retrieved by rough

estimations and sensitivity analyses, now their derivation must follow another rationale, in order to find values that match the biological behavior of the species under assessment. For the purpose, the experimental data were used to fit such additional model unknown parameters for two cyanobacterial species, namely *Anabaena* PCC 7122 and *Nostoc* PCC 7120. Although the model seems to work reasonably well, a more detailed investigation would be required, aimed at evaluating its predictive capabilities with respect to operating variables other than residence time. In this respect, further experimental analyses would be required, either to state potential correlations between biomass behavior and other operating variables, or to refine some of the model parameters involved.

References

Aaronson, S., & Dubinsky, Z. (1982). Mass production of microalgae. *Experientia*, *38*(1), 36–40. https://doi.org/10.1007/BF01944523/METRICS

Abed, R. M. M. (2009). *Interaction between cyanobacteria and aerobic heterotrophic bacteria in the degradation of hydrocarbons*. https://doi.org/10.1016/j.ibiod.2009.10.008

Allen, M. M., & Smith, A. J. (1969). Nitrogen chlorosis in blue-green algae. *Archiv Für Mikrobiologie*, *69*(2), 114–120. https://doi.org/10.1007/BF00409755

Alves De Oliveira, C., De Castro Oliveira, W., Machado, S., Ribeiro, R., Stringheta, P. C., & Galvão Do Nascimento, A. (2014). EFFECT OF LIGHT INTENSITY ON THE PRODUCTION OF PIGMENTS IN NOSTOC SPP. In *European Journal of Biology and Medical Science Research* (Vol. 2, Issue 1). www.ea-journals.org

Andrews, J. F. (1968). A mathematical model for the continuous culture of microorganisms utilizing inhibitory substrates. *Biotechnology and Bioengineering*, *10*(6), 707–723. https://doi.org/10.1002/BIT.260100602

Aroniada, M., Maina, S., Koutinas, A., & Kookos, I. K. (2020). Estimation of volumetric mass transfer coefficient (kLa)—Review of classical approaches and contribution of a novel methodology. *Biochemical Engineering Journal*, *155*, 107458. https://doi.org/10.1016/J.BEJ.2019.107458

Arrigo, K. R. (2005). Marine microorganisms and global nutrient cycles. *Nature*, *437*(7057), 349–355. https://doi.org/10.1038/NATURE04159

Assunção, J., Amaro, H. M., Malcata, F. X., & Guedes, A. C. (2022). Cyanobacterial pigments: photosynthetic function and biotechnological purposes. *The Pharmacological Potential of Cyanobacteria*, 201–256. https://doi.org/10.1016/B978-0-12-821491-6.00008-9

Barbera, E., Turetta, M., & Sforza, E. (2022). The effect of the internal nutrient quota accumulation on algal-based wastewater treatment: Decoupling HRT and SRT to improve the process. *Journal of Water Process Engineering*, *49*, 103112. https://doi.org/10.1016/J.JWPE.2022.103112

Barkia, I., Saari, N., & Manning, S. R. (2019). Microalgae for High-Value Products Towards Human Health and Nutrition. *Marine Drugs*, *17*(5). https://doi.org/10.3390/MD17050304

Baselga-Cervera, B., Balboa, C. G., Costas, E., & Lopez-Rodas, victoria. (2014). Why Cyanobacteria Produce Toxins? Evolutionary Game Theory Suggests the Key. *International Journal of Biology*, *7*(1), p64. https://doi.org/10.5539/IJB.V7N1P64

Batista, A. P., Gouveia, L., Bandarra, N. M., Franco, J. M., & Raymundo, A. (2013). Comparison of microalgal biomass profiles as novel functional ingredient for food products. *Algal Research*, *2*(2), 164–173. https://doi.org/10.1016/J.ALGAL.2013.01.004

Béchet, Q., Shilton, A., & Guieysse, B. (2013). Modeling the effects of light and temperature on algae growth: State of the art and critical assessment for productivity prediction during outdoor cultivation. *Biotechnology Advances*, *31*(8), 1648–1663. https://doi.org/10.1016/J.BIOTECHADV.2013.08.014

Bennett, A., & Bogobad, L. (1973). COMPLEMENTARY CHROMATIC ADAPTATION IN A FILAMENTOUS BLUE-GREEN ALGA. *Journal of Cell Biology*, *58*(2), 419–435. https://doi.org/10.1083/JCB.58.2.419

Bernard, O., & Rémond, B. (2012). Validation of a simple model accounting for light and temperature effect on microalgal growth. *Bioresource Technology*, *123*, 520–527. https://doi.org/10.1016/J.BIORTECH.2012.07.022

Borella, L. (2017). *UNO STUDIO SPERIMENTALE SULLA FISSAZIONE BIOLOGICA DELL'AZOTO MEDIANTE CIANOBATTERI, PER APPLICAZIONI INDUSTRIALI*.

Borella, L., Sforza, E., & Bertucco, A. (2021). Effect of residence time in continuous photobioreactor on mass and energy balance of microalgal protein production. *New Biotechnology*, *64*, 46–53. https://doi.org/10.1016/J.NBT.2021.05.006

Bothe, H., Schmitz, O., Yates, M. G., & Newton, W. E. (2010). Nitrogen Fixation and Hydrogen Metabolism in Cyanobacteria. *Microbiology and Molecular Biology Reviews*, *74*(4), 529–551. https://doi.org/10.1128/MMBR.00033-10/ASSET/6A89F896-E2C7-4CB2-B80B-3DABFEBFDB6F/ASSETS/GRAPHIC/ZMR9990922580010.JPEG

Brennan, L., & Owende, P. (2010). Biofuels from microalgae—A review of technologies for production, processing, and extractions of biofuels and co-products. *Renewable and Sustainable Energy Reviews*, *14*(2), 557–577. https://doi.org/10.1016/J.RSER.2009.10.009

Bulgac, A. (2021). *Nitrogen fixation in cyanobacteria towards new bio-based industrial approaches: experiments and process simulation*.

Cejudo, F. J., & Paneque, A. (1986). Short-term nitrate (nitrite) inhibition of nitrogen fixation in Azotobacter chroococcum. *Journal of Bacteriology*, *165*(1), 240. https://doi.org/10.1128/JB.165.1.240-243.1986

Cerri, M. O., Nordi Esperança, M., Badino, A. C., & Perencin de Arruda Ribeiro, M. (2016). A new approach for kLa determination by gassing-out method in pneumatic bioreactors. *Journal of Chemical Technology & Biotechnology*, *91*(12), 3061–3069. https://doi.org/10.1002/JCTB.4937

Chandra, R., Parra, R., & M. N. Iqbal, H. (2016). Phycobiliproteins: A Novel Green Tool from Marine Origin Blue-Green Algae and Red Algae. *Protein & Peptide Letters*, *24*(2), 118–125. https://doi.org/10.2174/0929866523666160802160222

Chen, S., Perathoner, S., Ampelli, C., & Centi, G. (2019). Electrochemical Dinitrogen Activation: To Find a Sustainable Way to Produce Ammonia. *Studies in Surface Science and Catalysis*, *178*, 31–46. https://doi.org/10.1016/B978-0-444-64127-4.00002-1

Chomel, M., Guittonny-Larchevêque, M., Fernandez, C., Gallet, C., DesRochers, A., Paré, D., Jackson, B. G., & Baldy, V. (2016). Plant secondary metabolites: a key driver of litter decomposition and soil nutrient cycling. *Journal of Ecology*, *104*(6), 1527–1541. https://doi.org/10.1111/1365-2745.12644

Costa, J. A. V., & de Morais, M. G. (2014). An Open Pond System for Microalgal Cultivation. *Biofuels from Algae*, 1–22. https://doi.org/10.1016/B978-0-444-59558-4.00001-2

Crini, G., & Lichtfouse, E. (2019). *Advantages and disadvantages of techniques used for wastewater treatment*. *17*, 145–155. https://doi.org/10.1007/s10311-018-0785-9

Delrue, F., Alaux, E., Moudjaoui, L., Gaignard, C., Fleury, G., Perilhou, A., Richaud, P., Petitjean, M., & Sassi, J. F. (2017). Optimization of Arthrospira platensis (Spirulina) growth: From laboratory scale to pilot scale. *Fermentation*, *3*(4). https://doi.org/10.3390/FERMENTATION3040059

Do Nascimento, M., Sanchez Rizza, L., Arruebarrena Di Palma, A., Dublan, M. de los A., Salerno, G., Rubio, L. M., & Curatti, L. (2015). Cyanobacterial biological nitrogen fixation as a sustainable nitrogen fertilizer for the production of microalgal oil. *Algal Research*, *12*, 142–148. https://doi.org/10.1016/J.ALGAL.2015.08.017

Droop, M. R. (1968). Vitamin B12 and Marine Ecology. IV. The Kinetics of Uptake, Growth and Inhibition in Monochrysis Lutheri. *Journal of the Marine Biological Association of the United Kingdom*, *48*(3), 689–733. https://doi.org/10.1017/S0025315400019238

Droop, M. R. (1983). 25 Years of Algal Growth Kinetics: A Personal View. *Botanica Marina*, *26*(3), 99–112. https://doi.org/10.1515/BOTM.1983.26.3.99

Facciola, S. (1990). *Cornucopia: a source book of edible plants*. https://worldveg.tind.io/record/15629

Fontes, A. G., Angeles Vargas, M., Moreno, J., Guerrero, M. G., & Losada, M. (1987). Factors affecting the production of biomass by a nitrogen-fixing blue-green alga in outdoor culture. *Biomass*, *13*(1), 33–43. https://doi.org/10.1016/0144-4565(87)90070-9

Gallon, J. R. (1992). Reconciling the incompatible: N2 fixation And O2. *New Phytologist*, *122*(4), 571–609. https://doi.org/10.1111/J.1469-8137.1992.TB00087.X

Gantar, M., & Svirčev, Z. (2008). MICROALGAE AND CYANOBACTERIA: FOOD FOR THOUGHT(1). *Journal of Phycology*, *44*(2), 260–268. https://doi.org/10.1111/J.1529-8817.2008.00469.X

Garcia-Pichel, F. (2009). Cyanobacteria. *Encyclopedia of Microbiology, Third Edition*, 107–124. https://doi.org/10.1016/B978-012373944-5.00250-9

Giddings, T. H., & Staehelin, L. A. (1981). Observation of microplasmodesmata in both heterocyst-forming and non-heterocyst forming filamentous cyanobacteria by freeze-fracture electron microscopy. *Archives of Microbiology*, *129*(4), 295–298. https://doi.org/10.1007/BF00414700

Grandi, A. (2018). *Biological nitrogen fixation by cyanobacteria for industrial applications: experimental investigation and process simulation*.

Grover, J. P., Scott, J. T., Roelke, D. L., Brooks, B. W., Grover, J. P., Scott, J. T., Roelke, D. L., & Brooks, B. W. (2019). Dynamics of nitrogen-fixing cyanobacteria with heterocysts: a stoichiometric model. *Marine and Freshwater Research*, *71*(5), 644–658. https://doi.org/10.1071/MF18361

Halliwell, B. (2003). Antioxidants in Human Health and Disease. *Https://Doi.Org/10.1146/Annurev.Nu.16.070196.000341*, *16*, 33–50. https://doi.org/10.1146/ANNUREV.NU.16.070196.000341

Handbook of Microalgal Culture. (2003). *Handbook of Microalgal Culture*. https://doi.org/10.1002/9780470995280

Havlik, I., Scheper, T., & Reardon, K. F. (2016). Monitoring of Microalgal Processes. *Advances in Biochemical Engineering/Biotechnology*, *153*, 89–142. https://doi.org/10.1007/10_2015_328

Heinisch, O. (1962). Steel, R. G. D., and J. H. Torrie: Principles and Procedures of Statistics. (With special Reference to the Biological Sciences.) McGraw-Hill Book Company, New York, Toronto, London 1960, 481 S., 15 Abb.; 81 s 6 d. *Biometrische Zeitschrift*, *4*(3), 207–208. https://doi.org/10.1002/BIMJ.19620040313

Henrikson, R., Yoro, C., & Ruppert, R. (1989). *Fifth Printing, Revised Edition Online*. www.spirulinasource.com

Ibraheem, I. B. M. (2010). BIODEGRADABILITY OF HYDROCARBONS BY CYANOBACTERIA1. *Journal of Phycology*, *46*(4), 818–824. https://doi.org/10.1111/J.1529-8817.2010.00865.X

Ivleva, N. B., & Golden, S. S. (2007). Protein extraction, fractionation, and purification from cyanobacteria. *Methods in Molecular Biology (Clifton, N.J.)*, *362*, 365–373. https://doi.org/10.1007/978-1-59745-257-1_26

Jiang, Y., Fan, K. W., Wong, R. T. Y., & Chen, F. (2004). Fatty acid composition and squalene content of the marine microalga Schizochytrium mangrovei. *Journal of Agricultural and Food Chemistry*, *52*(5), 1196–1200. https://doi.org/10.1021/JF035004C

Karthik, V., Saravanan, K., Bharathi, P., Dharanya, V., & Meiaraj, C. (2015). *An overview of treatments for the removal of textile dyes*.

Ketchum, B. H. (1939). The Absorption of Phosphate and Nitrate by Illuminated Cultures of Nitzschia Closterium. *American Journal of Botany*, *26*(6), 399. https://doi.org/10.2307/2436840

Khajepour, F., Hosseini, S. A., Ghorbani Nasrabadi, R., & Markou, G. (2015). Effect of Light Intensity and Photoperiod on Growth and Biochemical Composition of a Local Isolate of Nostoc calcicola. *Applied Biochemistry and Biotechnology*, *176*(8), 2279–2289. https://doi.org/10.1007/S12010-015-1717-9/TABLES/1

Khalifa, S. A. M., Shedid, E. S., Saied, E. M., Jassbi, A. R., Jamebozorgi, F. H., Rateb, M. E., Du, M., Abdel-Daim, M. M., Kai, G. Y., Al-Hammady, M. A. M., Xiao, J., Guo, Z., &

El-Seedi, H. R. (2021). Cyanobacteria—From the Oceans to the Potential Biotechnological and Biomedical Applications. *Marine Drugs 2021, Vol. 19, Page 241*, *19*(5), 241. https://doi.org/10.3390/MD19050241

Khan, M. I., Shin, J. H., & Kim, J. D. (2018). The promising future of microalgae: current status, challenges, and optimization of a sustainable and renewable industry for biofuels, feed, and other products. *Microbial Cell Factories 2018 17:1*, *17*(1), 1–21. https://doi.org/10.1186/S12934-018-0879-X

KUENZLER, E. J., & KETCHUM, B. H. (1962). RATE OF PHOSPHORUS UPTAKE BY PHAEODACTYLUM TRICORNUTUM. *Https://Doi.Org/10.2307/1539510*, *123*(1), 134–145. https://doi.org/10.2307/1539510

Kumar, J., Singh, D., Tyagi, M. B., & Kumar, A. (2018). Cyanobacteria: Applications in Biotechnology. *Cyanobacteria: From Basic Science to Applications*, 327–346. https://doi.org/10.1016/B978-0-12-814667-5.00016-7

Kumar, K., Mella-Herrera, R. A., & Golden, J. W. (2010). Cyanobacterial heterocysts. *Cold Spring Harbor Perspectives in Biology*, *2*(4). https://doi.org/10.1101/CSHPERSPECT.A000315

Lane, N. (2017). Serial endosymbiosis or singular event at the origin of eukaryotes? *Journal of Theoretical Biology*, *434*, 58–67. https://doi.org/10.1016/J.JTBI.2017.04.031

Lee, N. K., Oh, H. M., Kim, H. S., & Ahn, C. Y. (2017). Higher production of C-phycocyanin by nitrogen-free (diazotrophic) cultivation of Nostoc sp. NK and simplified extraction by dark-cold shock. *Bioresource Technology*, *227*, 164–170. https://doi.org/10.1016/J.BIORTECH.2016.12.053

Liu, H. (2014). Ammonia synthesis catalyst 100 years: Practice, enlightenment and challenge. *Chinese Journal of Catalysis*, *35*(10), 1619–1640. https://doi.org/10.1016/S1872-2067(14)60118-2

Loreto, C., Rosales, N., Bermúdez, J., & Morales, E. (2003). PRODUCCION DE PIGMENTOS Y PROTEINAS DE LA CIANOBACTERIA ANABAENA PCC 7120 EN RELACION A LA CONCENTRACION DE NITROGENO E IRRADIANCIA. *Gayana. Botánica*, *60*(2), 83–89. https://doi.org/10.4067/S0717-66432003000200001

Lundell, D. J., Williams, R. C., & Glazer, A. N. (1981). Molecular architecture of a light-harvesting antenna. In vitro assembly of the rod substructures of Synechococcus 6301

phycobilisomes. *Journal of Biological Chemistry*, *256*(7), 3580–3592. https://doi.org/10.1016/s0021-9258(19)69648-1

Maltsev, Y., Maltseva, K., Kulikovskiy, M., & Maltseva, S. (2021). Influence of Light Conditions on Microalgae Growth and Content of Lipids, Carotenoids, and Fatty Acid Composition. *Biology 2021, Vol. 10, Page 1060*, *10*(10), 1060. https://doi.org/10.3390/BIOLOGY10101060

Mao, R., & Guo, S. (2018). Performance of the mixed LED light quality on the growth and energy efficiency of Arthrospira platensis. *Applied Microbiology and Biotechnology*, *102*(12), 5245–5254. https://doi.org/10.1007/S00253-018-8923-7

Martín-Figueroa, E., Navarro, F., & Florencio, F. J. (2000). The GS-GOGAT pathway is not operative in the heterocysts. Cloning and expression of glsF gene from the cyanobacterium Anabaena sp. PCC 7120. *FEBS Letters*, *476*(3), 282–286. https://doi.org/10.1016/S0014-5793(00)01722-1

Martins, A. A., Marques, F., Cameira, M., Santos, E., Badenes, S., Costa, L., Vieira, V. V., Caetano, N. S., & Mata, T. M. (2018). Water footprint of microalgae cultivation in photobioreactor. *Energy Procedia*, *153*, 426–431. https://doi.org/10.1016/J.EGYPRO.2018.10.031

Masojídek, J., Torzillo, G., & Koblízek, M. (2013). Photosynthesis in Microalgae. *Handbook of Microalgal Culture: Applied Phycology and Biotechnology: Second Edition*, 21–36. https://doi.org/10.1002/9781118567166.CH2

Mazard, S., Penesyan, A., Ostrowski, M., Paulsen, I. T., & Egan, S. (2016). Tiny Microbes with a Big Impact: The Role of Cyanobacteria and Their Metabolites in Shaping Our Future. *Marine Drugs 2016, Vol. 14, Page 97*, *14*(5), 97. https://doi.org/10.3390/MD14050097

Meeks, J. C., Campbell, E. L., Summers, M. L., & Wong, F. C. (2002). Cellular differentiation in the cyanobacterium Nostoc punctiforme. *Archives of Microbiology*, *178*(6), 395–403. https://doi.org/10.1007/S00203-002-0476-5

Mekonnen, M. M., & Hoekstra, A. Y. (2010). *Value of Water Research Report Series No. 48 Value of Water*.

Monod, J. (1942). Recherches sur la croissance des cultures bactériennes. *(No Title)*. https://cir.nii.ac.jp/crid/1130282273101108736

Mostert, E. S., & Grobbelaar, J. U. (1987). The influence of nitrogen and phosphorus on algal growth and quality in outdoor mass algal cultures. *Biomass*, *13*(4), 219–233. https://doi.org/10.1016/0144-4565(87)90061-8

Muro-Pastor, A. M., & Hess, W. R. (2012). Heterocyst differentiation: from single mutants to global approaches. *Trends in Microbiology*, *20*(11), 548–557. https://doi.org/10.1016/J.TIM.2012.07.005

Nasr, M. (2018). Modeling applications in environmental bioremediation studies. *Phytobiont and Ecosystem Restitution*, 143–160. https://doi.org/10.1007/978-981-13-1187-1_7

Nitin Thukral, M. S. (2015). Microalgae as Future Fuel: Real Opportunities and Challenges. *Journal of Thermodynamics and Catalysis*, *06*(01). https://doi.org/10.4172/2157-7544.1000139

OECD-FAO Agricultural Outlook 2021-2030. (2021). https://doi.org/10.1787/agr-outl-data

Opeolu, B. O., Bamgbose, O., Arowolo, T. A., & Adetunji, M. T. (2010). Utilization of biomaterials as adsorbents for heavy metals' removal from aqueous matrices. *Scientific Research and Essays*, *5*(14), 1780–1787. http://www.academicjournals.org/SRE

Pancha, I., Chokshi, K., George, B., Ghosh, T., Paliwal, C., Maurya, R., & Mishra, S. (2014). Nitrogen stress triggered biochemical and morphological changes in the microalgae Scenedesmus sp. CCNM 1077. *Bioresource Technology*, *156*, 146–154. https://doi.org/10.1016/J.BIORTECH.2014.01.025

Pawar, S. B. (2016). Process Engineering Aspects of Vertical Column Photobioreactors for Mass Production of Microalgae. *ChemBioEng Reviews*, *3*(3), 101–115. https://doi.org/10.1002/CBEN.201600003

Pedersen, D., & Miller, S. R. (2017). Photosynthetic temperature adaptation during niche diversification of the thermophilic cyanobacterium Synechococcus A/B clade. *The ISME Journal*, *11*(4), 1053–1057. https://doi.org/10.1038/ISMEJ.2016.173

Peter, A. P., Koyande, A. K., Chew, K. W., Ho, S. H., Chen, W. H., Chang, J. S., Krishnamoorthy, R., Banat, F., & Show, P. L. (2022). Continuous cultivation of microalgae in photobioreactors as a source of renewable energy: Current status and future challenges. *Renewable and Sustainable Energy Reviews*, *154*, 111852. https://doi.org/10.1016/J.RSER.2021.111852

Piazza, F. (2021). *Produzione di cianoficina con cianobatteri diazotrofi: ottimizzazione delle condizioni di coltura*.

Posten, C. (2009). Design principles of photo-bioreactors for cultivation of microalgae. *Engineering in Life Sciences*, *9*(3), 165–177. https://doi.org/10.1002/ELSC.200900003

Pratte, B. S., Eplin, K., & Thiel, T. (2006). Cross-Functionality of Nitrogenase Components NifH1 and VnfH in Anabaena variabilis. *Journal of Bacteriology*, *188*(16), 5806. https://doi.org/10.1128/JB.00618-06

Rafiqul, I., Weber, C., Lehmann, B., & Voss, A. (2005). Energy efficiency improvements in ammonia production—perspectives and uncertainties. *Energy*, *30*(13), 2487–2504. https://doi.org/10.1016/J.ENERGY.2004.12.004

Raqiba H, & Sibi G. (2019). Light Emitting Diode (LED) Illumination For Enhanced Growth And Cellular Composition In Three Microalgae. *Advances in Microbiology Research*, *3*(1), 1–6. https://doi.org/10.24966/AMR-694X/100007

Rastogi, R. P., Sonani, R. R., Madamwar, D., & Incharoensakdi, A. (2016). Characterization and antioxidant functions of mycosporine-like amino acids in the cyanobacterium Nostoc sp. R76DM. *Algal Research*, *16*, 110–118. https://doi.org/10.1016/J.ALGAL.2016.03.009

Raven, J. A., & Ralph, P. J. (2015). Enhanced biofuel production using optimality, pathway modification and waste minimization. *Journal of Applied Phycology*, *27*(1), 1–31. https://doi.org/10.1007/S10811-014-0323-5/TABLES/3

Razzak, S. A., Hossain, M. M., Lucky, R. A., Bassi, A. S., & De Lasa, H. (2013). Integrated CO2 capture, wastewater treatment and biofuel production by microalgae culturing - A review. *Renewable and Sustainable Energy Reviews*, *27*, 622–653. https://doi.org/10.1016/j.rser.2013.05.063

Richmond, A., & Preiss, K. (1980). The Biotechnology of Algaculture. *Interdisciplinary Science Reviews*, *5*(1), 60–70. https://doi.org/10.1179/030801880789767891

Riethman, H., Bullerjahn, G., Reddy, K. J., & Sherman, L. A. (1988). Regulation of cyanobacterial pigment-protein composition and organization by environmental factors. *Photosynthesis Research*, *18*(1–2), 133–161. https://doi.org/10.1007/BF00042982

Rippka, R., Deruelles, J., & Waterbury, J. B. (1979). Generic assignments, strain histories and properties of pure cultures of cyanobacteria. *Journal of General Microbiology*, *111*(1), 1–61. https://doi.org/10.1099/00221287-111-1-1/CITE/REFWORKS

Rosales Loaiza, N., Vera, P., Aiello-Mazzarri, C., & Morales, E. (2016). Comparative growth and biochemical composition of four strains of Nostoc and Anabaena (Cyanobacteria, Nostocales) in relation to sodium nitrate. *Acta Biologica Colombiana*, *21*(2), 347–354. https://doi.org/10.15446/ABC.V21N2.48883

Saini, D. K., Pabbi, S., & Shukla, P. (2018). Cyanobacterial pigments: Perspectives and biotechnological approaches. *Food and Chemical Toxicology*, *120*, 616–624. https://doi.org/10.1016/J.FCT.2018.08.002

Sanz-Alférez, S., & del Campo, F. F. (1994). Relationship between nitrogen fixation and nitrate metabolism in the Nodularia strains M1 and M2. *Planta*, *194*(3), 339–345. http://www.jstor.org/stable/23383258

Sasongko, N. A., Noguchi, R., Ito, J., Demura, M., Ichikawa, S., Nakajima, M., & Watanabe, M. M. (2018). Engineering Study of a Pilot Scale Process Plant for Microalgae-Oil Production Utilizing Municipal Wastewater and Flue Gases: Fukushima Pilot Plant. *Energies 2018, Vol. 11, Page 1693*, *11*(7), 1693. https://doi.org/10.3390/EN11071693

Schulze, P. S. C., Barreira, L. A., Pereira, H. G. C., Perales, J. A., & Varela, J. C. S. (2014). Light emitting diodes (LEDs) applied to microalgal production. *Trends in Biotechnology*, *32*(8), 422–430. https://doi.org/10.1016/J.TIBTECH.2014.06.001

Sforza, E., Gris, B., De Farias Silva, C. E., Morosinotto, T., & Bertucco, A. (2014). Effects of Light on Cultivation of Scenedesmus Obliquus in Batch and Continuous Flat Plate Photobioreactor. *Chemical Engineering Transactions*, *38*, 211–216. https://doi.org/10.3303/CET1438036

Sforza, E., Pastore, M., Barbera, E., & Bertucco, A. (2019). Respirometry as a tool to quantify kinetic parameters of microalgal mixotrophic growth. *Bioprocess and Biosystems Engineering*, *42*(5), 839–851. https://doi.org/10.1007/S00449-019-02087-9/FIGURES/6

Shaikh, R., Rizvi, A., Pandit, S., Desai, N., & Patil, R. (2022). Microalgae: Classification, bioactives, medicinal properties, industrial applications, and future prospectives. *An Integration of Phycoremediation Processes in Wastewater Treatment*, 451–486. https://doi.org/10.1016/B978-0-12-823499-0.00004-3

Singh, D. P., Prabha, R., Verma, S., Meena, K. K., & Yandigeri, M. (2017). Antioxidant properties and polyphenolic content in terrestrial cyanobacteria. *3 Biotech*, *7*(2), 1–14. https://doi.org/10.1007/S13205-017-0786-6/TABLES/4

Singh, R. N., & Sharma, S. (2012). Development of suitable photobioreactor for algae production - A review. *Renewable and Sustainable Energy Reviews*, *16*(4), 2347–2353. https://doi.org/10.1016/j.rser.2012.01.026

Soeder, C. J. (1980). Massive cultivation of microalgae: Results and prospects. *Hydrobiologia*, *72*(1–2), 197–209. https://doi.org/10.1007/BF00016247/METRICS

Sonani, R. R., Roszak, A. W., Ortmann de Percin Northumberland, C., Madamwar, D., & Cogdell, R. J. (2018). An improved crystal structure of C-phycoerythrin from the marine cyanobacterium Phormidium sp. A09DM. *Photosynthesis Research*, *135*(1–3), 65–78. https://doi.org/10.1007/S11120-017-0443-2/FIGURES/7

Tan, T., Yu, J., & Shang, F. (2011). Biorefinery Engineering. *Comprehensive Biotechnology, Second Edition*, *2*, 815–828. https://doi.org/10.1016/B978-0-08-088504-9.00138-0

Tavanandi, H. A., Mittal, R., Chandrasekhar, J., & Raghavarao, K. S. M. S. (2018). Simple and efficient method for extraction of C-Phycocyanin from dry biomass of Arthospira platensis. *Algal Research*, *31*, 239–251. https://doi.org/10.1016/J.ALGAL.2018.02.008

Teo, C. L., Atta, M., Bukhari, A., Taisir, M., Yusuf, A. M., & Idris, A. (2014). Enhancing growth and lipid production of marine microalgae for biodiesel production via the use of different LED wavelengths. *Bioresource Technology*, *162*, 38–44. https://doi.org/10.1016/J.BIORTECH.2014.03.113

Touliabah, H. E. S., El-Sheekh, M. M., Ismail, M. M., & El-Kassas, H. (2022). A Review of Microalgae- and Cyanobacteria-Based Biodegradation of Organic Pollutants. *Molecules*, *27*(3). https://doi.org/10.3390/MOLECULES27031141

Trainor, F. R. (Francis R. (1978). *Introductory phycology*. 525. https://books.google.com/books/about/Introductory_Phycology.html?hl=it&id=L9sUAQAAIAAJ

Trentin, G., Piazza, F., Carletti, M., Zorin, B., Khozin-Goldberg, I., Bertucco, A., & Sforza, E. (2023). Fixing N2 into cyanophycin: continuous cultivation of Nostoc sp. PCC 7120. *Applied Microbiology and Biotechnology*, *107*(1), 97–110. https://doi.org/10.1007/S00253-022-12292-4/FIGURES/6

Valderrama, J. C. (1981). The simultaneous analysis of total nitrogen and total phosphorus in natural waters. *Marine Chemistry*, *10*(2), 109–122. https://doi.org/10.1016/0304-4203(81)90027-X

Vargas, M. A., Rodríguez, H., Moreno, J., Olivares, H., Del Campo, J. A., Rivas, J., & Guerrero, M. G. (1998). BIOCHEMICAL COMPOSITION AND FATTY ACID CONTENT OF FILAMENTOUS NITROGEN-FIXING CYANOBACTERIA. *Journal of Phycology*, *34*(5), 812–817. https://doi.org/10.1046/J.1529-8817.1998.340812.X

Vedana, M. (2022). *Coltivazione diazotrofica di Nostoc PCC 7120 in fotobioreattori continui per la produzione industriale di proteine*.

Venkata Mohan, S., Rohit, M. V., Chiranjeevi, P., Chandra, R., & Navaneeth, B. (2015). Heterotrophic microalgae cultivation to synergize biodiesel production with waste remediation: progress and perspectives. *Bioresource Technology*, *184*, 169–178. https://doi.org/10.1016/J.BIORTECH.2014.10.056

Villaró, S., Viñas, I., & Lafarga, T. (2021). Consumer acceptance and attitudes toward microalgae and microalgal-derived products as food. *Cultured Microalgae for the Food Industry: Current and Potential Applications*, 367–385. https://doi.org/10.1016/B978-0-12-821080-2.00001-0

Vincent, W. F., & Quesada, A. (2011). *Ultraviolet radiation effects on cyanobacteria: Implications for Antarctic microbial ecosystems*. 111–124. https://doi.org/10.1029/AR062P0111

Walsby, A. E. (1985). The permeability of heterocysts to the gases nitrogen and oxygen. *Proceedings of the Royal Society of London. Series B. Biological Sciences*, *226*(1244), 345–366. https://doi.org/10.1098/RSPB.1985.0099

Walsby, A. E. (2007). Cyanobacterial heterocysts: terminal pores proposed as sites of gas exchange. *Trends in Microbiology*, *15*(8), 340–349. https://doi.org/10.1016/j.tim.2007.06.007

Wang, H., Garcia, P. V., Ahmed, S., & Heggerud, C. M. (2022). Mathematical comparison and empirical review of the Monod and Droop forms for resource-based population dynamics. *Ecological Modelling*, *466*, 109887. https://doi.org/10.1016/J.ECOLMODEL.2022.109887

Wanner, U., & Egli, T. (1990). Dynamics of microbial growth and cell composition in batch culture. *FEMS Microbiology Letters*, *75*(1), 19–43. https://doi.org/10.1016/0378-1097(90)90521-Q

Wellburn, A. R. (1994). The Spectral Determination of Chlorophylls a and b, as well as Total Carotenoids, Using Various Solvents with Spectrophotometers of Different Resolution. *Journal of Plant Physiology*, *144*(3), 307–313. https://doi.org/10.1016/S0176-1617(11)81192-2

Wolk, C. P., Ernst, A., & Elhai, J. (1994). Heterocyst Metabolism and Development. *The Molecular Biology of Cyanobacteria*, 769–823. https://doi.org/10.1007/978-94-011-0227-8_27

World Population Prospects - Population Division - United Nations. (2022). https://population.un.org/wpp/Download/Standard/MostUsed/

Yu, Y., You, L., Liu, D., Hollinshead, W., Tang, Y. J., & Zhang, F. (2013). Development of Synechocystis sp. PCC 6803 as a phototrophic cell factory. *Marine Drugs*, *11*(8), 2894–2916. https://doi.org/10.3390/MD11082894

Yustinadiar, N., Manurung, R., & Suantika, G. (2020). Enhanced biomass productivity of microalgae Nannochloropsis sp. in an airlift photobioreactor using low-frequency flashing light with blue LED. *Bioresources and Bioprocessing*, *7*(1), 1–15. https://doi.org/10.1186/S40643-020-00331-9/FIGURES/8

Zhang, X. (2015). *Microalgae removal of CO 2 from flue gas*. www.iea-coal.org

Zuccaro, G., Yousuf, A., Pollio, A., & Steyer, J. P. (2020). Microalgae Cultivation Systems. *Microalgae Cultivation for Biofuels Production*, 11–29. https://doi.org/10.1016/B978-0-12-817536-1.00002-3

Żymańczyk-Duda, E., Samson, S. O., Brzezińska-Rodak, M., & Klimek-Ochab, M. (2022). Versatile Applications of Cyanobacteria in Biotechnology. *Microorganisms 2022, Vol. 10, Page 2318*, *10*(12), 2318. https://doi.org/10.3390/MICROORGANISMS10122318

Web sites

Algae Fuel Market - Global Industry Analysis 2023. Retrieved June 17, 2023, from https://www.transparencymarketresearch.com/algae-fuel-market.html

Alternative proteins top the bill for the latest FAO–International Sustainable Bioeconomy Working Group webinar | Sustainable and circular bioeconomy for food systems transformation | Food and Agriculture Organization of the United Nations. (2022). Retrieved June 11, 2023, from https://www.fao.org/in-action/sustainable-and-circular-bioeconomy/resources/news/details/en/c/1507553/

Microalgae Market by Size, Share, Forecasts, & Trends Analysis. (2023). Retrieved June 13, 2023, from https://www.meticulousresearch.com/product/microalgae-market-5197#description

Microalgae Market to Reach $3.08 billion by 2030 - Market Size, Share, Forecasts, & Trends Analysis Report with COVID-19 Impact - Bloomberg. (2023). Retrieved June 12, 2023, from https://www.bloomberg.com/press-releases/2023-01-31/microalgae-market-to-reach-3-08-billion-by-2030-market-size-share-forecasts-trends-analysis-report-with-covid-19-impact

Ringraziamenti

In primo luogo, vorrei ringraziare la prof.ssa Eleonora Sforza, che mi ha concesso l'opportunità di poter prendere parte a questo progetto e sapientemente guidato in ogni sua fase realizzativa, alimentando il mio interesse verso il mondo della ricerca.

Un sentito ringraziamento va a tutti i compagni di laboratorio con cui ho condiviso questa esperienza e grazie ai quali sono riuscito ad ampliare le mie conoscenze, sia in campo teorico che applicativo. In particolare, menzione d'onore va a Veronica, che nonostante la distanza è stata un punto di riferimento fondamentale per lo sviluppo di questo lavoro.

Infine, vorrei ringraziare di cuore i miei genitori, che hanno sempre riposto fiducia incondizionata nelle mie capacità ed ambizioni, e sostenuto di fronte ad ogni sfida.